12-2009

# STRAIGHT LINE BRAKING PERFORMANCE OF A ROAD VEHICLE WITH NON LINEAR TIRE STIFFNESS FORMULATION

Anup Khekare
*Clemson University*, akhekar@g.clemson.edu

# STRAIGHT LINE BRAKING PERFORMANCE OF A ROAD VEHICLE WITH NON LINEAR TIRE STIFFNESS FORMULATION

---

A Thesis
Presented to
the Graduate School of
Clemson University

---

In Partial Fulfillment
of the Requirements for the Degree
Master of Science
Mechanical Engineering

---

by
Anup D. Khekare
December 2009

---

Accepted by:
Dr. E. Harry Law, Co-Committee Chair
Dr. Beshahwired Ayalew, Co-Committee Chair
Dr. John Ziegert

# Abstract

The capability of a road vehicle equipped with an Anti-Lock Braking System (ABS) to come to a safe stop depends on factors such as dynamic force between tire and road, surface adhesion coefficient, and the vertical profile of the road. When in panic, a driver's reaction is to step hard on the brakes to make the vehicle stop as soon as possible. Although the use of modern technologies such as ABS and Electronic Stability Control (ESC) have reduced the number of accidents significantly, any further improvement in stopping distance would only complement these technologies.

Michelin has undertaken the development of a non-pneumatic tire (called the TWEEL™) which can decouple the ride comfort and handling capability of road vehicles. Studies in the ride comfort area have shown reductions in the tire-to-road dynamic force using the TWEEL™. This might lead to shorter stopping distances while braking. The primary focus area of this thesis is to evaluate the straight line braking performance of a 2007 BMW Mini Cooper with TWEELs™ on randomly irregular roads. Different vertical road profiles were utilized to evaluate their effect on braking. A comparison of results is made between the original equipment (OE) tires and the TWEEL™. Additionally, the effect on vehicle braking of tuning the shock absorbers was also studied.

A eight degree-of-freedom model that focuses on vertical and longitudinal dynamics was developed in Simulink. A rather simple brake system with an ideal antilock system (ABS) was used to avoid wheel lock-up in hard braking scenarios. A Pacejka tire model was employed as well. The nonlinear tire stiffness and the nonlinear shock absorber curves were incorporated in the model using look-up tables. The model was validated in the time

domain using the results from a vehicle model in CarSim for similar tests.

For simulation on a road profile similar to weathered asphalt at Michelin's Laurens Proving Grounds (WA-LPG), the selection between TWEEL™ and OE tire does not affect braking performance. Also, the frequency content of the "smooth" road profile had minimal effect on stopping distance. However, as RMS roughness of road profiles increased, the stopping distance increased for both the TWEEL™ and the OE tire and the "softer" TWEEL™ yielded a shorter stopping distance than the OE tire. When shock damping was altered, no change in stopping distance was found on "smooth" roads and "firmer" shocks performed better on "rough" road profiles.

# Acknowledgments

I am thankful to my advisors Dr. E. Harry Law and Dr. Beshahwired Ayalew for their guidance and financial support during the course of this work. I appreciate their efforts to keep me on track and focused on the goal. I would like to extend my gratitude to Dr. John Ziegert, also on my graduate committee, for his input and support during this work. I also appreciate the efforts of the Mechanical Engineering Department to fund part of my study and to make my experience at Clemson a delightful one.

The help and feedback provided by Michelin and BMW were equally important for the success of this work and their efforts are deeply acknowledged. Special thanks go to Mr. Judhajit Roy for the insight he provided. I also appreciate the company of my friends, who helped me stay motivated and kept my spirits up while working on this thesis.

# Dedication

I would like to dedicate this work to my parents Mr. Dewarao Khekare and Mrs. Anuradha Khekare and my sister Mrs. Swati Khekare Ghotekar, all of whom gave me the opportunity to come to the United States to pursue my dream and be where I am today. Without your continuous support and encouragement, I would not have been able to pursue this work and my Masters degree. I would also like to remember my late sister, Ms. Deepti Khekare whose memories were always by my side during the course of this work.

# Table of Contents

# List of Tables

# List of Figures

# Chapter 1

# Introduction

## 1.1 Introduction

Modern automotive technologies aim at making the automobile more safe and efficient. Antilock brakes, active suspensions, active brake proportioning, and dynamic stability control are a few of these technologies. Researchers are constantly trying to improve these technologies by either investigating newer control strategies or fine-tuning the available vehicle parameters to achieve maximum efficiency with the existing systems. Vehicle braking is a very important aspect when it comes to automobile safety, since in situations like panic stops, a properly designed brake system can save lives and help avoid damage to property. The braking performance of a vehicle depends on factors such as tire-to-road force, surface conditions, type of tire tread, suspension, and brake configuration.

Previous work done in the area of braking of road vehicles investigated various suspension and brake configurations. The vehicle models that were utilized ranged from rather simple quarter-car models to more detailed CarSim models. Sophisticated control strategies such as active brake proportioning [3] and active control of weight distribution [2] are also discussed in literature. In the end, all these strategies aimed at controlling and/or minimizing the dynamic tire-to-road force to improve vehicle performance in braking.

Michelin has undertaken development of a non-pneumatic tire design called the

TWEEL™. With this design researchers aim to reduce tire rolling resistance to reduce fuel consumption. Also, Michelin aims to improve the ride and handling characteristics of cars by equipping them with TWEELs™.

This work focuses on effect of the nonlinear tire stiffness on the dynamic tire-to-road force and hence on braking performance of a vehicle equipped with these new tires. The effect of different road profiles and shock absorbers on braking performance is also discussed. The developed model considers the vertical and longitudinal dynamics of a road vehicle and does not ignore coupling between the two. This was not the case with most of the previous work in the area [1, 7, 5]. This work aims to develop the vehicle model and simulations and to give more conclusive information about the effectiveness of this new tire design on braking performance.

## 1.2 Research Motivation and Problem Statement

Researchers at Michelin Americas Research and Corporation (MARC) have conceived a revolutionary new non-pneumatic tire design called the TWEEL™. With the TWEEL™, Michelin's aim is to meet or exceed the ride, handling, and the acoustic characteristics of the OE tire on current vehicles while lowering rolling resistance to increase gas mileage. TWEEL™ designers have characterized the vertical stiffness by a nonlinear law which can be realized by a mathematical equation. Previous work done in evaluating the ride characteristics of the current vehicle equipped with nonlinear TWEELs™ showed that lower root mean square (RMS) tire-to-road forces are possible by adopting the TWEEL™ design [15]. Further study showed that tuning the shock absorbers will compliment the reduction in dynamic tire-to-road force [13]. Theoretically, this should translate into improved braking and handling performance. The results of this study will help quantify the effect of the nonlinear stiffness law on the braking performance of the vehicle. Additionally, parametric studies will examine vehicle behavior in different braking maneuvers when equipped with the TWEEL™ and the OE tire. A step by step plan of action is as follows,

1. Develop a vehicle model to account for the longitudinal and vertical dynamics of an automobile.

2. Incorporate a model of an anti-lock braking system in the vehicle model for simulation of hard braking tests.

3. Simulate straight line braking tests on a simulated weathered asphalt road similar to that at Michelin's Laurens Proving Grounds (WA-LPG) and perform a sensitivity analysis of the stopping distance to the parameters of the nonlinear TWEEL™ stiffness law.

4. Study and compare the braking performance of the TWEEL™ to the OE tire on roads rougher than the WA-LPG road.

5. With stopping distance as a performance metric, perform a sensitivity analysis to study the effect of shock absorber damping on the vehicle equipped with OE tires and TWEELs™ when braked on a simulated road similar to the WA-LPG road and rougher than the WA-LPG road.

## 1.3 Organization of the Thesis

Chapter 1 gives an overview of the problem statement and the motivation underlying this study. The previous work conducted in this field is reviewed in Chapter 2. The derivation of physical models and the modeling is discussed next, in Chapter 3. Chapter 4 introduces the user to various sensitivity studies performed and also discusses the results. Finally, Chapter 5 summarizes the conclusions and recommendations based on the results of the study. Appendix A includes detailed derivation of the equations of motion used in modeling the vehicle. The input parameters used for the model are tabulated in Appendix B. The details of the Simulink model can be found in Appendix C. The Matlab codes used in the study are included in Appendix D.

# Chapter 2

# Literature Review

Cars today come installed with technologies such as Anti-Lock Braking (ABS); furthermore, technologies such as Electronic Brake force Distribution (EBD) make vehicle behavior during an emergency maneuvers relatively safer. Any improvements in the performance of these systems by tuning the available vehicle and tire parameters is an effort well worth the result. In the past, experimental and analytical efforts have been made to study the braking performance. Literature for this field discusses several computer models which simulate the associated physics using different modeling techniques; several approaches were used to model anti-lock systems as well. In its initial part, this chapter summarizes relevant vehicle models from the literature followed by anti-lock brake system models.

## 2.1 Vehicle Model

In [1], Rangelov discusses the development of the quarter car model to study the braking performance of an automobile in a straight line on flat and uneven roads in a Matlab-Simulink environment. The vehicle model includes a suspension, a Short Wavelength Intermediate Frequency Tire (SWIFT) model, and an anti-lock braking system. The author compared the effect of using various wheel-lock criteria to warn the ABS controller about impending wheel lock up. A few of these include tire torque, wheel angular decel-

eration, wheel longitudinal slip or a combination of wheel angular deceleration and wheel longitudinal slip. The author found out that tire torque (defined by the author as tangential force $\times$ the rolling radius of tire + polar moment of inertia of belt $\times$ tire angular acceleration) when used as a wheel lock criteria yields the best stopping distance. The next best criterion was found to be the ratio of the wheel angular acceleration and the wheel angular velocity. However, the quarter car model, used in [1] lacked the weight shift in vertical load from back to front due to deceleration and hence is not considered very accurate.

Ashrafi [2] developed three vehicle models with different levels of complexity to investigate sophisticated control strategies in braking. These models were validated with the available experimental data and the best of the three was selected to study concepts like suspension control, different braking configurations, and active control of weight distribution. He also investigated the effect of location of center of gravity, road adhesion, split-$\mu$ surface, and different ABS configurations. Perhaps the most interesting concept investigated by Ashrafi was the active control of weight distribution to increase the normal reaction forces during braking and increase the performance. He achieved this by embedding an inertia element (free to accelerate in the fore/aft or vertical direction at a controlled rate) in the chassis. Ashrafi found that when under hard braking, the longitudinal position of center of gravity (C.G.) affects vehicle stability more so than the transverse position. In case of a brake failure, Ashrafi suggests that the failure of front brakes while rear wheels are locked can lead to a dangerous spin out of the vehicle. Lastly, he concluded that the fore/aft motion of the inertia element slightly improved the stopping distance but the vertical acceleration of the inertia element was ineffective in improving the braking performance.

Nantais [3] investigated the effect of Active Brake Proportioning on braking performance. His work dealt with actively proportioning the brake pressure at each wheel according to the available traction at the tires. He investigated the performance of cars with and without Active Brake Proportioning (ABP) using "CarSim" models. He concluded that a vehicle equipped with ABP outperformed the baseline vehicle in straight line braking, braking in a turn, and braking while avoiding obstacles.

In [4], Nigam developed a detailed brake model in MATRIXx (software for control system application) and a vehicle model in ADAMS (Automatic Dynamic Analysis of Mechanical Systems). Control strategies were developed to effectively use vehicle information to improve stopping distance and stability. He compared the performance of three and four channel ABS systems to a car without ABS. He also evaluated the performance on road surfaces ranging from ice to dry asphalt with non-uniform surface conditions like split $\mu$, transition of surfaces, checker board patterns etc. A simplified driver model using the vehicle's yaw angle and linear deviations from path as control inputs was developed. Nigam concluded that a four channel ABS matters only when the road surface condition as seen by the tires is not similar for all the wheels. He added that wheel accelerations are a very good control input for ABS and vehicle yaw information is vital when designing stability control systems.

Delaigue and Eskandarian [5] developed a vehicle braking model to predict the stopping distance under various braking conditions. They considered numerous parameters like pavement properties, roadway slope, presence of drag/wind, vehicle-related components such as general specifications (i.e. load distribution, pitch inertia and several dimensional factors), tire properties (i.e. dimensions, load and pressure), presence of ABS, suspension characteristics, and types of brake (drums or discs). The model was developed in a Matlab-Simulink environment and validated with test data from sources like National Highway Traffic Safety Administration and Car and Driver magazine. The study showed that the experimental and simulated data compared well. The authors concluded that the model can be used as a reliable and accurate tool for simulations of vehicle straight line stopping events.

Paradiso [15] discusses the effect of TWEELs™ on ride comfort of a 2007 BMW Mini Cooper. He implemented a five degree of freedom vehicle model in Matlab/Simulink environment. His model also included nonlinear shock curves. Field data and four post test data was used by Paradiso to validate his vehicle model. To achieve desired fidelity with the model, Paradiso had to tune parameters like engine mounting stiffness, engine mass,

and rear shock damping. The reasons mentioned were unavailability of relevant parameters or incorrect data. In the end, he concluded that the overall ride comfort would increase with the adoption of this nonlinear tire design. Additionally, he stated that the dynamic tire-to-road force is reduced using the TWEEL™ design and that this might mean more available grip.

## 2.2 Anti-Lock Brake System (ABS) Model

Anti-lock brake systems avoid wheel lock under hard braking thus preserving the lateral force generation capacity of the tires. Note that for simulations investigating braking performance, it is theoretically possible to calculate wheel slip and utilize it as a control input for ABS algorithms, but this is purely an academic exercise. Wheel slip is an impractical parameter to measure in the real world and hence practical ABS algorithms use different control inputs than wheel slip, viz. wheel angular acceleration or angular velocity.

Infantini, et al. [7] proposed a proportional and derivative (PD) control strategy for ABS by controlling wheel slip. His aim was to achieve desired longitudinal wheel slip during braking. The simulations were performed for snow, wet and dry asphalt with a controller that was implemented in Matlab-Simulink environment. Infantini concluded that the proposed ABS control logic reduces the stopping distance relative to passive braking. This approach however, could not control the slip in a desired range.

In [8], Day and Roberts discuss the implementation of two ABS algorithms, a relatively straight forward tire slip algorithm and a more sophisticated Bosch ABS algorithm which is closer to what many passenger cars have today. The Bosch system was developed in the Human Vehicle Environment (HVE) - an integrated environment for setting up and executing simulation models. The HVE Bosch algorithm was based on wheel spin acceleration and a critical tire slip threshold. In conclusion, the authors state that the experimental results compare favorably with simulation.

Cabrera, Ortiz, Castillo, and Simon[9] and Jun [10] discuss a fuzzy logic approach

to ABS. The fuzzy controllers differ from traditional controllers in that they use a set of fuzzy IF-THEN decision rules to describe mapping relationships between inputs (states) and outputs (control action). Jun [10] discusses the development of a fuzzy logic-based controller for a light bus. The author concludes that the fuzzy controller is robust and provides good control over both dry and icy roads.

Alptekin [6] studied the interaction of the suspension and braking systems in automobiles with and without ABS. He used a quarter car model and a seven degree of freedom model to simulate straight line braking maneuvers. Both random and discrete road inputs were used to excite the vehicle. He used an "ideal" anti-lock system to avoid wheel lock up. Several damper or shock absorber configurations like linear, nonlinear, and idealized "sky-hook" dampers were implemented in the model. A semi-active suspension with control logic to hold the suspension damper in a "firm" setting during a severe braking maneuver was also investigated. Stopping distance was used as a metric to compare these different configurations. Alptekin concluded that a "firm" passive damper was most effective in reducing the dynamic force between the tire and road and hence has the best braking performance. The bicycle model used by Alptekin was of particular interest since it considered all the necessary degrees of freedom required to accurately simulate the physics and yet was simple enough to model within the given time frame. Similarly, the ABS algorithm and the brake system model used by Alptekin were deemed accurate for the purpose of this work.

Law and Hazare [13] used a simplified method to determine the "best" shock configuration with respect to front and rear grip and vertical acceleration. They used the ride model developed by Paradiso [15]. This method involves a weighting function J which includes the vertical ride acceleration and both front and rear grip. A value of $J < 1$ indicates an improvement over the OE tire. The different shock effects ("firm" and "soft") were approximated by scaling the shock force vs. velocity curve with a constant gain K. A five degree of freedom ride model was then simulated at of 30 and 60 mph on a road profile similar to the weathered asphalt road at Lauren's Proving Grounds (WA-LPG road). This road profile was generated by comparing simulated and tested ISO RMS vertical accelera-

tion for the vehicle [15]. The ride and grip responses were then obtained. The smallest J values were obtained when the RMS acceleration was weighted 50%, the front grip 37.5%, and the rear grip 12.5%. Also, softer shocks at the front and rear were found to reduce the RMS ride acceleration and improve front grip while the rear grip was found to be best with nominal shocks at the rear and was independent of the front shocks. While Law and Hazare evaluated the effect of shocks on ride, the authors of [14] present similar work where they study the effect of a worn and a new shock absorber on the braking performance. They modeled a mid-sized European sedan in CarSim and performed a hard braking maneuver from 100 km/h without the aid of ABS. They discovered that on smooth roads the shocks did not affect the stopping distance. However if the roads were rough, the shock characteristics significantly affect the stopping distance. The car with worn shock absorbers had a longer stopping distance than the car equipped with new shocks.

Paradiso [15] modeled and validated the vertical dynamics of the vehicle under consideration. As will be discussed in detail in Chapter 3 in this study, the longitudinal dynamics, brake system model, and anti-lock system algorithm from Alptekin's work [6] were incorporated into Paradiso's vehicle model [15] to obtain a longitudinal and vertical vehicle dynamic model used to study braking performance.

# Chapter 3

# Model Description

## 3.1 Introduction

This chapter discusses the various models used in this work. This includes the vehicle model, tire model, brake and ABS models, and suspension model. It also discusses the generation of road profiles for the study. The vehicle considered in this work is a 2007 BMW Mini Cooper S in curb + driver (C+D) loading condition. A simple eight degree freedom model was developed and simulated in the Matlab/Simulink environment. This model includes the vertical and longitudinal dynamics to evaluate braking performance. The commercial software package CarSim was also used to develop a vehicle model of the Mini. The latter takes detailed geometric data, inertial parameters, steering and suspension kinematics, tire force data, and suspension compliance data as input and uses inbuilt solvers to obtain the solutions to the equations of motions . The Simulink model was validated by comparing the results to those obtained from CarSim.

## 3.2 Description of the Vehicle Dynamic Model

The so-called "bicycle model" used in this study assumes that the vehicle is symmetric about a vertical plane that passes through the C.G.. Also, the left and right wheels are assumed to see similar road inputs at any given time. For simulation purposes, the two

wheels on the front and rear axle can thus be lumped to a single wheel per axle; hence the name "bicycle model".

The eight degree of freedom model is based on the ride model developed in Simulink by Law and Paradiso [15] which was modified by including longitudinal dynamics. Since the model was realized in Simulink environment, it was easy to incorporate the nonlinear tire force curves, and the nonlinear shock absorber curves. The equations of motions used were derived using the Newton-Euler approach and the derivation is included in Appendix A. Figure 3.1 shows the vehicle model used in this study. The model uses lumped parameters to represent the masses of the components. Following are the degrees of freedom considered for this vehicle:

$$
\begin{aligned}
z_s &= Sprung\,Mass\,C.G.\,Heave \\
theta &= Sprung\,Mass\,Pitch \\
z_{tf} &= Front\,Axle\,Heave \\
z_{tr} &= Rear\,Axle\,Heave \\
z_e &= Engine\,Heave \\
\nu &= Longitudinal\,Velocity \\
\omega_f &= Front\,Wheel\,Angular\,Velocity \\
\omega_r &= Rear\,Wheel\,Angular\,Velocity
\end{aligned}
$$

This study utilized the SAE vehicle coordinate system [20] to develop the equations of motion. Figure 3.2 shows the coordinate system. The longitudinal X axis points forward. The lateral Y axis is positive to the right of the driver. The vertical Z axis points down.

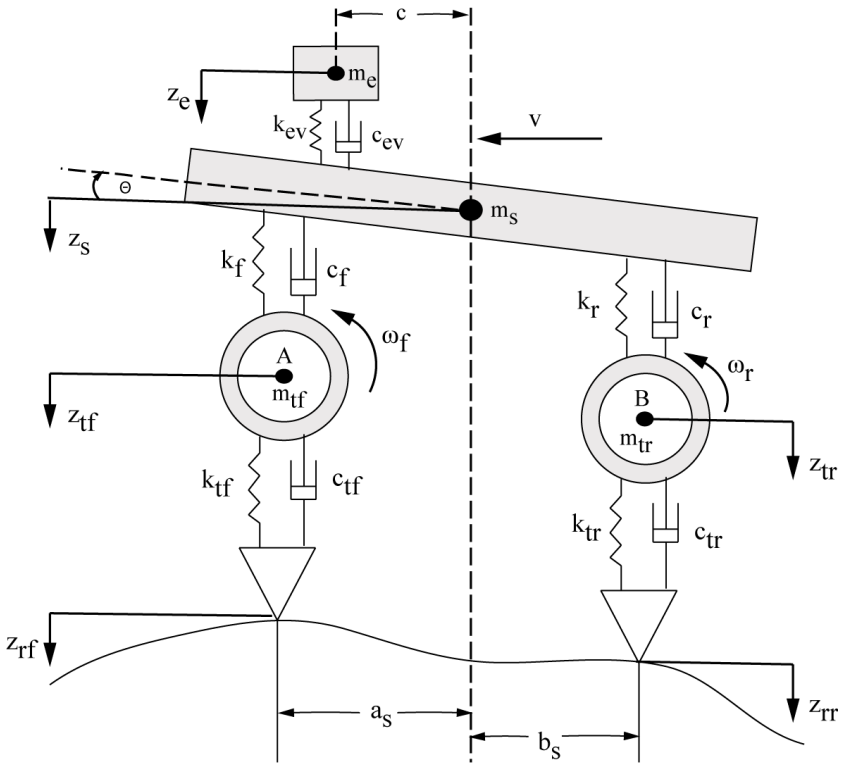


Figure 3.1: Eight Degree of Freedom model

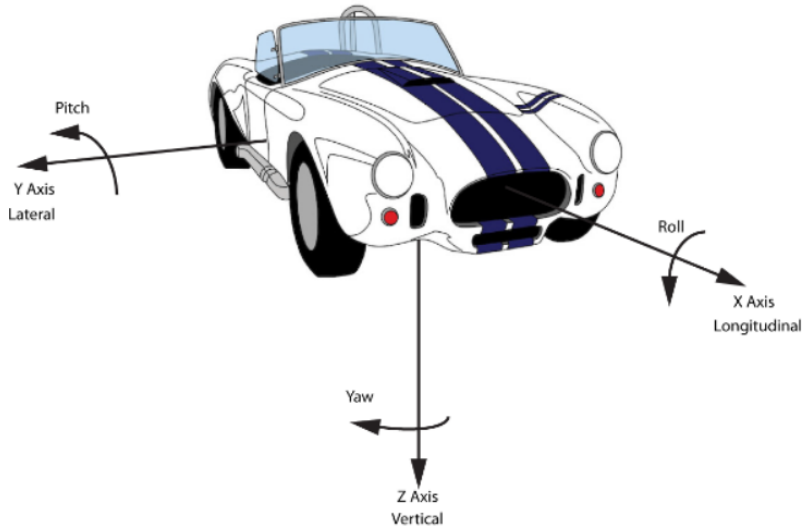


Figure 3.2: SAE Coordinate system

The sprung mass is defined as the portion of the mass of the vehicle which is supported by the suspension. It typically includes the mass of the body, chassis, engine, cargo, and passengers. Sometimes, it can include approximately half the weight of suspension itself. This study models the sprung mass as a rigid body. Any additional passenger or cargo load is added to this body. The sprung mass is connected to the unsprung mass via suspension components and finally to the ground through the tires.

The locations of C.G. and other inertial parameters for the vehicle configurations under consideration were calculated by Law [19] and are tabulated in Appendix B.

## 3.3 Suspension System Modeling

The suspension system is composed of parallel spring and damper elements connecting the sprung and unsprung masses. The spring is modeled as a linear element and the stiffnesses were calculated by Law in [19]. Since it is assumed that the left and right wheels are identical and have similar inputs, the stiffness is lumped into per-axle values. Law [19] also provided the per axle damping values of 7840 $\frac{N}{m/s}$ and 5180 $\frac{N}{m/s}$ for front and rear, respectively.

Practically though, the dampers used in shock absorbers have a highly nonlinear and hysteretic behavior. Obviously, more accurate results are expected by using the nonlinear curves in simulation. Michelin [18] provided the force vs. velocity curves for the shock absorber as tested on a shock dynamometer. Tests were conducted for a 100 mm stroke cycled at 3.16 Hz (maximum shock velocity = 1 m/s) and also for a 19 mm stroke cycled at 2.15 Hz (maximum shock velocity = 0.1 m/s). Preliminary simulations of braking tests in CarSim (from 60mph to 0) were carried out on a road profile similar to the WA-LPG road. The results showed that during braking on the WA-LPG road, maximum shock velocities of 0.13 m/s were reached. Similar simulation on a rougher road registered a maximum shock velocity of 0.75 m/s. Thus the data from 19 mm stroke cycled at 2.15 Hz run (maximum shock velocity = 0.1 m/s) would not have been accurate for any of these simulations. To

maintain accuracy, it was decided that the data from 100 mm stroke cycled at 3.16 Hz (maximum shock velocity = 1 m/s) will be used for this work. Figures 3.3 and 3.4 show the comparison of the linear and nonlinear force vs. velocity curves (100 mm stroke cycled at 3.16 Hz).

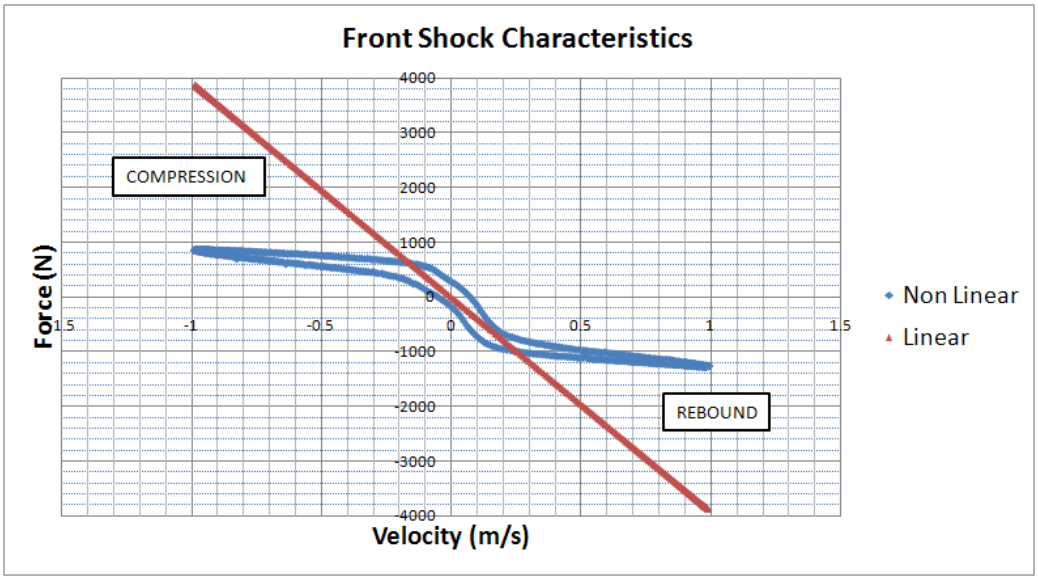


Figure 3.3: Front Shock Absorber - Force vs. Velocity (100 mm stroke at 3.16 Hz)

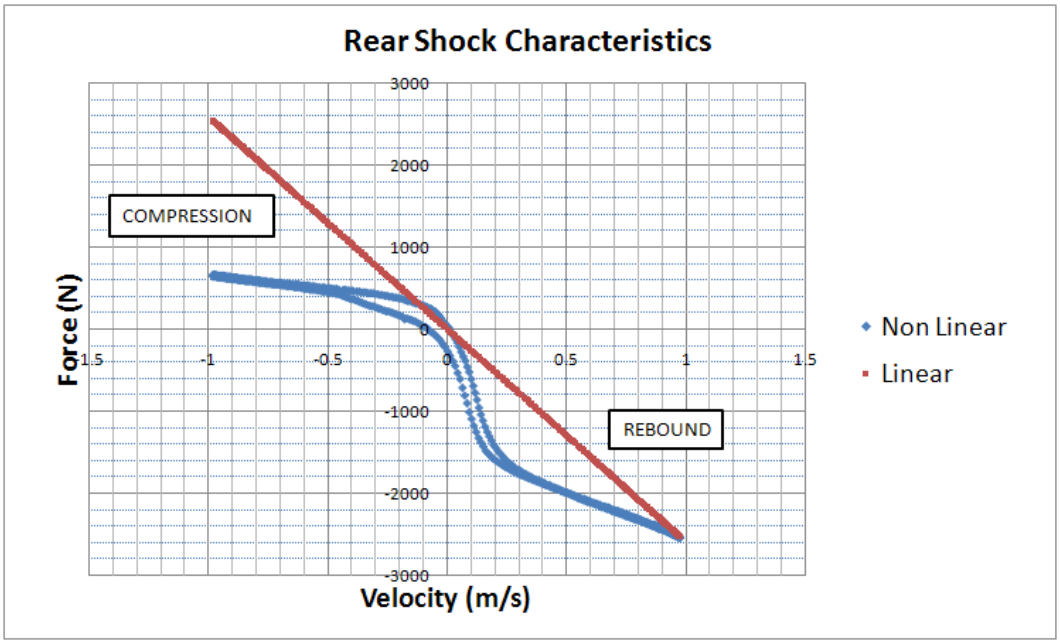


Figure 3.4: Rear Shock Absorber - Force vs. Velocity (100 mm stroke at 3.16 Hz)

As mentioned earlier, shock absorbers are highly hysteretic in nature. In this work, however, hysteresis is ignored for simplicity. Paradiso [15] explains the method he adopted to approximate the shock dynamometer data obtained from Michelin [18]. Paradiso segmented the data into sections and fitted lines to these sections. The curves were then augmented to ensure both continuity and zero damping force at zero velocity. Equations 3.1 and 3.2 were used by Paradiso for defining the nonlinear shock dynamometer data in his work. The equations correspond to the run for a 100 mm stroke cycled at 3.16 Hz .

For the front shocks, the equations are:

$$F_f = \begin{cases} -497.52 \cdot V + 358.48 & -1 \leq V \leq -.25 \\ 88768 \cdot V^5 + 110931 \cdot V^4 + 14449 \cdot V^3 - 10290 \cdot V^2 - 4031.1 \cdot V & -.24 \leq V \leq 0.2 \\ -468.75 \cdot V - 801.25 & 0.21 \leq V \leq 1 \end{cases} \tag{3.1}$$

For the rear shocks, the equations are:

$$F_r = \begin{cases} -391.7 \cdot V + 273.3 & -1 \leq V \leq -0.4 \\ -649.8 \cdot V + 170.1 & -0.39 \leq V \leq -0.1 \\ 208662 \cdot V^4 + 39380 \cdot V^3 - 26550 \cdot V^2 - 5177.8 \cdot V & -0.09 \leq V \leq 0.13 \\ 208662 \cdot V^4 + 39380 \cdot V^3 - 26550 \cdot V^2 - 5177.8 \cdot V - 88 & 0.14 \leq V \leq 0.22 \\ -1237.3 \cdot V - 1339.8 & 0.23 \leq V \leq 1 \end{cases} \tag{3.2}$$

where

$$\begin{aligned} F_f, F_r &= Front\,and\,Rear\,Shock\,Force\,(N) \\ V &= Shock\,Velocity\left(\frac{m}{sec}\right) \end{aligned}$$

Figures 3.5 and 3.6 show the fits to the force vs. velocity curves generated by Paradiso. These are also used in this work.

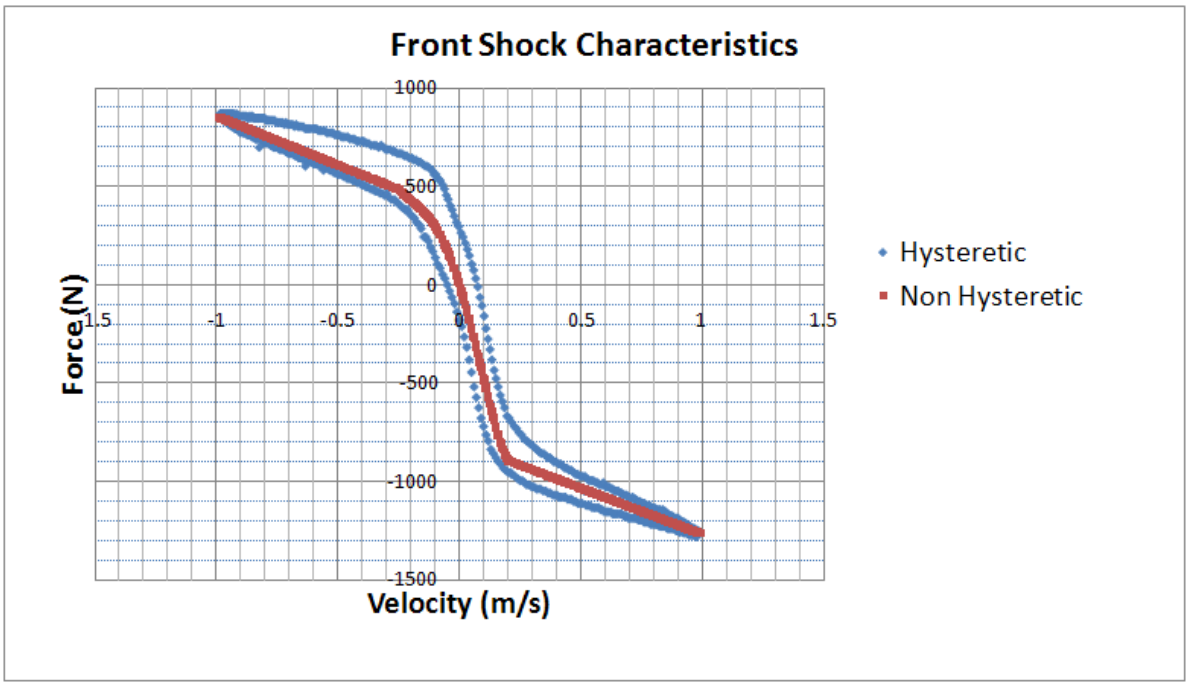


Figure 3.5: Front Shock Absorber - Force vs. Velocity (100 mm stroke at 3.16 Hz)

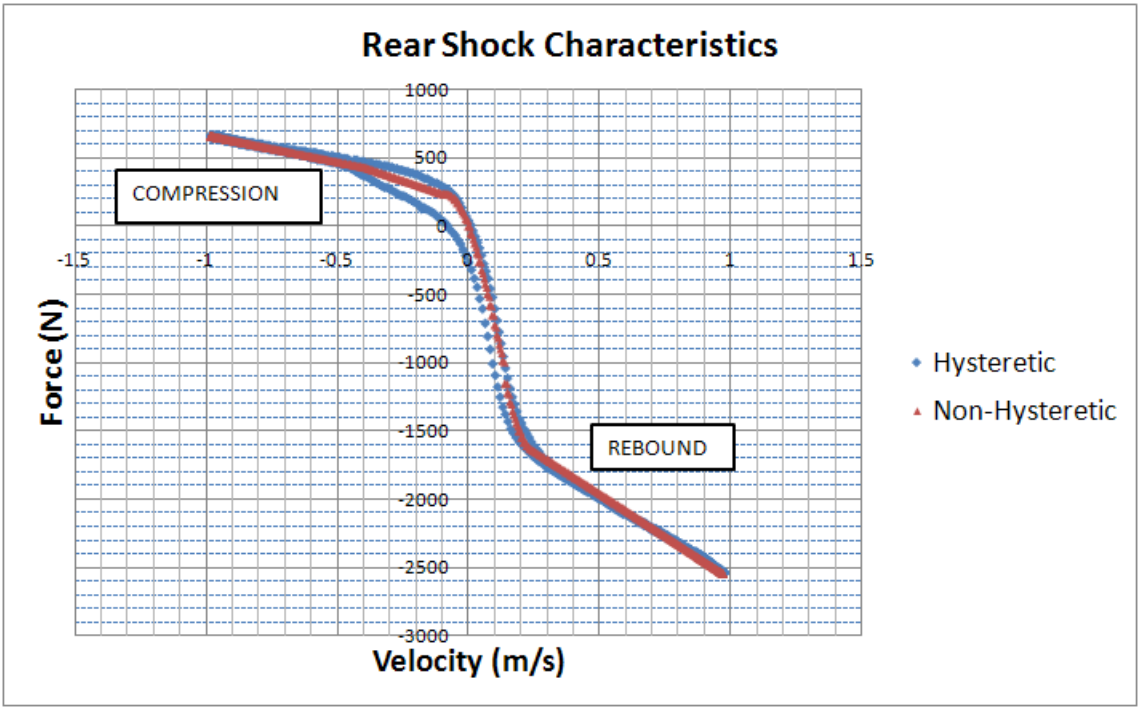


Figure 3.6: Rear Shock Absorber - Force vs. Velocity (100 mm stroke at 3.16 Hz)

## 3.4 Brake System Model

### 3.4.1 Introduction

The braking system on an modern automobile is comprised of many components. The major components are master cylinder, booster, brake lines, wheel calipers, brake pads, and brake discs and/or drums. To brake the vehicle, the driver depresses the brake pedal attached to the master cylinder creating fluid pressure in brake lines which is transferred to the brake cylinders and thus to the calipers that press the brake pads against the brake drum or disc. Previous work done in modeling and simulation of brake system dynamics varied from a simple first order system approximation to a component by component dynamic model of the complete braking system. This section discusses the modeling of the brake system and its components. Further, it discusses the concept of brake pressure proportioning to front and rear as well as anti-lock braking systems.

In [26] the authors modeled the major components of a brake system in AMEsim®. The authors paid special attention to booster modeling. The model was validated with a test bench set up. Finally, chassis systems like ABS and vehicle dynamic control (VDC) were integrated with the vehicle dynamics model. Yamada and Sawada [25] discuss a similar approach towards modeling of brake components in the Matlab-Simulink environment. Pang and Agnew [27] modeled the fluid flow dynamics in the system when the brakes are applied. According to the authors, the response time of a brake system depends on the brake fluid dynamics and the functionality of each sub-component. The work models the fluid pressure differentials through the system components when the brakes are applied. The authors conclude that their study would help the brake performance engineer predict pressure differentials and hence brake response time. While all these approaches to brake system modeling are excellent, they are quite detailed and do not fit the context of this work. Furthermore, unlike the aforementioned references, this work does not aim to model the brake system in detail. Hence simpler models were considered for the work.

Fisher [21] analyzed the dynamic performance of automotive braking systems and

discovered that the dynamics of the booster and the brake lines are the most important. According to Schafer, Howard, and Carp [22] the frequency response of a typical brake system is similar to that of a first order system with a time constant of 0.1 sec. The Bosch Automotive Handbook [24] under the section "Braking Systems for Passenger Cars" mentions that the pressure build up (when brakes are applied) is a slower process than the pressure drop (when brakes are released). It also mentions that the pressure drop process is ten times faster than the build up process. A study by Aurora [23] shows that for pressure build up, a time constant of 0.1 sec is a good approximation. Alptekin [6] combined these system parameters to formulate a brake system model which was simple but could approximately emulate the actual system. His concept was hence adopted for this work.

It is further assumed that there is a linear relationship between brake fluid pressure in the hydraulic lines and available brake torque at the wheels. This allows us to use brake torque as input rather than the hydraulic fluid pressure in the master cylinder. Hence for this study a time constant of 0.1 sec was used for brake torque build up whereas a time constant of 0.01 sec was used for torque release.

### 3.4.2 Brake Proportioning

The concept of brake proportioning can be explained as distributing the brake torque generation capacity between front and rear wheels of an automobile. Practically, this is done by controlling the size of wheel cylinders, brake pads, discs/drums, and proportioning valves themselves. It is known that the longitudinal or lateral force generated by a tire is proportional to the normal load on it. Brake proportioning plays an important role in brake system design since during braking the normal loads between tires and road increase at the front and decrease at the rear. This is called "weight shift". Thus, weight shift reduces the longitudinal force generation capacity of the rear tires and increases that of the front tires. If overbraked, the rear tires will lock and spin-out may occur. On the other hand, if the front wheels are overbraked, they might lock, and the driver would lose steering control. To avoid the spin out scenario, rear brakes on modern cars are always designed to produce less

torque than the front. The so-called ideal brake distribution is when the front and rear wheels reach the adhesion limits at the same time. The equations necessary for evaluating the braking performance of a car are presented in [17]. Chapter 9 in [17] discusses the derivation for the ideal brake force distribution curve. The equations are,

$$\begin{aligned} \frac{F_{xf}}{W} &= \left(\frac{b}{L} + \frac{h}{L} \cdot \frac{a_x}{g}\right) \cdot \frac{a_x}{g} \\ \frac{F_{xr}}{W} &= \left(\frac{a}{L} - \frac{h}{L} \cdot \frac{a_x}{g}\right) \cdot \frac{a_x}{g} \end{aligned} \tag{3.3}$$

where,

$$\begin{aligned} F_{xf} &= Front\ Braking\ Force,\ N \\ F_{xr} &= Rear\ Braking\ Force,\ N \\ W &= Normal\ Load,\ N \\ b &= Sprung\ Mass\ CG\ to\ Rear\ Axle,\ m \\ a &= Sprung\ Mass\ CG\ to\ Front\ Axle,\ m \\ a_x &= Longitudinal\ Acceleration,\ \frac{m}{s^2} \\ g &= Acceleration\ due\ to\ Gravity,\ \frac{m}{s^2} \end{aligned}$$

The derivation neglects aerodynamic drag and rolling resistance and assumes a level road. Hence,

$$\mu W = \frac{W}{g} a_x$$

$$\mu = \frac{a_x}{g} \tag{3.4}$$

The program Ideal_brake_distribution.m was written in Matlab to plot the ideal

proportioning curve for the vehicle under consideration. Figure 3.7 shows the output of the program.

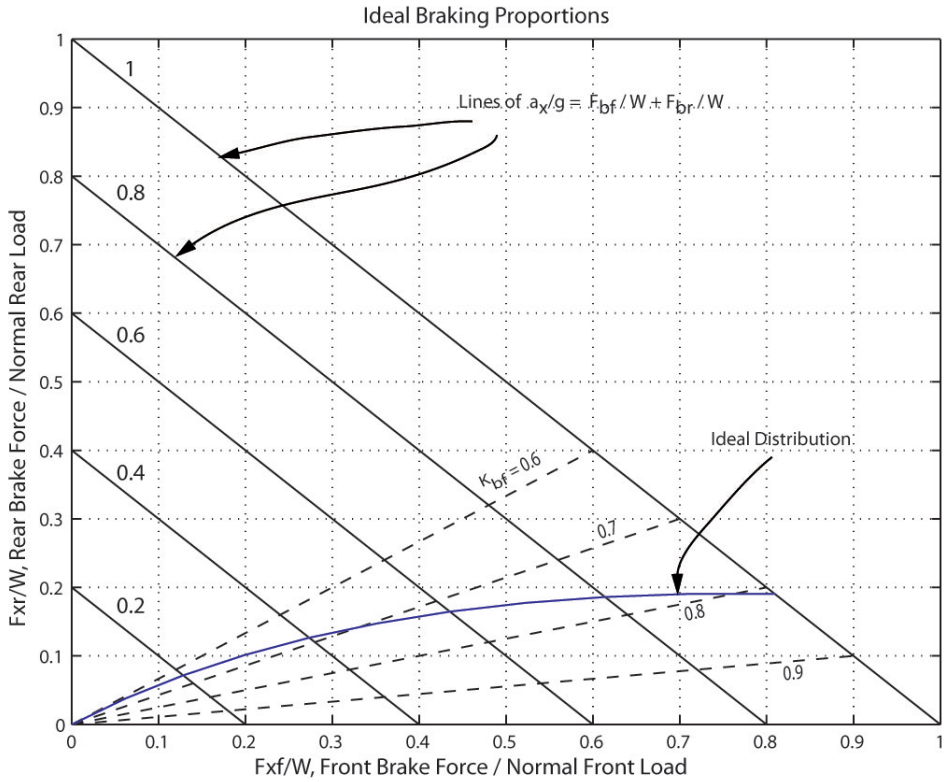


Figure 3.7: Ideal Braking Proportion for BMW Mini Cooper (C+D Configuration)

The lines of constant $\frac{a_x}{g}$ lines are obtained by the equation below:

$$\frac{-a_x}{g} = (\frac{F_{xf} + F_{xr}}{W}) \tag{3.5}$$

where

$$\begin{aligned}
a_x &= Longitudinal\, Acceleration\, of\, the\, Vehicle\, (\frac{m}{sec^2}) \\
g &= Acceleration\, due\, to\, Gravity\, (\frac{m}{sec^2}) \\
W &= Weight\, of\, the\, Car\, (N) \\
F_{xf} &= Longitudinal\, Force\, for\, Front\, Tires\, (N) \\
F_{xr} &= Longitudinal\, Force\, for\, Rear\, Tires\, (N) \\
K_{bf} &= \%\, Braking\, on\, Front
\end{aligned}$$

Corresponding to each value of $\frac{F_{xf}}{W}$ on the curve marked "Ideal Distribution", the corresponding $\frac{F_{xr}}{W}$ value is such that maximum adhesion level is achieved simultaneously in front and rear. Current production cars however, do not feature valves capable of producing this nonlinear proportioning. Most systems use linear or bi-linear proportioning .

This study uses linear proportioning where only 30 % of the braking torque is diverted to the rear wheels. Notice that in Figure 3.7, we see that the "Ideal Distribution" curve and the $K_{bf} = 0.7$ curve intersect at approximately $\frac{a_x}{g} = 0.45$ . This means that without ABS if braked , up to 0.45 g's the rear wheels are under-braked and hence would lock after the front wheels. For $a_x > 0.45$ g's, however, the rear wheels are overbraked i.e. the applied brake torque is more than the ideal brake torque.

### 3.4.3 Anti-lock Braking System

The longitudinal force generated by a tire depends on the non dimensional parameter wheel slip ratio ($\kappa$) and the vertical load on tire.

The slip ratio ($\kappa$) is defined as

$$\kappa = \frac{v - r\omega}{v} \tag{3.6}$$

where

$$\begin{aligned} \omega &= Angular\,Velocity\,of\,the\,Wheel\,(\frac{rad}{sec}) \\ v &= Linear\,Velocity\,of\,Wheel\,Center\,(\frac{m}{sec}) \\ r &= Rolling\,Radius\,(m) \end{aligned}$$

Figure 3.8 shows the longitudinal force curves generated using Pacejka magic formula [16] and data from [31]. Note that the tire force data (longitudinal force vs. slip ratio curve) was an estimate. Further details about the tire model can be found in section 3.6. In Figure 3.8 the longitudinal force increases linearly with wheel slip up to about 6 % and then gradually drops down to about 70 % of the peak value at a wheel slip of 100 % (locked wheel). This is true at almost all the vertical loads. This can be explained by Figure 3.9 which shows the so-called $\mu$-slip curve for the same tire. The surface adhesion coefficient $\mu$ governs the available grip from a pneumatic tire. The factor $\mu$ depends on a number of variables such as road surface conditions, type of rubber compound, and dynamics in the tire-road interface. As shown in Figure 3.9, with increasing wheel slip, $\mu$ increases linearly to about 6 % wheel slip and then drops down to 70 % of peak when the tire slides while being locked.

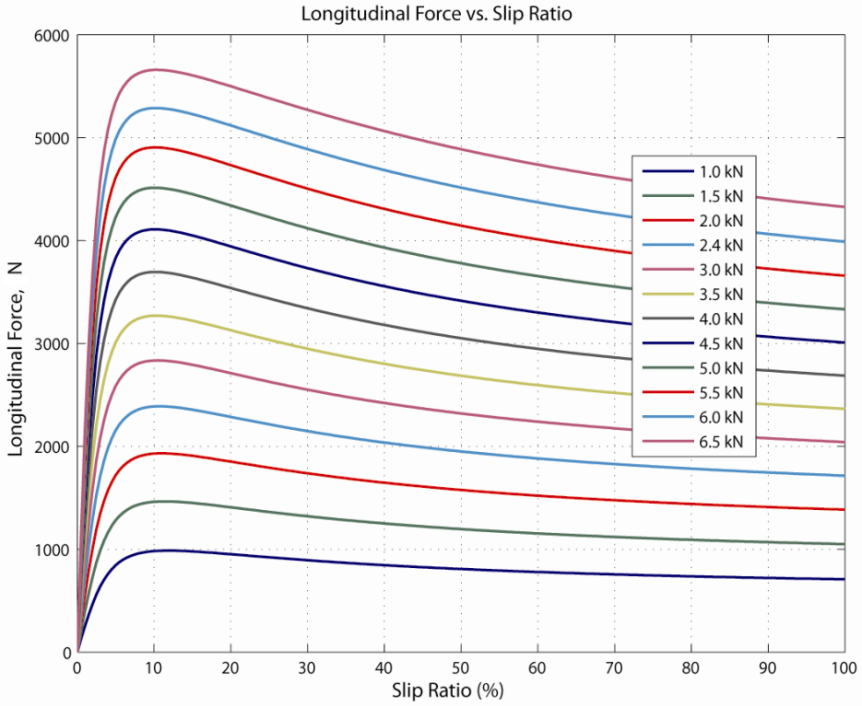


Figure 3.8: Longitudinal Force Curve

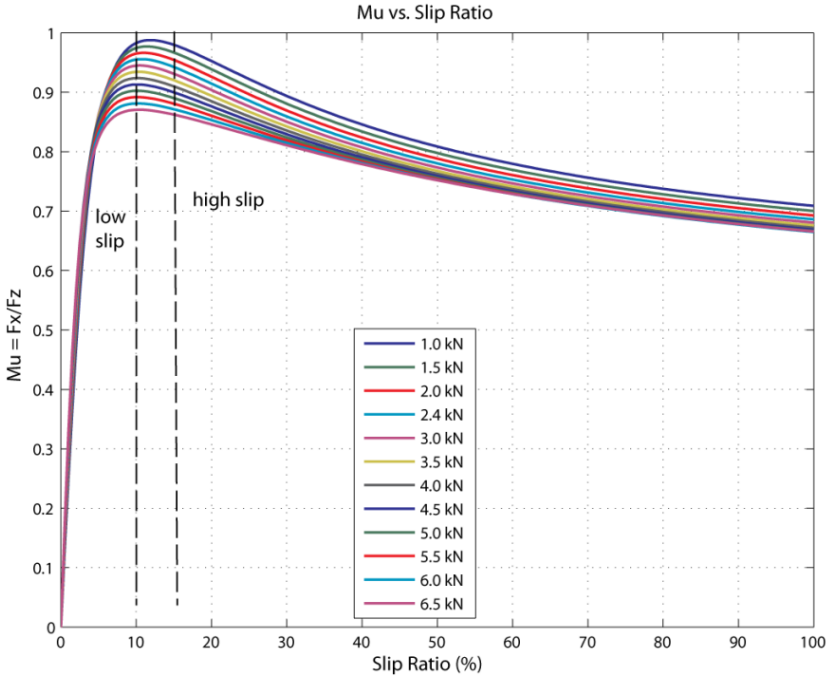


Figure 3.9: Mu Slip Curve

During emergency maneuvers, average drivers react by stepping on to the brake to come to a stop as soon as possible. Depending on the surface conditions, eventually the wheels would lock and start sliding. As seen in Figures 3.8 and 3.9, the effective $\mu$ and longitudinal force generated decrease at higher wheel slip. Hence, when a wheel is locked, the tire does not utilize maximum available traction. Modern cars equipped with ABS avoid this situation by avoiding wheel lock. Theoretically, these systems try to cycle the wheel slip in the range marked above a certain *low slip* and below a certain *high slip* as shown by the vertical dashed lines on Figure 3.9. This is often achieved by a set of sensors, ABS control unit, pumps, and actuators. There are various control strategies for ABS in literature which are discussed in Chapter 2. Practical ABS controllers monitor the wheel speed continuously and modulate the brake fluid pressure as deemed necessary to avoid wheel lock.

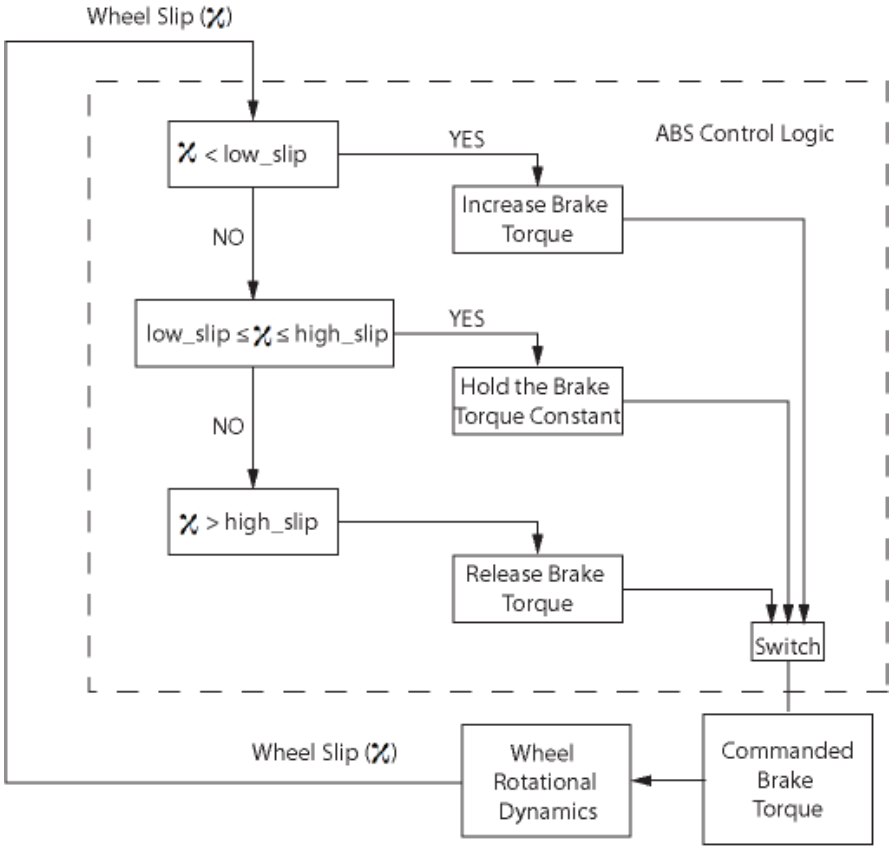


Figure 3.10: ABS control Algorithm

Since the primary objective of this thesis is to utilize the ABS and not to perform an in-depth study on ABS systems, a simple logic based controller was utilized. This logic is based on the work done by Alptekin [6]. He calls this system an "ideal" ABS system- "ideal" in that it tries to emulate the functioning of the actual ABS control system which in most cases is proprietary to manufacturers. Figure 3.10 shows the logic used. This algorithm is based on wheel slip, i.e., it uses wheel slip as an input for control purposes. As soon as the brakes are applied, the brake torque increases through a first order lag with a time constant of 0.1 sec. This causes the angular speed of the wheel to decrease, and increases the slip ratio. As soon as the slip ratio increases above *low slip* but is smaller than *high slip* the controller holds the brake torque constant. If wheel slip goes above *high slip,* the controller releases the brake and the torque goes to zero with a time lag of 0.01 sec. The time lags for torque application and release were chosen as discussed in Section 3.4.1.

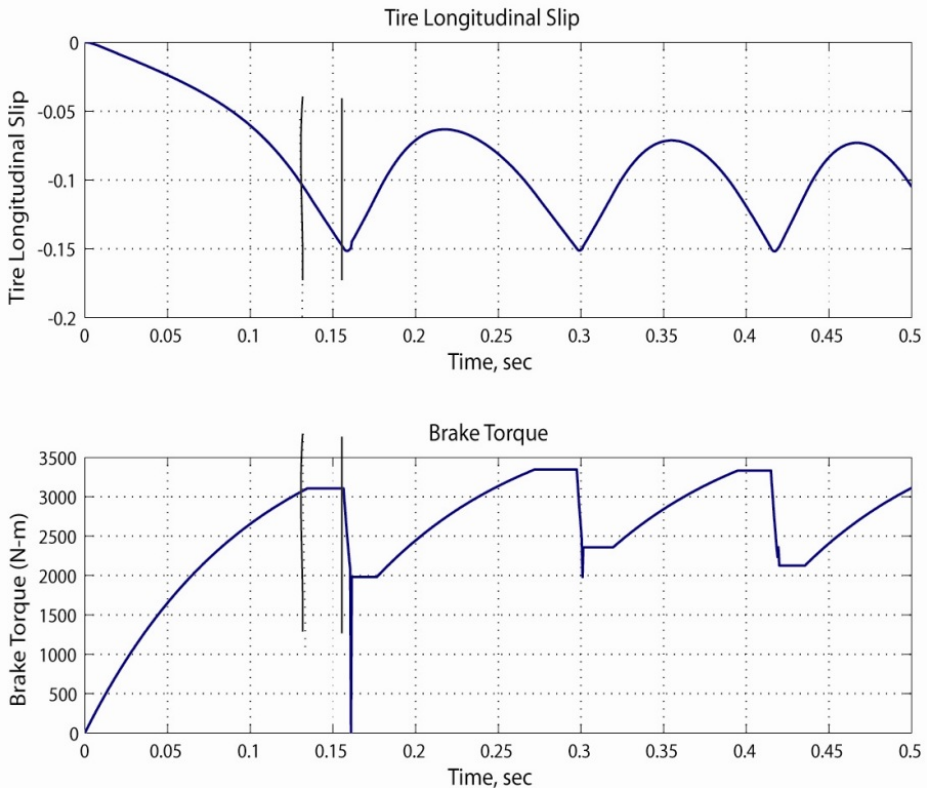


Figure 3.11: ABS operation

From Figure 3.9 it can be seen that for this analysis the range of slip ratio values to achieve maximum traction is

$$\begin{aligned} low\,slip &= 0.11 \\ high\,slip &= 0.15 \end{aligned}$$

Figure 3.11 shows the ABS in operation for a per axle commanded torque of 4200 Nm for the front axle. The vertical marker lines indicate the time at which the slip crosses the respective slip limits. Initially when the brakes are applied, the brake torque increases with a time lag equal to 0.1 sec, and the wheel slip starts increasing. As soon as the slip reaches the value of 0.11 (0.13 sec) the commanded brake torque is held constant at about 3100 Nm. This constant torque is still enough to increase slip; hence as soon as the slip reaches the value of 0.15 (around 0.15 sec) the brake torque is released to zero through a smaller time lag of 0.01 sec. Due to the decrease in brake torque the slip starts to decrease and as soon as it falls below 0.15, the brake torque is again held constant at a lower value of 2000 Nm. When the slip decreases below the *low slip* value of 0.11 the brake torque is again increased from 2000 Nm to the full commanded torque through a lag of 0.1 sec. This cycle is repeated again until the longitudinal velocity drops to some predefined minimum (5 mph in this case). Once the longitudinal speed drops to 5 mph the ABS controller is switched OFF and the brakes are allowed to lock.

### 3.4.4 Locked Wheel Dynamics

The equation for dynamics of a rotating wheel is given by

$$\dot{\omega} = \frac{1}{I_t}\left[F_x \cdot r - T_b\right] \tag{3.7}$$

where

$$
\begin{aligned}
\dot{\omega} = &\quad Angular\,Acceleration\left(\tfrac{rad}{sec^2}\right)\\
I_t = &\quad Rotational\,Inertia\,(kg\cdot m^2)\\
F_x = &\quad Longitudinal\,Force\,(N)\\
r = &\quad Rolling\,Radius\,(m)\\
T_b = &\quad Brake Torque\left(\tfrac{N}{m}\right)
\end{aligned}
$$

In Equation 3.7 for a positive $T_b$ such that $T_b$ is greater than$F_x \cdot r$, the angular acceleration in next integration step would decrease to a smaller value compared to the prior step. This represents the correct physics, but only until the wheel is locked. Numerically, the integrator used in the model would allow $\dot{\omega} < 0$ if $T_b$ is greater than $F_x \cdot r$. This is not physically possible. To curb this, when the wheels are locked ($\omega = 0$) the equations for rotational dynamics are altered. In this case, when the wheel locks, the brake torque $T_b$ is matched to the equilibrium torque $F_x \cdot r$ so that the resulting $\dot{\omega}$ remains zero.

## 3.5 TWEEL™ Nonlinear Vertical Stiffness Law

As mentioned earlier in this work, the TWEEL™ is characterized by a nonlinear stiffness. The law is given by Equation 3.8,

$$F = C \cdot \delta^N \tag{3.8}$$

Where,

$$
\begin{aligned}
F &= Force \quad (kg)\\
C &= Constant\,\left(\frac{kg}{mm^N}\right)\\
N &= Constant\,(dimensionless)\\
\delta &= Deflection\,(mm)
\end{aligned}
$$

For a given $N$ value, the value of $C$ can be calculated with a known maximum static

deflection $\delta_{max}$ and the maximum load $F_{max}$ corresponding to $\delta_{max}$. $F_{max}$ was known to be 438 kg corresponding to weight on a front wheel in the Gross Vehicle Weight configuration (GVW). This is the heaviest load the wheel would see in any static condition for the vehicle under consideration. From Equation 3.8 we have,

$$C = F_{max} \cdot \delta_{max}^{-N} \tag{3.9}$$

Then, with the value of $C$ known and the value of static loading $F$ for the given vehicle configuration (garage loads at GVW rear, C+D front, and C+D rear), we should be able to calculate the static deflection by,

$$\log(\delta_{stat}) = \frac{\log(F) - \log(C)}{N} \tag{3.10}$$

Figure 3.12 shows the implementation of this nonlinear stiffness law in Simulink. The block "Fcn" houses the nonlinear formulation. The input to block "Fcn " is the total (static + dynamic) deflection in $m$. It is converted to $mm$ and multiplied by gravitational constant $g$ to get the output force in Newtons.

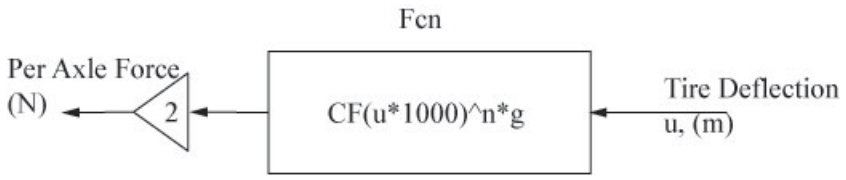


Figure 3.12: Implementation of Non-Linear Stiffness Law in Simulink

Figure 3.13 shows the nonlinear law for $\delta_{max} = 15\,mm$ and $N = 0.6$; it also shows the corresponding linear characteristics of the OE tire. Note that the horizontal solid lines on Figure 3.13 indicate the static loading conditions for the front and rear wheels. Also, note the differences in the static deflections due to different stiffness characteristics of the TWEEL™ and the OE tire. Owing to the nonlinear stiffness, the TWEEL™ has lower static deflection than the OE tire for both the front and rear loading. Table 3.1 shows the stiffness for the TWEEL™ and the OE tire at garage loads in the C+D and GVW configuration. The front TWEEL™ is "softer" compared to the OE tire while the rear TWEEL™ is about the same stiffness as the OE tire in C+D configuration. In GVW configuration both the front and rear TWEELs™ are relatively "softer" than the OE tire and the TWEEL™ in C+D configuration.

In [33], Paradiso discusses the ride comfort of the vehicle under consideration for a range of static deflections. In his conclusion, he states that the case for a TWEEL™ with $\delta_{max}$= 15 mm, N = 0.6, while yielding a less comfortable overall ride than other TWEEL™ cases examined, keeps the low frequency acceleration response closer to that found with the OE tire, and has a lower value of the ISO RMS weighted acceleration than the car with OE tires. It also has better grip than the OE tire-equipped car with potentially better handling and braking. Also, it was known that Michelin is aiming towards a maximum static deflection of 15 mm. Hence, this case was considered to be a good starting point for

this work.

| | Garage Load (N) | TWEEL™ ($\delta_{max} = 15\,mm$, $N = 0.6$) Stiffness $\left(\frac{N}{m}\right)$ | OE Tire Stiffness $\left(\frac{N}{m}\right)$ |
|---|---|---|---|
| Curb+Driver (Front) | 3894.6 | 183.51 $e3$ | 232.02 $e3$ |
| Curb+Driver (Rear) | 2599.7 | 240.26 $e3$ | 232.02 $e3$ |
| GVW (Front) | 4296.8 | 171.87 $e3$ | 232.02 $e3$ |
| GVW (Rear) | 3374.6 | 201.9 $e3$ | 232.02 $e3$ |

Table 3.1: TWEEL™ and Tire Stiffness (Garage Loads)

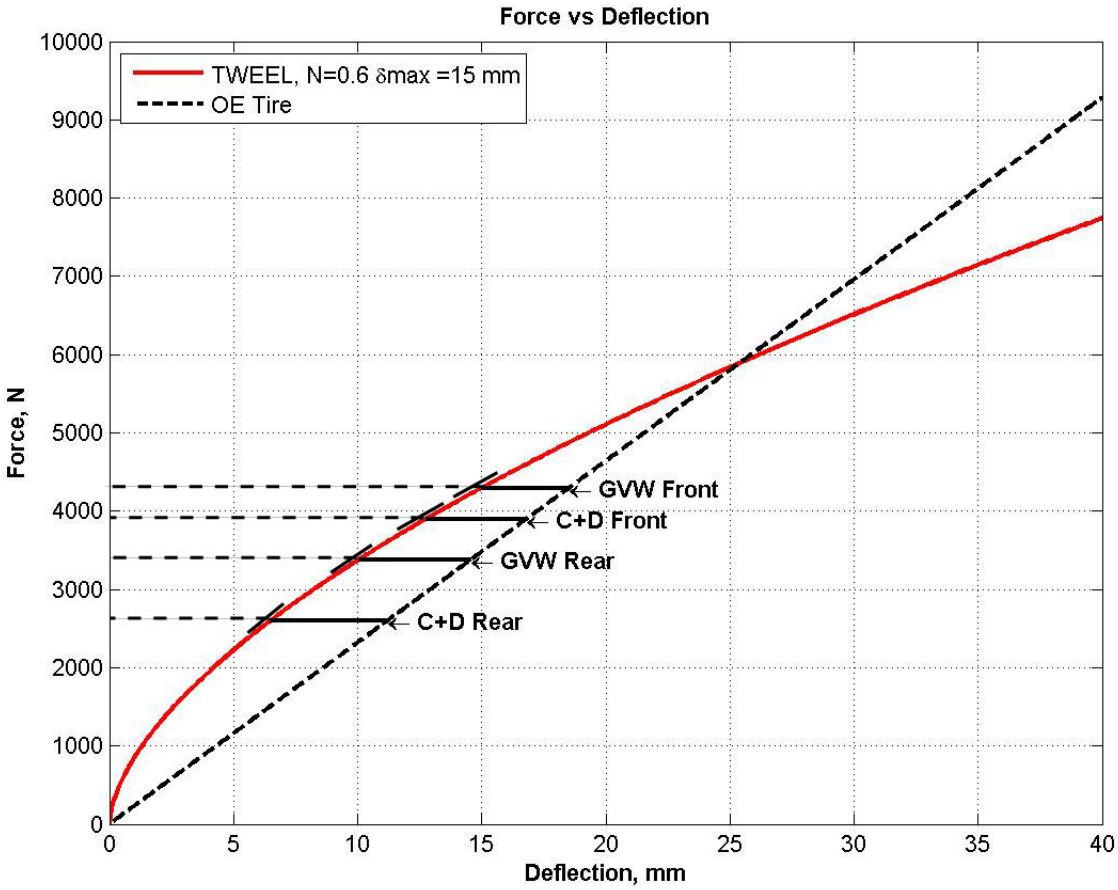


Figure 3.13: TWEEL™ Non-Linear Stiffness: Force (N) vs. $\delta(mm)$

## 3.6 Tire Model

Tire modeling has been a topic of interest amongst researchers for a long time. The complexity of tire design coupled with its highly nonlinear response to dynamic inputs makes tire modeling for simulations a very difficult job. Literature on tire modeling has both analytical and empirical approaches to the problem.

The analytical model in [30] uses mechanical analogs to describe longitudinal and lateral deflections for tread and sidewall. Longitudinal deflections are determined using a simple elastic spring model and lateral deflections are calculated using elastic beam formulations. Source code was developed to include the model in a commercially available software called Dynamic Analysis Design System (DADS). The authors conclude that the model is computationally efficient and only requires a few easily obtainable parameters. Salaani [29] discusses the development and validation of an analytical tire model. His theoretical model uses standard mechanical properties that characterize the force generating capacity of tires. Some of these properties are lateral and longitudinal stiffness, aligning moment, pneumatic trail, overturning moment arm, lateral force relaxation length, and friction properties. He validated the analytical model by comparing the results to experimental data for four different tires. Miyashitaa, Kawazuraa, and Kab [28] extended the so-called Fiala–Sakai model meant for use in braking studies. This was done using a generalized skewed parabola to express contact pressure profile in circumferential direction which is otherwise approximated by a quadratic parabola function.

Perhaps the most widely used model for tire simulation is the "Pacejka Magic Formula". The magic formula is an empirical formulation of measured data for longitudinal force, lateral force, and aligning moment. Each tire is characterized by a set of coefficients, the number of which varies and depends on the particular output parameter, viz. longitudinal force, lateral force and aligning moment. The equations developed are then used to calculate the force or moment depending on the inputs of vertical load, slip and camber angle. The "Magic Formula" is used in majority of vehicle dynamics simulations, owing to its

reasonable accuracy, ease of programming, faster computation, and lower CPU utilization. This work therefore utilizes the magic formula presented in [31] for longitudinal force. The formula is given by:

$$F_x = D\sin(C\tan^{-1}(B\phi)) \tag{3.11}$$

Where

$$\begin{aligned}
\phi &= (1-E)\kappa + \left(\frac{E}{B}\right)\tan^{-1}(B\kappa) \\
D &= a_1 F_z^2 + a_2 F_z \\
C &= 1.65 \\
B &= \frac{a_3 F_z^2 + a_4 F_z}{CDe^{a_5 F_z}} \\
E &= a_6 F_z^2 + a_7 F_z + a_8 \\
\kappa &= Slip\,Ratio\,in\,\% \\
F_z &= Vertical\,Load\,in\,kN
\end{aligned}$$

No test data were available for longitudinal force data. The data used for this study were estimated based on characteristics available in the literature and experience. Empirically, it was known that the peak longitudinal force is generated at about 10% slip ratio and that for full lock (i.e., sliding $\mu$) conditions, the magnitude of longitudinal force is approximately 70% of the peak [37]. This is true over the range of vertical loads. The coefficients for the "Magic Formula" were then tuned to get this desired longitudinal force vs. slip ratio curve. They are as shown in Table 3.2.

| $a_1$ | $a_2$ | $a_3$ | $a_4$ | $a_5$ | $a_6$ | $a_7$ | $a_8$ |
|---|---|---|---|---|---|---|---|
| -21.3 | 1009 | 49.6 | 226 | 0.069 | -0.001 | 0.056 | 0.486 |

Table 3.2: Longitudinal Force Coefficients

Figures 3.8 and 3.9 show the corresponding longitudinal force curves and the $\mu - slip$ curve:

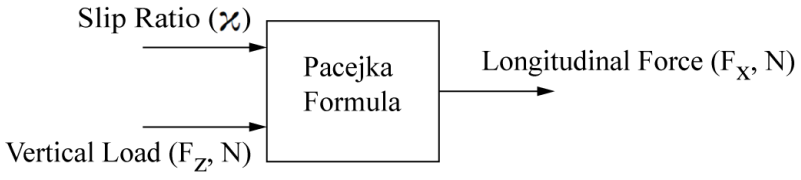


Figure 3.14: Tire Model Implementation

Since the tire model requires wheel slip ratio and vertical load to generate the longitudinal force, calculation of the tire-to-road normal force is imperative. Figure 3.15 shows the vertical dynamic model of the front tire and the corresponding free body diagram.

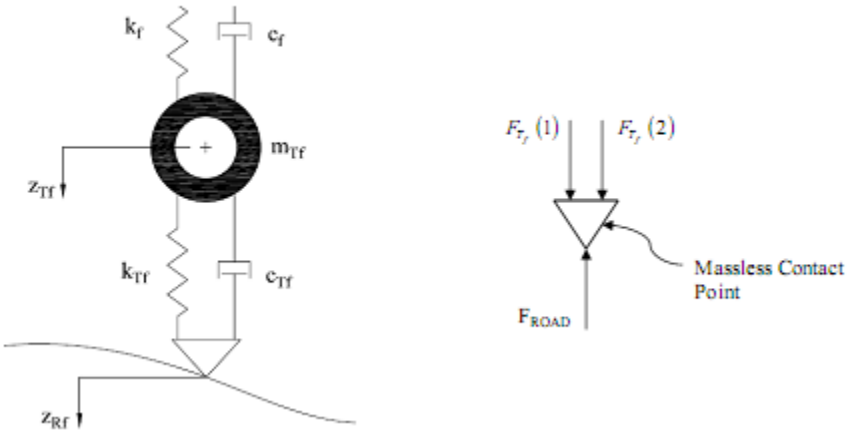


Figure 3.15: tire-to-road Interface: Model and Free Body Diagram

As can be seen, the two components that contribute to the dynamic tire-to-road force are the tire spring and damper. The damper force is given by

$$F_{Tf}(2) = c_{tf}(\dot{z_{tf}} - \dot{z_{rf}}) \tag{3.12}$$

where

$$
\begin{aligned}
c_{tf} &= Tire\,Damping\left(\frac{N}{\frac{m}{s}}\right) \\
\dot{z_{tf}} &= Wheel\,Center\,Vertical\,Velocity\left(\frac{m}{s}\right) \\
\dot{z_{rf}} &= Road\,Input\,Velocity\left(\frac{m}{s}\right)
\end{aligned}
$$

The spring force is governed by the nonlinear stiffness law and is given by,

$$F_{Tf}(1) = C(\delta_{stat} + z_{tf} - z_{rf})^N \cdot g \tag{3.13}$$

The total force is given by,

$$F_z = F_{Tf}(1) + F_{Tf}(2) \tag{3.14}$$

### 3.6.1 Wheel Lift-off

Wheel lift-off is the condition when contact between the tire and road is lost. When this contact is lost, the only vertical force acting on the wheel/tire is the static weight. When the wheel is lifted off the ground the tire cannot generate any longitudinal/retarding forces and hence would not contribute to braking. Wheel lift-off is handled as a special case within this simulation model.

Under static loading, the tire or TWEEL™ is compressed by $\delta_s$. When the tire unloads, it will rebound an equivalent amount before losing contact with the ground. To model wheel lift-off, the equations are modified as soon as the tire rebounds back by $\delta_s$, this is done by reducing the forces through the tire spring and damper to zero. Thus, mathematically,

$$c_t, k_t = \begin{cases} c_t, k_t & \delta \leq \delta_s \\ 0 & \delta > \delta_s \end{cases} \tag{3.15}$$

where,

$$\begin{aligned} c_t = &\quad Tire\,Damping\left(\frac{N}{\frac{m}{s}}\right) \\ k_t = &\quad Tire\,Stiffness\,(\frac{N}{m}) \end{aligned} \tag{3.16}$$

## 3.7 Generation of Random Rough Road Profile

To simulate the vehicle during braking, it was imperative to model the vertical irregularities of the road. During braking the longitudinal velocity of the vehicle decreases with time. Hence, the road profile was included as a function of longitudinal (x) coordinate of the road. The road profile chosen was the weathered asphalt section of the track at the Laurens Proving Ground (WA-LPG). Additionally, other "rougher" road profiles were also required. This section discusses the algorithm for the generation of random road profiles used for these studies. It also details the steps taken by Paradiso [15] to generate a road profile similar to the weathered asphalt road at LPG (WA-LPG) which is used in this work.

Wong [32] states that when a surface is regarded as randomly irregular, it can be represented by a power spectral density function (PSD) as in Equation 3.17.

$$S(\Omega) = C_{sp} \cdot \Omega^{-N} \quad \left(\frac{m^2}{\frac{cycle}{m}}\right) \tag{3.17}$$

Where

$$\begin{aligned} \Omega &= Spatial\,Frequency\,\left(\frac{cycle}{m}\right) \\ C_{sp}, N &= Constants \end{aligned}$$

Since this work is done in the temporal domain, Equation 3.17 must be converted to a function of frequency in $Hz$ or $\frac{rad}{sec}$. This is achieved using the relationships between spatial wavelength ($\Omega$) and the vehicle speed ($\nu$) which are given by Equations 3.18 and 3.19 below,

$$f\left(\frac{cycle}{sec}\right) = \Omega\left(\frac{cycle}{m}\right)\cdot v\left(\frac{m}{sec}\right) \tag{3.18}$$

$$\omega\left(\frac{rad}{sec}\right) = 2\pi\cdot\Omega\left(\frac{rad}{m}\right)\cdot v\left(\frac{m}{sec}\right) \tag{3.19}$$

The PSD in the temporal domain is then expressed as

$$S(\omega) = \frac{(2\pi\cdot\nu)^{N-1}C_{sp}}{\omega^N} \quad \left(\frac{m^2}{\frac{rad}{sec}}\right) \tag{3.20}$$

In order to create a road profile , the program "Braking_Road_PSD.m" was written in Matlab. The input to this program are the $C_{sp}$ and $N$ coefficients and the velocity $v$ of the vehicle. The program is based on the program "road_psd_mp6.m" written by M. Paradiso for his study[15]. The original author of this code is D. Moline. The code also uses the Simulink model file "road_test.mdl" to create the desired road.

The development of road profiles for roads other than WA-LPG was relatively straightforward since no validation with test data was involved. The $C_{sp}$ and $N$ coefficients used for generating respective road profiles are listed in Table 3.3. A detailed description on the choice of the coefficients is included in section 4.3.2.

| Description | $N$ | $C_{sp}$ |
|---|---|---|
| Road 1 | 2.6 | $1.079\times10^{-7}$ |
| Road 2 | 2.1 | $5.5\times10^{-7}$ |
| Gravel Highway | 2.1 | $4.4\times10^{-6}$ |
| Smooth Highway | 2.1 | $4.8\times10^{-7}$ |

Table 3.3: List of Coefficients for Road Profile Generation [32]

Figure 3.16 and the following text gives an explanation of the procedure of creating the road profile when the $C_{sp}$ and $N$ coefficients are known. There are two major steps,

1. Generate the road profile for user defined $C_{sp}$ and $N$ values. To achieve this, files "road_test.mdl" and "Braking_road_test.m" are used.

   (a) A linear vector of frequencies in Hz (*freq*) that the road should contain (0.5-50 Hz) is created.

   (b) The road amplitude properties are set by multiplying each frequency by an amplitude, A, and raising it to a power, Q,

   $$amp = A \cdot freq^{Q} \tag{3.21}$$

   (c) The value of A corresponds to the resulting value of $C_{sp}$ and Q corresponds to resulting value of N for the PSD of created roadway.

   (d) Multiple sinusoidal waves are then created with a sine wave generator in Simulink. The output is,

   $$O_j(t) = AMP_j \cdot \sin(FREQ_j \cdot t + phase) \tag{3.22}$$

   $$\begin{aligned} j &= length\,of\ freq\,vector \\ AMP &= \frac{amp}{\frac{freq}{\frac{2}{\pi}}} \\ FREQ &= Frequency\,vector\ freq\,in\ \frac{rad}{sec} \\ phase &= Pseudo\,random\,vector\,with\,same\,length\,as\,the\,frequency\,vector, \\ &\quad drawn\,from\,a\,normal\,distribution\,with\,zero\,mean\,and\,standard \\ &\quad deviation\,of\,one. \end{aligned}$$

   (e) Then, at each time step, the current values of the sine waves in the vector are added together to get the random road profile.

2. Tune the road profile,

(a) Once the road profile for the given values of Q and A is created, the PSD of this resulting roadway is calculated.

(b) A power curve is fit to this PSD and the slope of the line in logarithmic domain is compared to desired value of N. The value of Q (Equation 3.21) is adjusted until the slope is within 1 percent of the desired value of N.

(c) Once the value of Q has been set, the area under the desired PSD (calculated for the same frequency range as in *freq* vector) is compared to the area under the line fitted to the PSD of the created roadway. The value of A (Equation 3.21) is then adjusted until the difference in areas is within 0.1 percent.

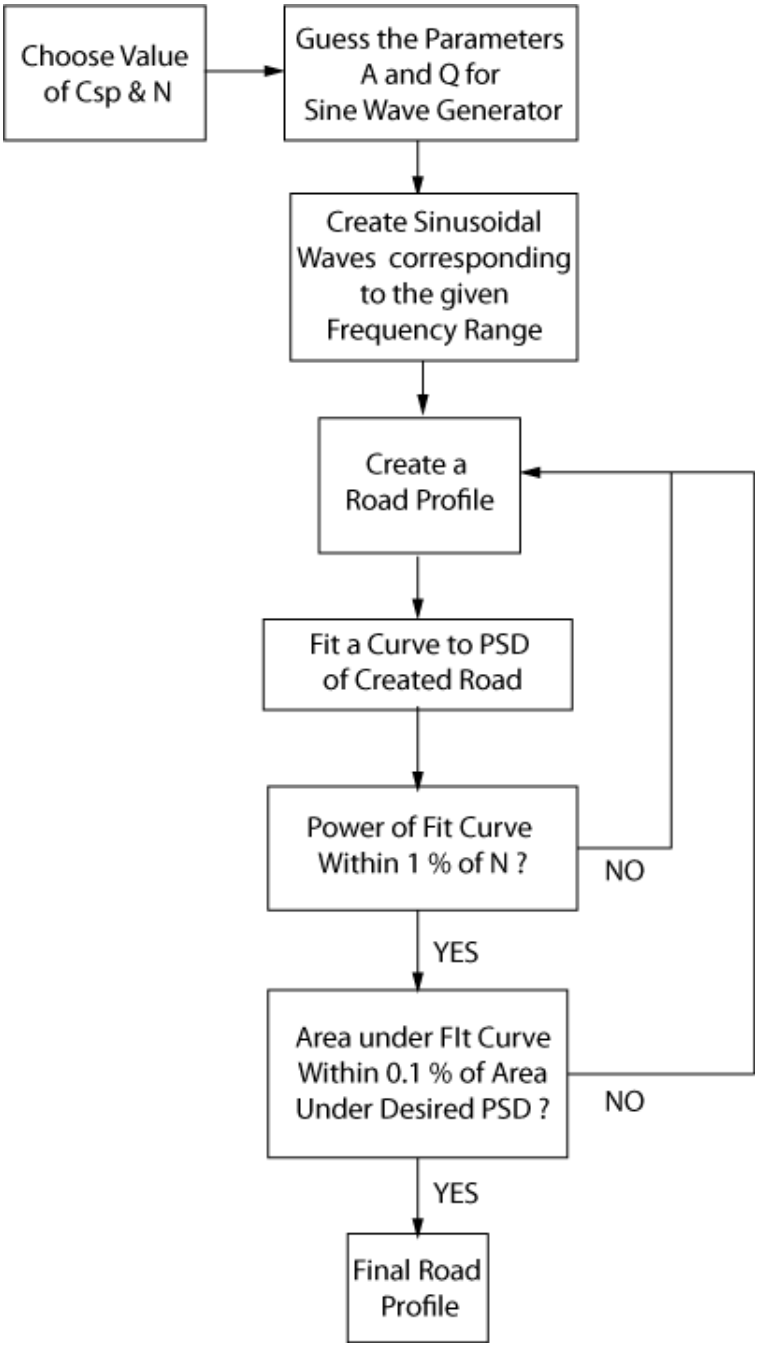


Figure 3.16: Road Profile Generation

To create a road profile similar to the WA-LPG road requires a few additional steps. The following text explains the procedure to create the road profile similar to the WA-LPG road (Paradiso [15]),

1. Various roadways were created using a set of $C_{sp}$ and $N$ coefficients. The ride model was used to simulate the five DOF car model running on these created roadways.

2. Then the value of the ISO RMS vertical acceleration was calculated for each created road profile. This was compared to the test data.

3. Paradiso [15] calculated the ISO RMS accelerations for both 30 mph and 60 mph runs and then plotted the observed differences.

4. From his exercise, Paradiso found out that for 30 mph runs $C_{sp} = 3.0e-8$ and *N=2.2* provided the closest match to the WA-LPG test data, while for the 60 mph runs the corresponding values were $C_{sp} = 2.0e-8$ and *N=2.4*. Table 3.4 summarizes the findings. Figure 3.17 shows the corresponding plots.

| | $C_{sp}$ | $N$ | Desired RMS Acceleration ($\frac{m}{s^2}$) | Calculated RMS Acceleration ($\frac{m}{s^2}$ ) |
|---|---|---|---|---|
| 30 mph Simulation | 3 e-8 | 2.2 | 0.1638 | 0.16451 |
| 60 mph Simulation | 2 e-8 | 2.4 | 0.206 | 0.20472 |

Table 3.4: Road Profile Match, [15]

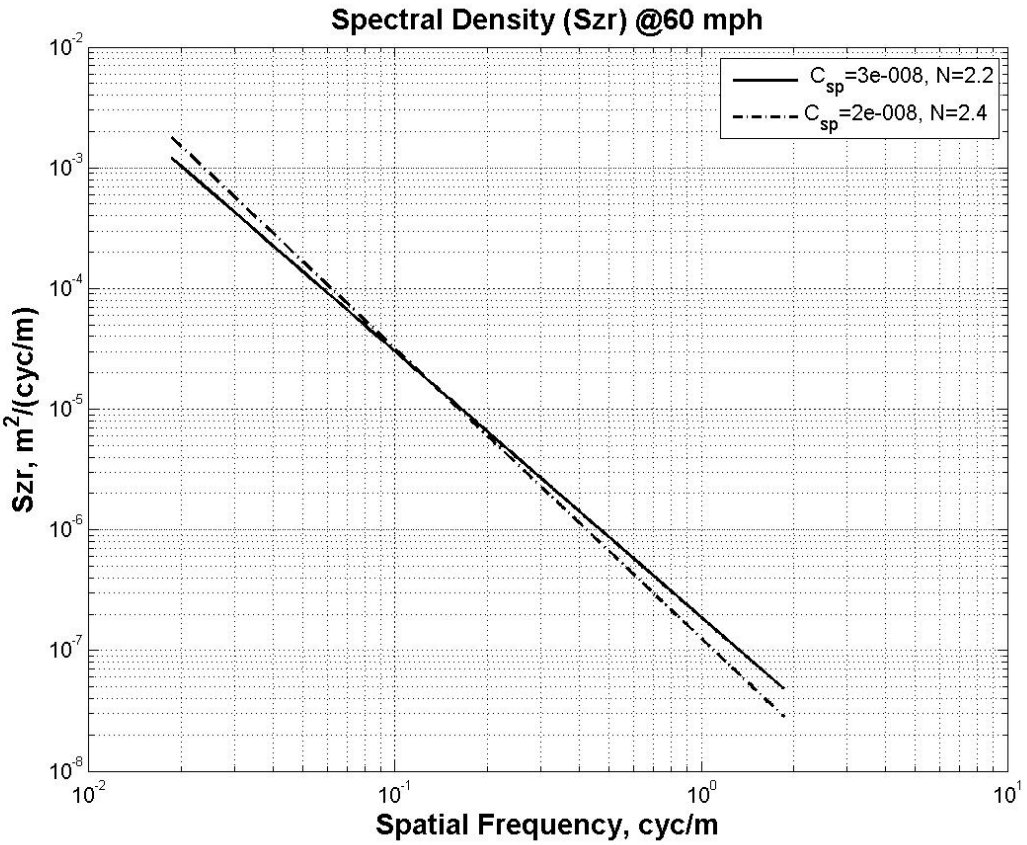


Figure 3.17: Spatial PSDs

Paradiso chose $C_{sp} = 2.5e^{-8}$ and $N = 2.3$ for his study because it yielded best compromise between the 30 mph and 60 mph simulations. This work utilizes the same coefficients to create the profile for the WA-LPG road. For the Simulink model, road input is included as a table of road profile versus longitudinal distance along the road. The block obtains the longitudinal position of the vehicle from solving the equations of motion and then outputs the ground vertical inputs under each wheel.

## 3.8 Summary and Overview of the Matlab/Simulink Model

This section discussed the modeling of the vehicle, its components and the realization of the equations of motion in the Matlab/Simulink environment. A representative block diagram for the very first level is shown in Figure 3.18. Each of the seven subsystems contain an assembly of blocks to realize the equations of motion which are derived in Appendix A. Additionally, there is a block for the brake model and the tire model. This model is solved using a variable step solver "ode45 (Dormand-Prince)". The variable step solver in Simulink is advantageous in the fact that it takes bigger time steps when it detects slower change in states. This saves computation time without compromising accuracy. Also, the maximum time step allowed is limited to 0.005 sec which is equivalent to 200 Hz. This is orders of magnitude greater than the system natural frequencies known from [15]. This means that the time step is small enough not to compromise accuracy of results.

The Simulink model is run within a Matlab code which initializes the workspace for the simulation. The code is used to select vehicle configuration, the initial speed, the road type, and the shock absorber type. It also initializes the parameters for the brake system, tire model, and ABS operation. The ABS can be turned ON or OFF using the code. Finally, the post processing and data plotting features of Matlab are used to display the results.

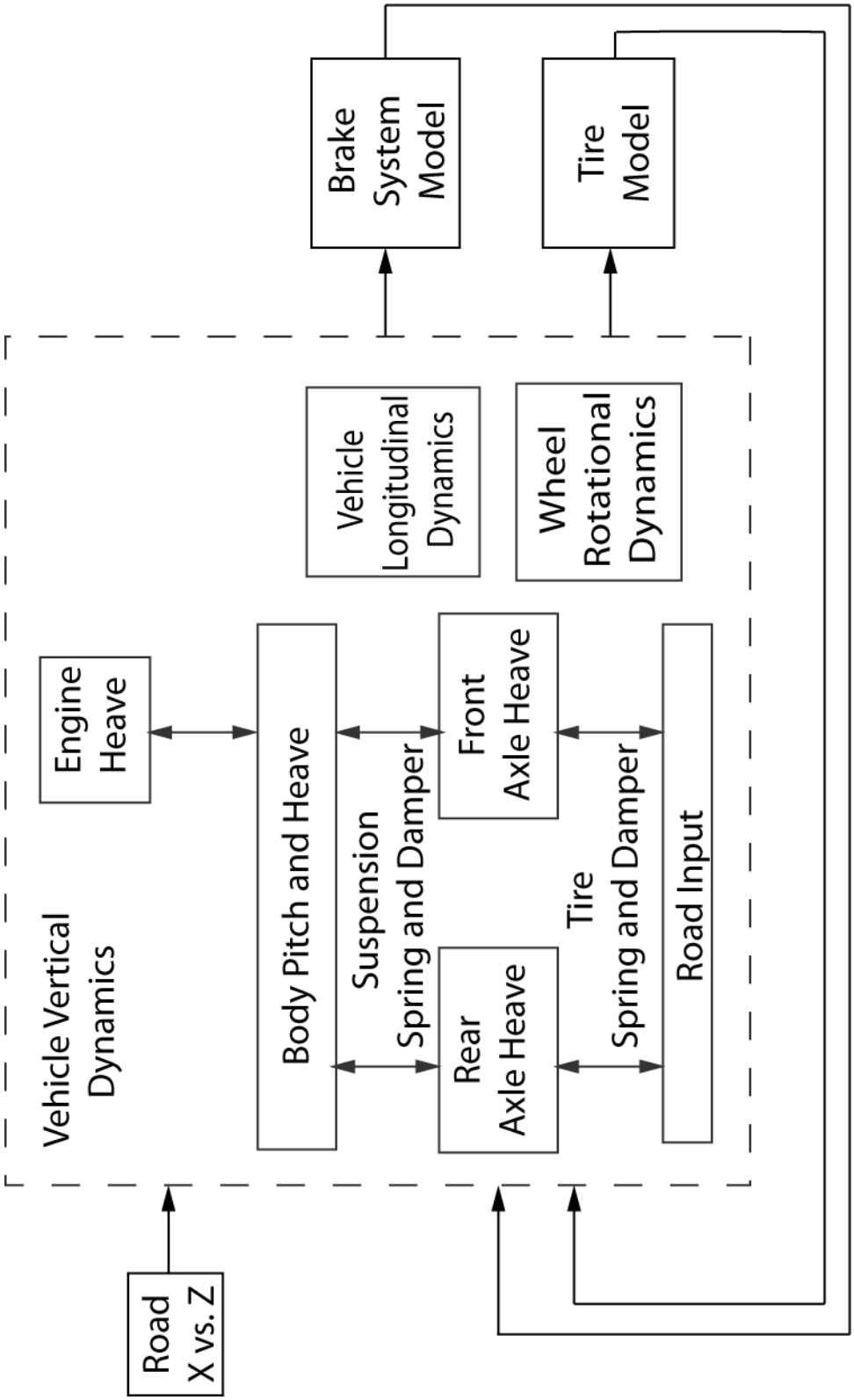


Figure 3.18: Simulink Block Diagram

# Chapter 4

# Results

## 4.1 Introduction

Chapter 3 discussed the modeling of the vehicle, brake system, tire, and the ABS. First, multiple TWEELs™ with different vertical stiffness characteristics were formulated and then simulated in conjunction with the vehicle model. Simulations of straight line braking tests from 60 mph for the vehicle in C+D configuration were run for different sensitivity studies and the stopping distance was recorded. Note that all the studies use the MKS system of units, but some data is post processed to show the results in different units for the sake of familiarity. For example, the stopping distance was calculated in meters but is shown in feet. This chapter discusses the results from these sensitivity studies. It also discusses the validation of the vehicle model. The Simulink block diagrams and the Matlab code used for this part of study can be found in Appendices C and D.

## 4.2 Model Validation

Recall that the vehicle model used in this thesis is an extension of the ride model (vertical dynamics) by Paradiso [15]. He validated the Simulink model with test data from four post tests and weathered asphalt runs. His study stated that the simulation results had the same trend as the test data. However, he had to tune some parameters (viz, engine

mass, engine mount stiffness, and rear shock damping) to get a good match. A rationale for tuning the model was provided as either unavailability of relevant data and/or that some of the available data were incorrect.

Validation of the complete model (including both vertical and longitudinal dynamics) was a difficult task, since no physical tests were performed to evaluate braking performance. In addition, test data for tire longitudinal force were not available.

A detailed model for the 2007 BMW Mini in C+D configuration was already developed in CarSim using the kinematics and compliance data from [18] provided by Michelin. CarSim is a proprietary vehicle dynamics simulation module developed and marketed by Mechanical Simulation Inc. It uses inbuilt data libraries and set of equations of motion for a vehicle model. The overall model is composed of user configurable individual systems such as the steering, brakes, suspension kinematics and compliance, tire data, inertial parameters etc. for a given car and are input using the graphic user interface (GUI). Specific roads and tracks can also be set up. Choices for numerical integration methods, sample time, and output data processing/plotting are available on the so-called "Home Screen".

The vehicle model for the Mini developed in the handling report [34] was validated by data from random steer and understeer tests carried out at Michelin's Lauren's Proving Ground (LPG). It was hence plausible that the longitudinal and vertical dynamics of the Simulink model can be compared for accuracy to this relatively detailed model in CarSim. A hard braking test was simulated both in CarSim and in Simulink for the same car and similar test conditions and input parameters. The results for braking without ABS on a perfectly flat road are shown in Figure 4.1 and 4.2. The two models were found to be in good agreement with each other.

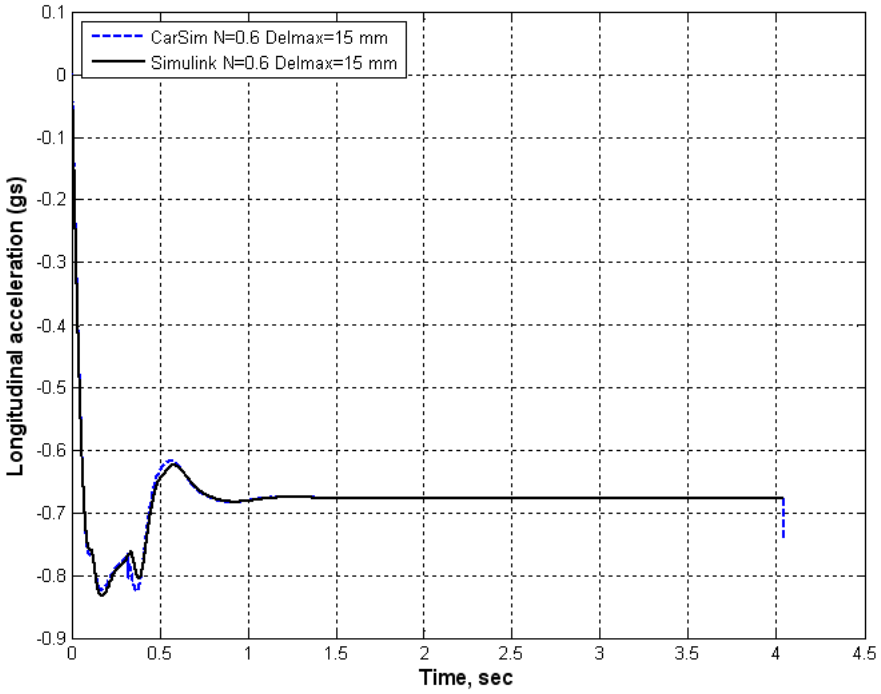


(a) Longitudinal Acceleration of C.G. (CarSim vs. Simulink)

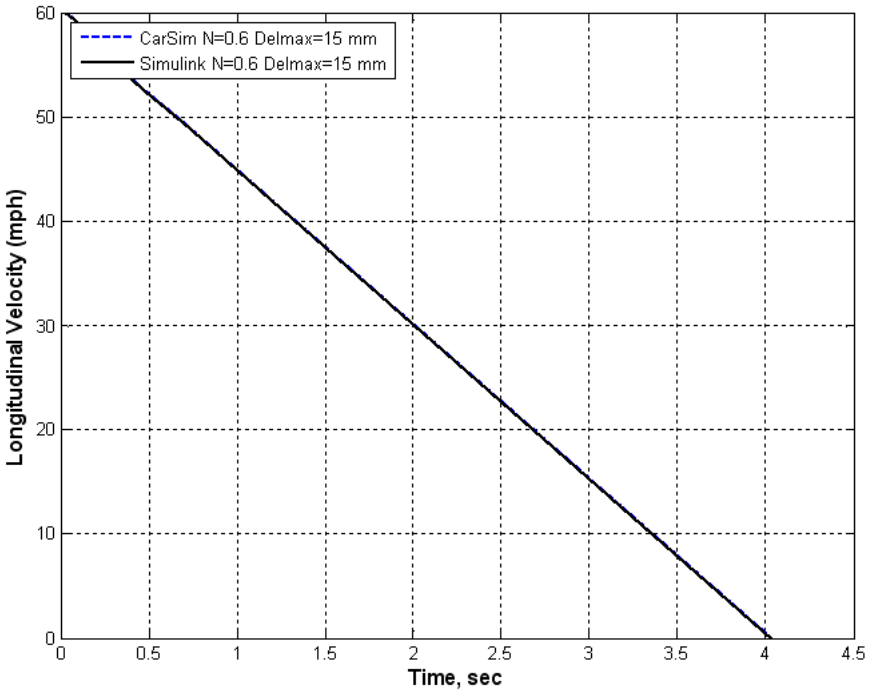


(b) Longitudinal Velocity of C.G. (CarSim vs. Simulink)

Figure 4.1: Model Validation

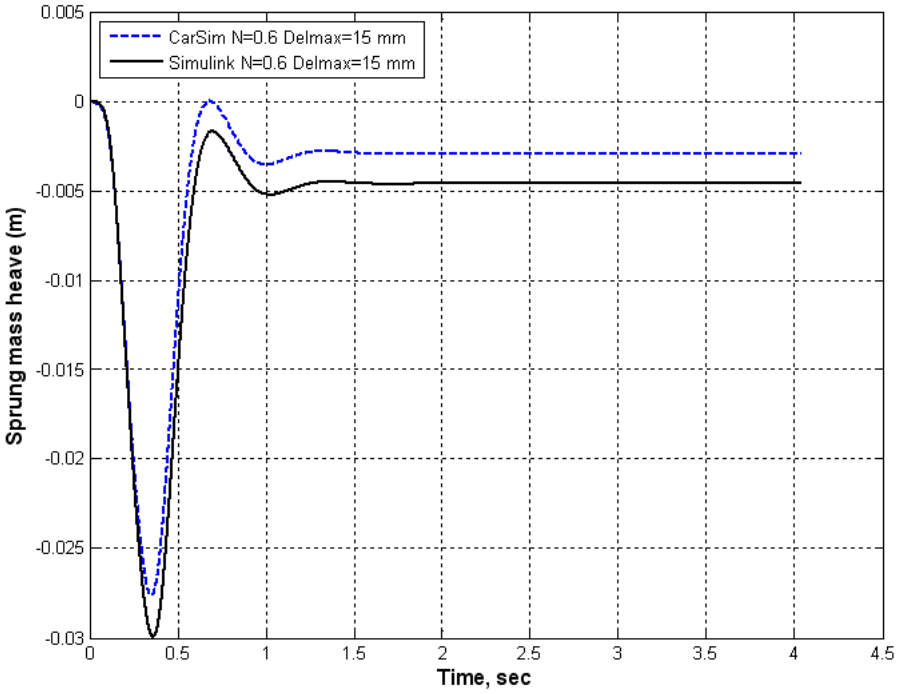


(a) Sprung Mass Heave (CarSim vs. Simulink)

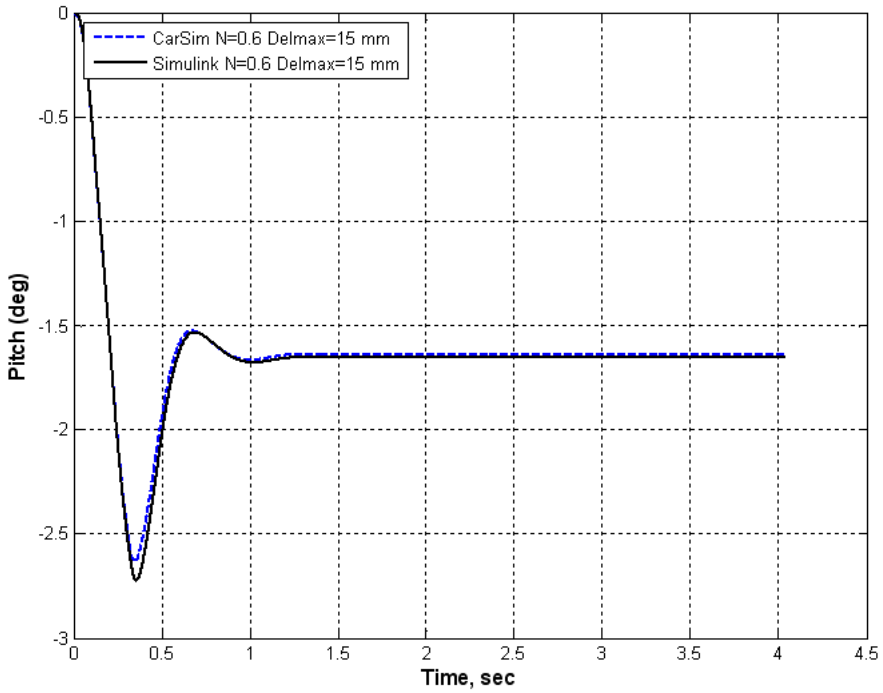


(b) Sprung Mass Pitch Angle (CarSim vs. Simulink)

Figure 4.2: Model Validation

## 4.3 Sensitivity Studies

Sensitivity studies are a good means to isolate the effects of a single parameter on a given test/simulation. A sensitivity study was conducted to evaluate the effect of TWEEL™ parameters on stopping distance on a randomly rough road similar to the WA-LPG road. Other studies involved changing road roughness and shock damping to check for improvements in stopping distance with different hypothetical TWEELs™. Each study involved simulation of a hard braking test from 60 mph to a complete stop. The vehicle model was at steady state condition at the beginning of simulation. Full brake torque was applied as a step input at $t = 0\,sec.$ Stopping distance was recorded and reported as a performance metric. All the studies are detailed below.

### 4.3.1 Sensitivity to TWEEL™ parameter selection

The central theme of this thesis was to evaluate the effects of the nonlinear formulation of tire stiffness on braking performance. Section 3.5 formulates this nonlinear stiffness and its implementation in the Simulink model. The parameters $N$ and $\delta_{max}$ control the stiffness of the TWEEL™; larger $\delta_{max}$ and smaller $N$ values signify a "softer" TWEEL™. Thus, the tire-to-road force which depends on tire stiffness would also depend on the parameters selected for the TWEEL™. This was one of the conclusions in [15] by Paradiso. He also mentioned possible gains in braking performance and ride comfort with the choice of a appropriate TWEEL™. Figure 4.3 shows the variation of the simulated RMS tire-to-road vertical force on the WA-LPG road. These values were obtained from the ride model simulated on the WA-LPG road. Clearly, "softer" TWEELs™ have lower magnitude of dynamic forces and hence are expected to perform better under braking.

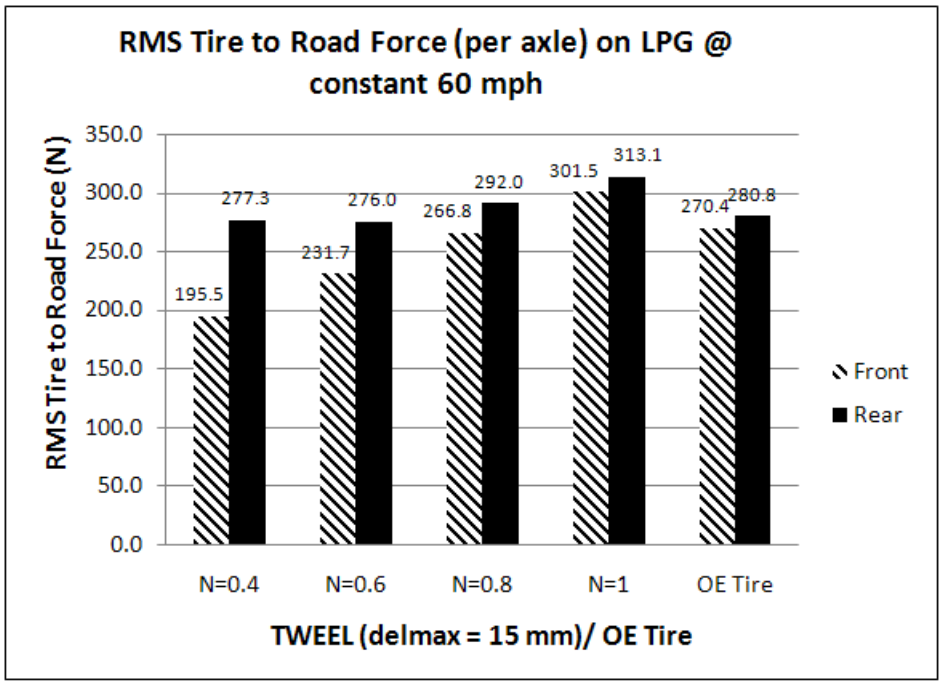


Figure 4.3: RMS tire-to-road Force (C+D Configuration, Constant 60 mph)

Based on the recommendations by Paradiso [15] and Michelin [35], four different TWEELs™ corresponding to a static deflection $\delta_{max} = 15\,mm$ and $N = 0.4$ through $N = 1$ were set up in Matlab/Simulink environment and simulated in conjunction with the vehicle model. The road profile used was similar to that of the WA-LPG road. The methodology used for obtaining the road profile is discussed in Section 3.7. The vehicle parameters used are presented in Tables B.1 through B.4. The results of the simulation are tabulated below,

| TWEEL™ / OE Tire | Stopping Distance from 60 mph |
|---|---|
| $\delta_{max} = 15\,mm,\ N = 0.4$ | 136 $ft$ |
| $\delta_{max} = 15\,mm,\ N = 0.6$ | 136 $ft$ |
| $\delta_{max} = 15\,mm,\ N = 0.8$ | 136 $ft$ |
| $\delta_{max} = 15\,mm,\ N = 1$ | 136 $ft$ |
| $OE Tire$ | 136 $ft$ |

Table 4.1: Stopping Distance on Simulated WA-LPG road (C+D Configuration)

Table 4.1 shows that stopping distance was insensitive to the selection of TWEEL™ parameters. In theory, stopping distance is a function of the braking force, which in turn depends on the adhesion coefficient $\mu$ and the vertical load $F_z$ . Since the simulation assumes that the adhesion coefficient is constant, braking force depends on the vertical load.

Referring back to Figure 4.3, note that between the OE Tire and the relatively "softer" TWEELs™, the latter had smaller dynamic RMS tire-to-road forces and hence were expected to have better grip. For the developed model, at a given instant in time during braking, the vertical load on a wheel depends on the weight shift due to deceleration and the dynamic tire-to-road force due to road profile.

| | Front Wheel | Rear Wheel |
|---|---|---|
| Static/Garage Vertical Load (N) | 3894.6 | 2599.7 |

Table 4.2: Garage Loads (per wheel) in C+D Configuration

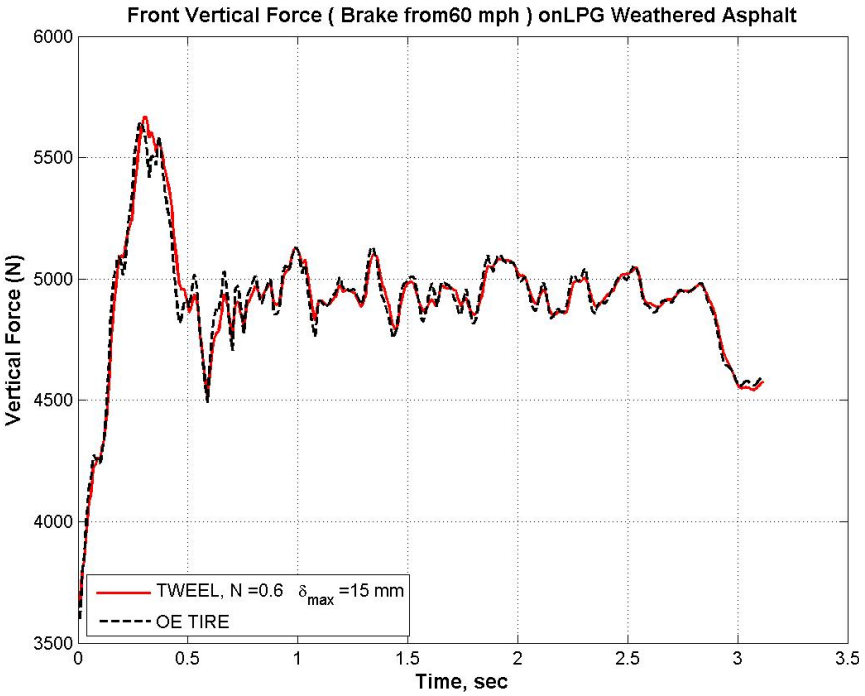


(a) Front Tire Vertical Load (per wheel)

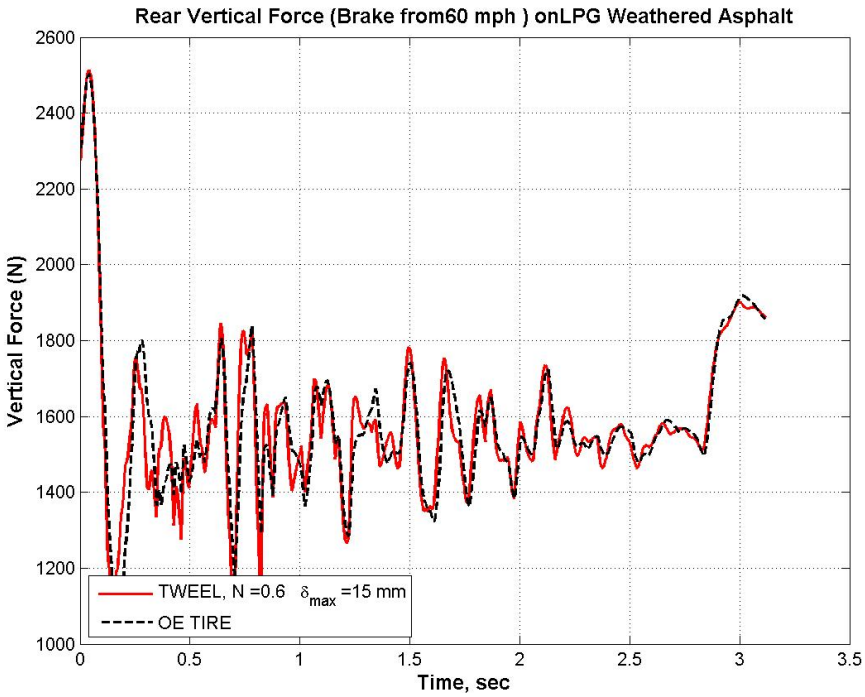


(b) Rear Tire Vertical Load (per wheel)

Figure 4.4: Vertical Force Response on the WA-LPG road (Simulation Results, C+D Configuration)

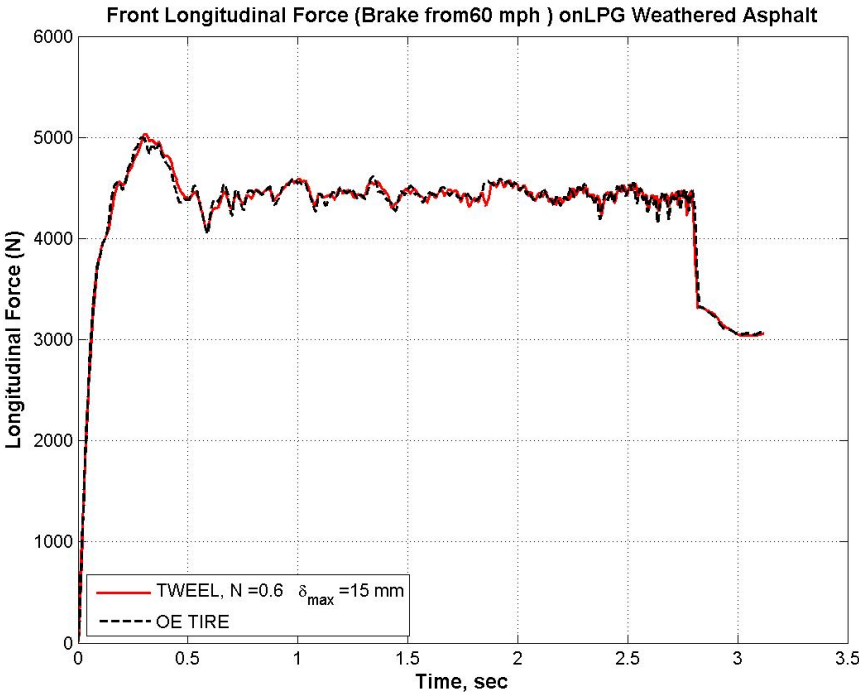


(a) Front Tire Longitudinal Force (per wheel)

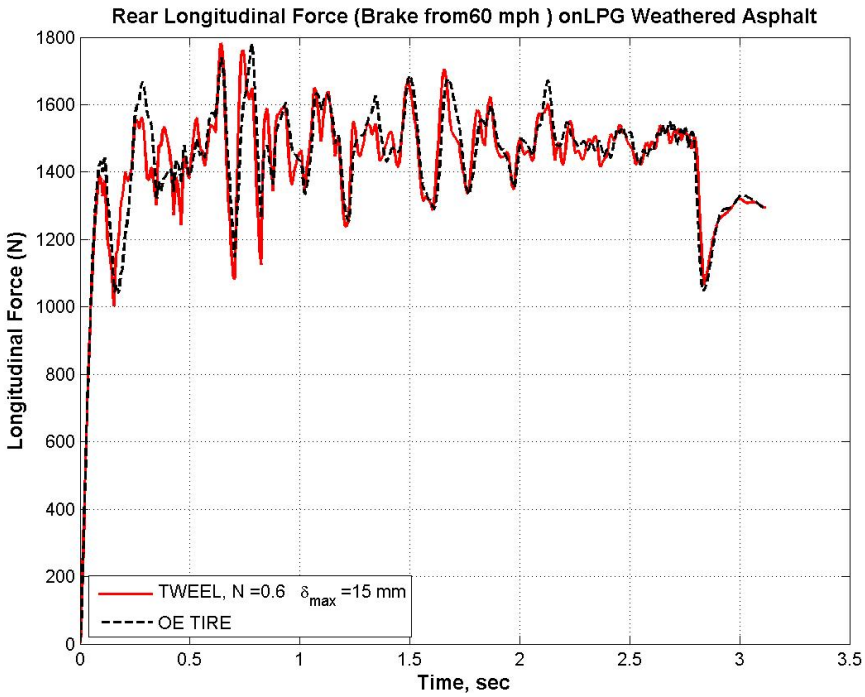


(b) Rear Tire Longitudinal Force (per wheel)

Figure 4.5: Longitudinal Force Response on the WA-LPG road (Simulation Results, C+D Configuration)

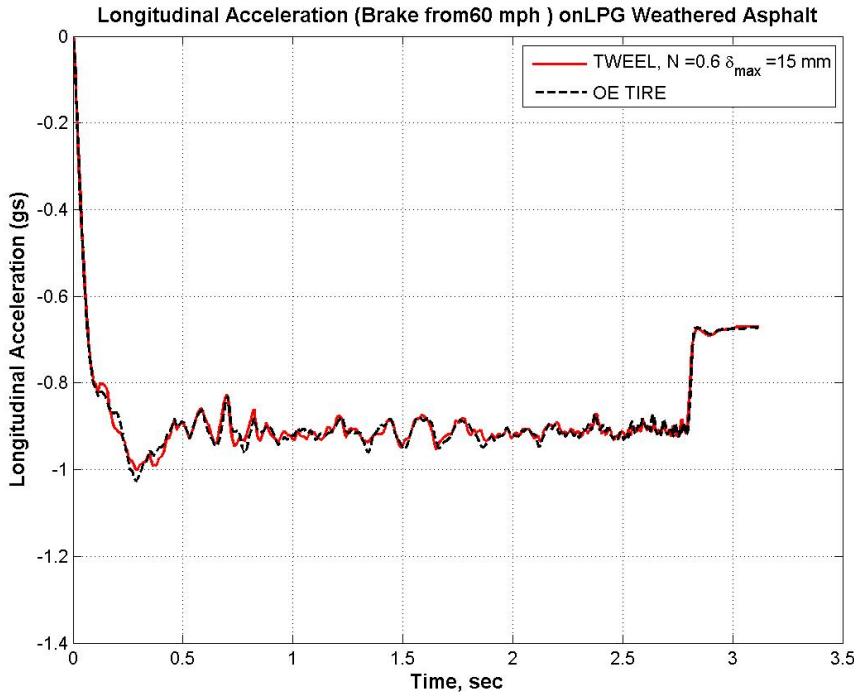


(a) Longitudinal Acceleration

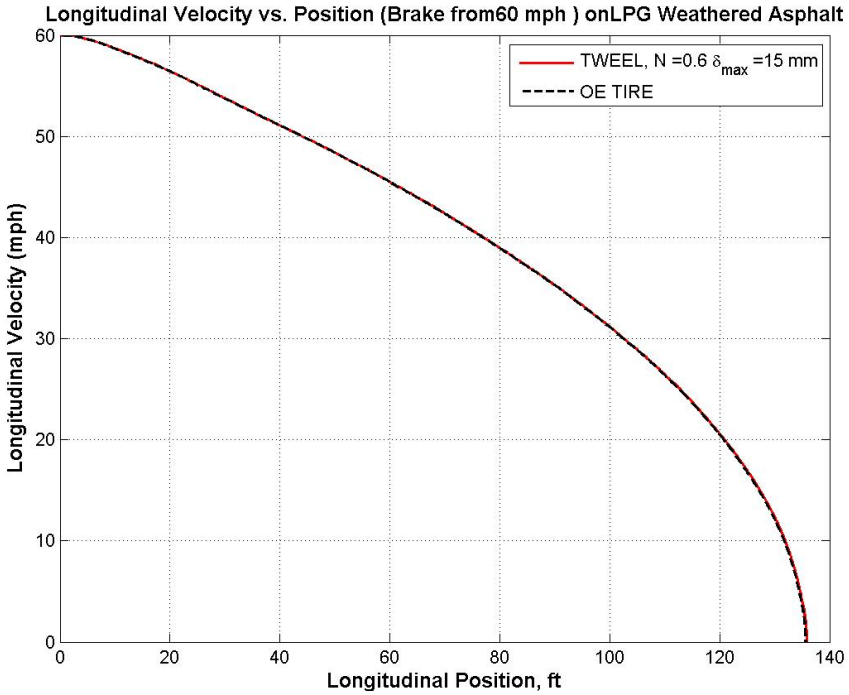


(b) Longitudinal Velocity vs. Position

Figure 4.6: Response on the WA-LPG road (Simulation Results, C+D Configuration)

Figures 4.4 and 4.5 show the vertical and longitudinal force (per wheel) history on the WA-LPG road. Notice the increase in front wheel vertical force and the corresponding decrease at the rear. This can be attributed to the weight shift from back to front axle. Although the majority of the change in vertical load is from weight shift due to the deceleration, it may be seen that the road roughness also contributes to the variations in vertical load. Table 4.3 shows the RMS vertical load and RMS longitudinal force at the front and rear wheels, and the longitudinal deceleration during braking.

In Table 4.3, for the TWEEL™ and the tire, both the vertical and longitudinal forces are comparable. The deceleration values are comparable as well. This explains the similar braking performance for both cases on the WA-LPG road. Tables 4.4 and 4.5 show the tangent stiffnesses of the TWEEL™ and the tire in the C+D configuration. Obviously, the OE tire has constant stiffness. During braking, weight shifts to the front from rear. Table 4.4 also includes the tangent stiffness for the TWEEL™ at total load = garage value + RMS for the front wheel, and total load = garage value - RMS for the rear wheel. Notice that the front TWEEL™ is "softer" than the OE tire while the rear is "stiffer". It would be interesting to see the corresponding results for the GVW configuration, since the loading is higher than the C+D configuration. Theoretically the TWEEL™ should get "softer" with higher loading.

| | RMS Front Fz (N) | RMS Front Fx (N) | RMS Rear Fz (N) | RMS Rear Fx (N) | RMS Longitudinal Deceleration (g's) |
|---|---|---|---|---|---|
| TWEEL™ $\delta_{max} = 15\,mm$, $N = 0.6$ | 1050 | 4351.2 | 1114.9 | 1425.5 | 0.89 |
| OE Tire | 1082 | 4453.2 | 1065.8 | 1474.9 | 0.91 |

Table 4.3: Results of Simulation on the WA-LPG road (Brake from 60 mph, C+D Configuration)

| Stiffness $\left(\frac{N}{m}\right)$ | At Garage Load (3894.6 N) | At Garage Load + RMS Vertical Load |
|---|---|---|
| TWEEL™ ($\delta_{max} = 15\,mm, N = 0.6$) | 183.51 $e3$ | 156.36 $e3$ |
| OE Tire | 232.02 $e3$ | 232.02 $e3$ |

Table 4.4: TWEEL™ and OE Tire Stiffness (per Wheel) (C+D, at Front Wheel when Braked from 60 mph on the WA-LPG road)

| Stiffness $\left(\frac{N}{m}\right)$ | At Garage Load (2599.7 N) | At Garage Load - RMS Vertical Load |
|---|---|---|
| TWEEL™ ($\delta_{max} = 15\,mm, N = 0.6$) | 240.26 $e3$ | 349.2 $e3$ |
| OE Tire | 232.02 $e3$ | 232.02 $e3$ |

Table 4.5: TWEEL™ and OE Tire Stiffness (per Wheel) (C+D, at Rear Wheel when Braked from 60 mph on the WA-LPG road)

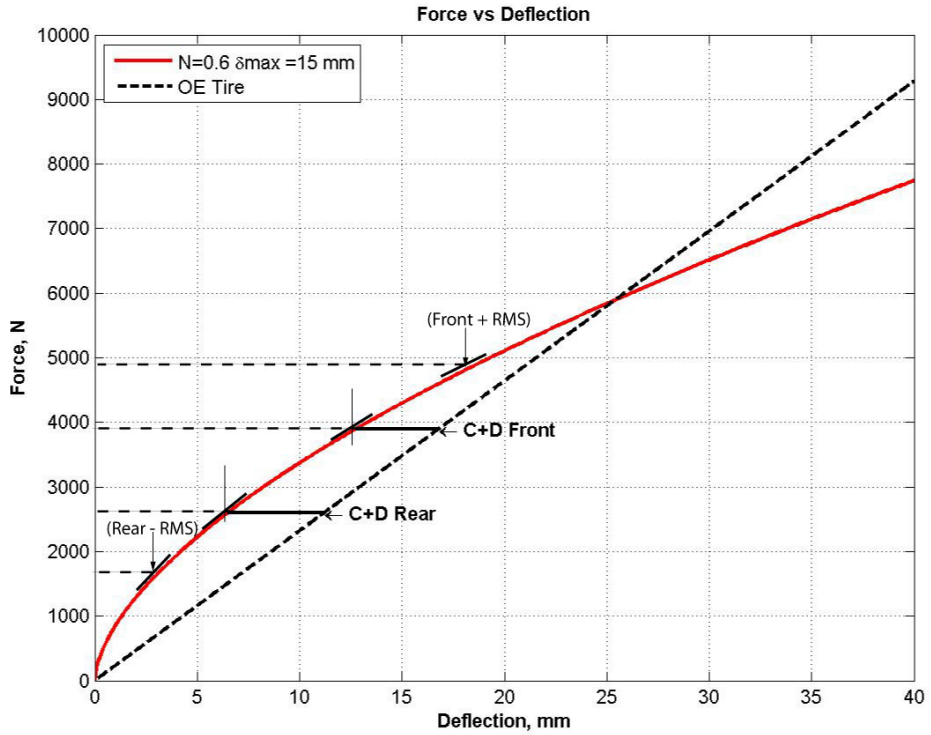


Figure 4.7: Force vs. Deflection Curve

Figure 4.8 shows the probaility density functions for vertical load when the braking simulation was performed on the WA-LPG road. The vertical arrows mark the front and rear garage loads in the C+D conditions. Table 4.6 shows the mean and standard deviation of the vertical load for braking simulations on the WA-LPG road. Obviously, the weight shifts from rear to front. The mean weight at front is hence higher than the garage value, vice-versa for rear. Note that the values of the mean and standard deviation are fairly close for both the TWEEL™ and the OE tire. The standard deviations for the TWEEL™ equipped car are slightly larger than for the car with the OE tires. This is very probably due to variation in stiffness for the TWEEL™ as it deflects.

| Variable | Mean (N) | Standard Deviation (N) |
|---|---|---|
| Front TWEEL™ ($\delta_{max} = 15\,mm$, $N = 0.6$) | 4840.2 | 205.1 |
| Front OE Tire | 4978.7 | 165.0 |
| Rear TWEEL™ ($\delta_{max} = 15\,mm$, $N = 0.6$) | 1470.2 | 170.2 |
| Rear OE Tire | 1524.6 | 119.2 |

Table 4.6: Post-processing of Vertical Force Data on the WA-LPG road (C+D Configuration, Brake from 60 mph)

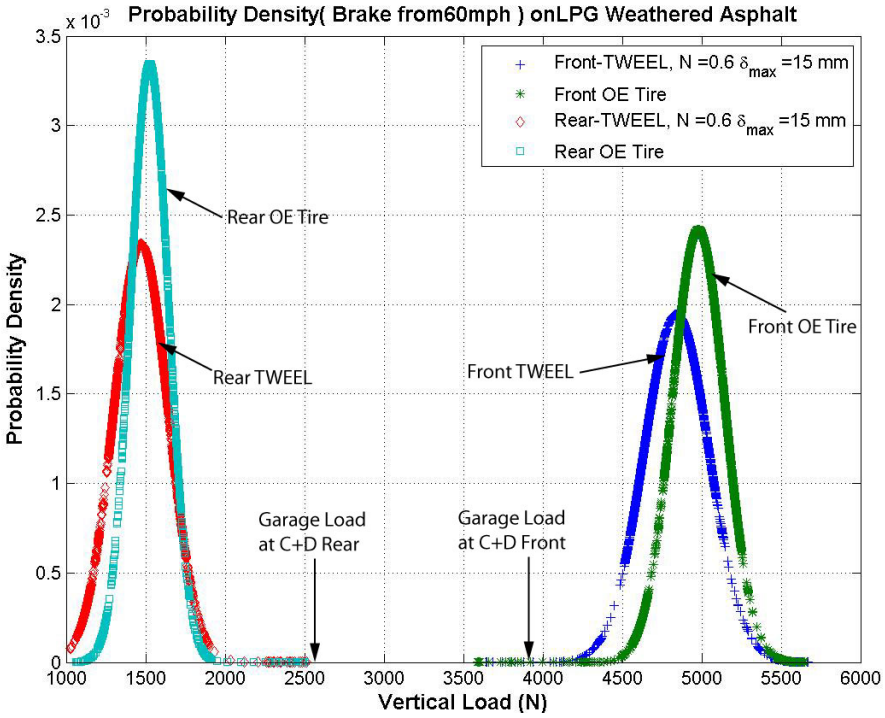


Figure 4.8: Probability Density Functions on the WA-LPG road (C+D Configuration, Brake from 60 mph)

### 4.3.2 Sensitivity to Road Roughness

The discussion in Section 4.3.1 pertains to the car traversing the simulated WA-LPG road which is a "relatively smooth" road. This section will discuss the sensitivity of the stopping distance to road roughness. Also, possible advantages with the adoption of the TWEEL™ on these "rough" roads will be discussed.

The roughness of road profiles is typically represented by power spectral density (PSD) curves. Figure 4.9 shows the PSD curves for various roads as given in Wong [32]. This representation uses the formulation in Equation 4.1 at a constant speed of 60 mph. The coefficients $C_{sp}$ and $N$ used for these roadways are available in Wong [32] and are listed in Table 4.7. The procedure to calculate the RMS roughness is detailed in the text after Table 4.7.

The temporal PSD is given by

$$S_{Z_r}(\omega) = \frac{(2\pi \cdot \nu)^{N-1} C_{sp}}{\omega^N} \quad \left( \frac{m^2}{\frac{rad}{sec}} \right) \tag{4.1}$$

where

$$\begin{aligned} C_{sp}, N &= Constants \\ \omega &= Temporal\, Frequency \left( \frac{rad}{sec} \right) \\ v &= Longitudinal\, Velocity \left( \frac{m}{sec} \right) \end{aligned}$$

| Description | $N$ | $C_{sp}$ | RMS Roughness (mm) |
|---|---|---|---|
| Rough Runway | 2.1 | $8.1 \times 10^{-6}$ | 24.7 |
| Gravel Highway | 2.1 | $4.4 \times 10^{-6}$ | 18.2 |
| Smooth Highway | 2.1 | $4.8 \times 10^{-7}$ | 6 |
| WA-LPG road | 2.3 | $2.5 \times 10^{-8}$ | 1.9 |

Table 4.7: Coefficients for Roadways (Wong [32])

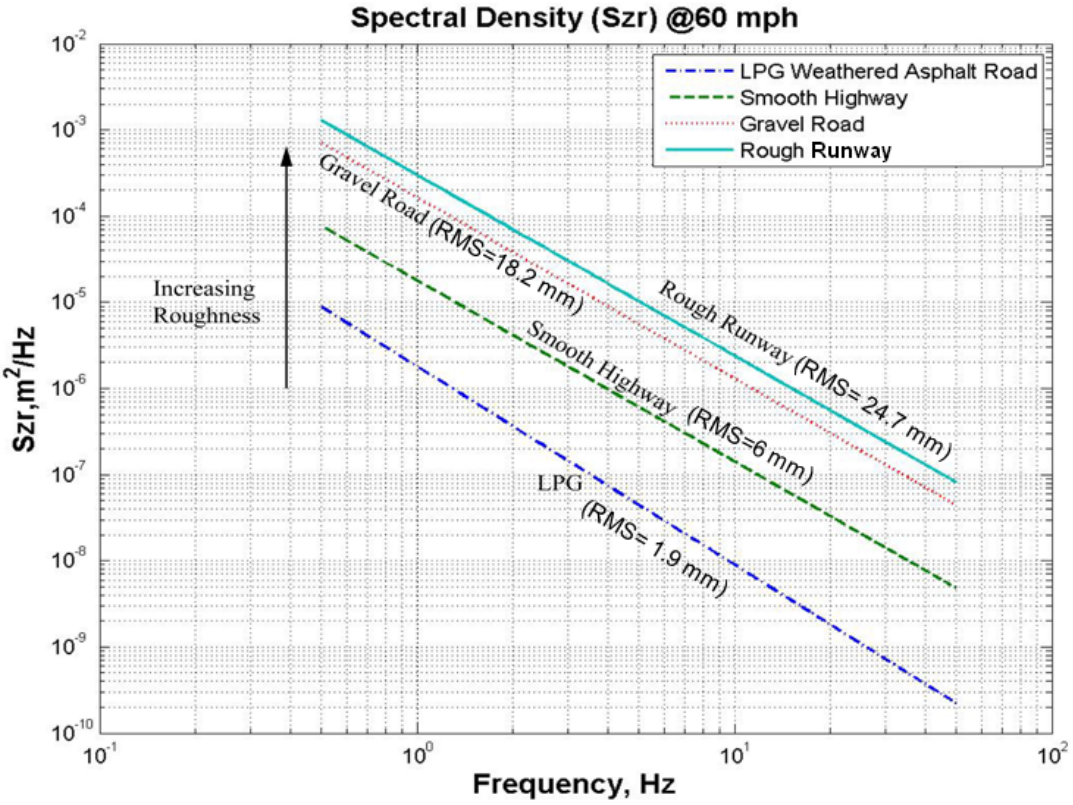


Figure 4.9: PSDs of Various Roadways (Wong [32])

For any curve on Figure 4.9 the mean square value in a frequency range $(\omega_1, \omega_2)$ can be calculated as

$$E(Z_r) = \int_{\omega_1}^{\omega_2} S_{Z_r}(\omega)\, d\omega \tag{4.2}$$

where,

$$\begin{aligned} \omega_1 &= Lower\,Frequency\left(Hz\,/\,\tfrac{rad}{sec}\right) \\ \omega_2 &= Higher\,Frequency\left(Hz\,/\,\tfrac{rad}{sec}\right) \end{aligned}$$

The Root Mean Square (RMS) can then be calculated as

$$RMS = \sqrt{E(Z_r)} \tag{4.3}$$

Obviously, the greater the RMS value, the rougher the road. In Figure 4.9 the RMS values were calculated over a temporal frequency range of 0.5 to 50 Hz. Table 4.8 shows the wavelengths corresponding to these frequency at different speeds.

| Temporal frequency/Speed | *20 mph* | *40 mph* | *60 mph* |
|---|---|---|---|
| 0.5 Hz | 17.88 $\frac{m}{cycle}$ | 35.76 $\frac{m}{cycle}$ | 53.64 $\frac{m}{cycle}$ |
| 50 Hz | 0.18 $\frac{m}{cycle}$ | 0.36 $\frac{m}{cycle}$ | 0.54 $\frac{m}{cycle}$ |

Table 4.8: Road Wavelengths

The dynamic tire-to-road force depends on the amplitude and the frequency content of road roughness. It is of interest for this work to evaluate the differences in braking performance when either of these two parameters are changed one at a time. Additionally, this study will also explore advantages of the TWEEL™ on these "new" roads. The two studies done to evaluate the effect of road roughness include:

1. Varying the frequency content of the roadway without changing RMS roughness.

2. Changing the roughness of the road profile.

Both of these studies are described in detail in the following sections.

#### 4.3.2.1 Varying the Frequency Content for Same Roughness

Figure 4.10 shows the RMS tire-to-road force for the front and rear axles plotted against frequency. This plot was obtained from the response of a ride model by Paradiso [15] on the WA-LPG road with OE tires at a constant speed of 60 mph. Note the increased response in the 9-11 Hz region. This is because the wheel hop modes are present in this frequency range. Recall that larger dynamic tire-to-road forces could lead to longer stopping distances. To understand if this would affect the braking performance, two different roads "Road 1" and "Road 2" were created using the method described in Section 3.7. The roads "Road 1" and "Road 2" are different in frequency content especially in the high frequency region around the wheel hop modes. Note that the RMS roughness given by Equation 4.3 is held constant.

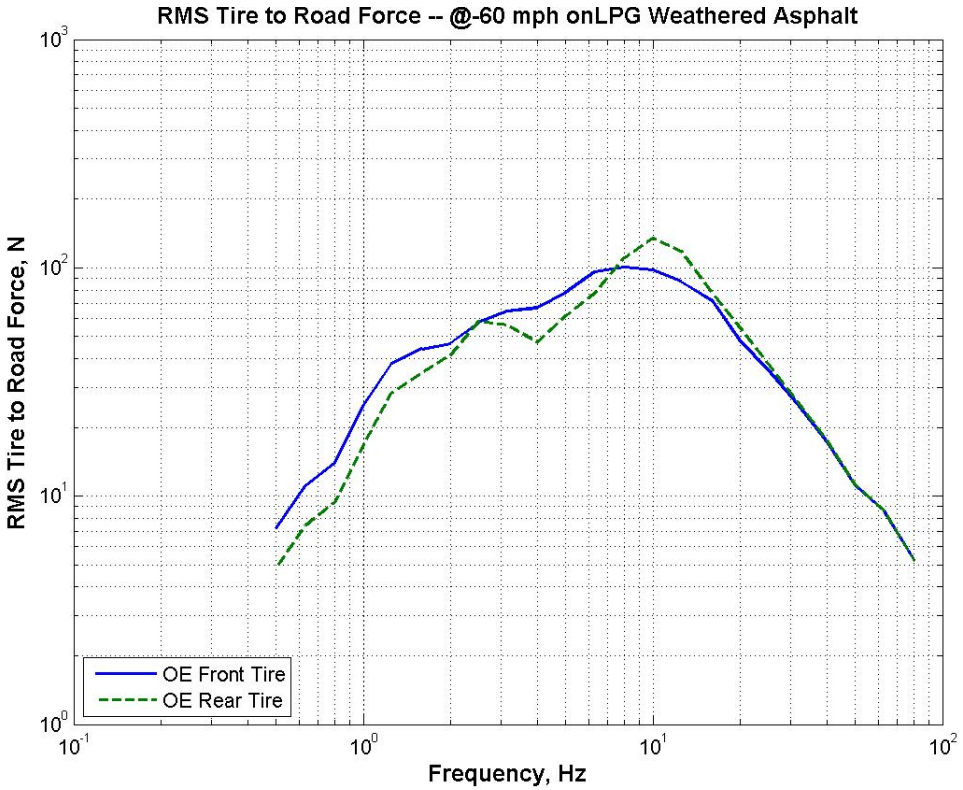


Figure 4.10: RMS tire-to-road (Per Axle) Force vs. Frequency

The road profiles were developed using the following steps,

1. For given $C_{sp}$ and $N$ values, the RMS value is calculated using Equation 4.3.

2. Starting with a new $N$ value and the RMS value calculated in step 1, a new $C_{sp}$ is value is determined to keep this RMS value constant.

3. Once known, the $C_{sp}$ and $N$ coefficients are used to construct new roadways using the technique in Section 3.7.

Both the roads compare to the "Smooth Highway" as far as RMS roughness is concerned. Figure 4.11 shows the aforesaid "Road 1" and "Road 2". As discussed earlier, "Road 2" has more content at higher frequencies than "Road 1". Table 4.9 shows the corresponding $C_{sp}$ and $N$ parameters used to generate the road profiles. The stopping distance for braking from 60 mph to a full stop were recorded and are shown in Table 4.10 and Figure 4.12.

| Description | $N$ | $C_{sp}$ | RMS Roughness (mm) |
|---|---|---|---|
| Road 1 | 2.6 | $1.079 \times 10^{-7}$ | 6.54 |
| Road 2 | 2.1 | $5.5 \times 10^{-7}$ | 6.54 |
| WA-LPG road | 2.3 | $2.5 \times 10^{-8}$ | 1.9 |

Table 4.9: $C_{sp}$ and $N$ for Roads with Constant RMS Roughness

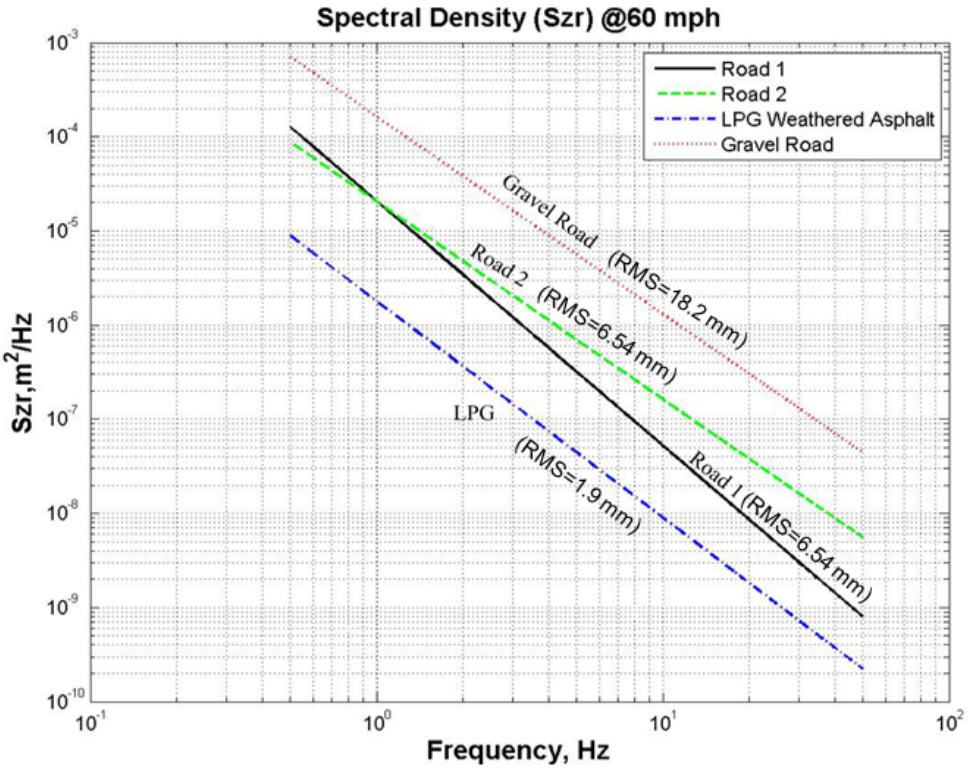


Figure 4.11: PSD with same RMS Roughness

The vehicle with "softer" TWEELs™ has shorter stopping distances than the car with OE tires or its "stiffer" counterparts on "Road 2". On "Road 1", there is very little difference in stopping distance for the various "tires". Among the three roadways, stopping distances on "Road 1" and "Road 2" are larger than on the WA-LPG road. This can be explained by the relatively larger RMS roughness of both roads compared to the WA-LPG road. "Road 2", which has more content at higher frequencies has relatively longer stopping distances compared to "Road 1". This can be attributed to the relatively greater excitation of the wheel hop modes in the case of "Road 2". Excitation of the wheel hop modes typically means more variation in the dynamic tire-to-road force that translates into longer stopping distances while braking.

| | Road 1 (RMS= 6.54 mm) | Road 2 (RMS= 6.54 mm) | WA-LPG road (RMS= 1.9 mm) |
|---|---|---|---|
| $\delta_{max} = 15mm, N = 0.4$ | 137.0 $ft$ | 139.0 $ft$ | 136 $ft$ |
| $\delta_{max} = 15mm, N = 0.6$ | 137.3 $ft$ | 139.1 $ft$ | 136 $ft$ |
| $\delta_{max} = 15mm, N = 0.8$ | 136.9 $ft$ | 139.6 $ft$ | 136 $ft$ |
| $\delta_{max} = 15mm, N = 1$ | 137.0 $ft$ | 139.8 $ft$ | 136 $ft$ |
| OE Tire | 136.7 $ft$ | 139.1 $ft$ | 136 $ft$ |

Table 4.10: Stopping Distance on Roads with same RMS Road Profile (Brake from 60 mph, C+D Configuration)

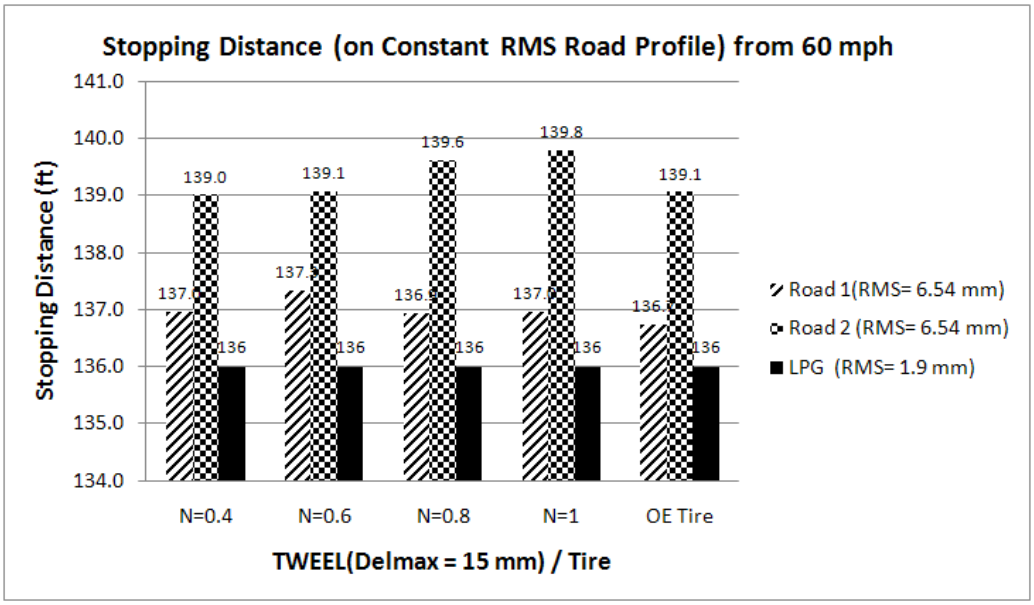


Figure 4.12: Stopping Distance on Roads with same RMS Road Profile (Brake from 60 mph, C+D Configuration)

Table 4.11 shows the results when braking was simulated on "Road 1". There are minimal differences between the TWEEL™ and the tire; this was expected since the stopping distance of the two cases is very similar. Tables 4.12 and 4.13 show the corresponding stiffnesses for the TWEEL™ and the tire. Tables 4.14 through 4.16 include corresponding information for the simulation on "Road 2". Again, no significant differences in stopping

distance were observed between the TWEEL™ and the tire in Table 4.14.

| | RMS Front Fz (N) | RMS Front Fx (N) | RMS Rear Fz (N) | RMS Rear Fx (N) | RMS Longitudinal Deceleration (g's) |
|---|---|---|---|---|---|
| TWEEL™ $\delta_{max} = 15\,mm$, $N = 0.6$ | 1063.9 | 4422.2 | 1098.9 | 1411.4 | 0.89 |
| OE Tire | 1090.3 | 4458.7 | 1094.4 | 1438.5 | 0.90 |

Table 4.11: Results of Simulation on "Road 1" (Brake from 60 mph , C+D Configuration)

| Stiffness $\left(\frac{N}{m}\right)$ | At Garage Load (3894.6 N) | At Garage Load + RMS Vertical Load |
|---|---|---|
| TWEEL™ ($\delta_{max} = 15\,mm$, $N = 0.6$) | 183.51 $e3$ | 156.20 $e3$ |
| OE Tire | 232.02 $e3$ | 232.02 $e3$ |

Table 4.12: TWEEL™ and OE Tire Stiffness (per Wheel) (C+D, at Front Wheel when Braked from 60 mph on "Road 1")

| Stiffness $\left(\frac{N}{m}\right)$ | At Garage Load (2599.7 N) | At Garage Load - RMS Vertical Load |
|---|---|---|
| TWEEL™ ($\delta_{max} = 15\,mm$, $N = 0.6$) | 240.26 $e3$ | 343.86 $e3$ |
| OE Tire | 232.02 $e3$ | 232.02 $e3$ |

Table 4.13: TWEEL™ and OE Tire Stiffness (per Wheel) (C+D, at Rear Wheel when Braked from 60 mph on "Road 1")

| | RMS Front Fz (N) | RMS Front Fx (N) | RMS Rear Fz (N) | RMS Rear Fx (N) | RMS Longitudinal Deceleration (g's) |
|---|---|---|---|---|---|
| TWEEL™ $\delta_{max} = 15\,mm$, $N = 0.6$ | 1070.6 | 4426.5 | 1031 | 1388.3 | 0.89 |
| OE Tire | 983.17 | 4338.6 | 1127.9 | 1343.8 | 0.87 |

Table 4.14: Results of Simulation on "Road 2" (Brake from 60 mph, C+D Configuration)

| Stiffness $\left(\frac{N}{m}\right)$ | At Garage Load (3894.6 N) | At Garage Load + RMS Vertical Load |
|---|---|---|
| TWEEL™ ($\delta_{max} = 15\,mm$, $N = 0.6$) | 183.51 $e3$ | 156.36 $e3$ |
| OE Tire | 232.02 $e3$ | 232.02 $e3$ |

Table 4.15: TWEEL™ and OE Tire Stiffness (per Wheel) (C+D, at Front Wheel when Braked from 60 mph on "Road 2")

| Stiffness $\left(\frac{N}{m}\right)$ | At Garage Load (2599.7 N) | At Garage Load - RMS Vertical Load |
|---|---|---|
| TWEEL™ ($\delta_{max} = 15\,mm$, $N = 0.6$) | 240.26 $e3$ | 327.18 $e3$ |
| OE Tire | 232.02 $e3$ | 232.02 $e3$ |

Table 4.16: TWEEL™ and OE Tire Stiffness (per Wheel) (C+D, at Rear Wheel when Braked from 60 mph on "Road 2")

#### 4.3.2.2 Varying the RMS Roughness

Figure 4.13 shows the PSDs for roads as determined in [32]. The corresponding $C_{sp}$, $N$, and RMS values are listed in Table 4.7. Both the "Gravel Road" and "Smooth Highway" are characterized by $N = 2.1$ but have different $C_{sp}$values, hence the different RMS

roughness values. The "Gravel Road" is obviously rougher than "Smooth Highway". Since the roughness over the entire frequency range is greater for "Gravel Road" it is expected that the dynamic tire-to-road forces would also increase as compared to the "Smooth Highway" and the WA-LPG road.

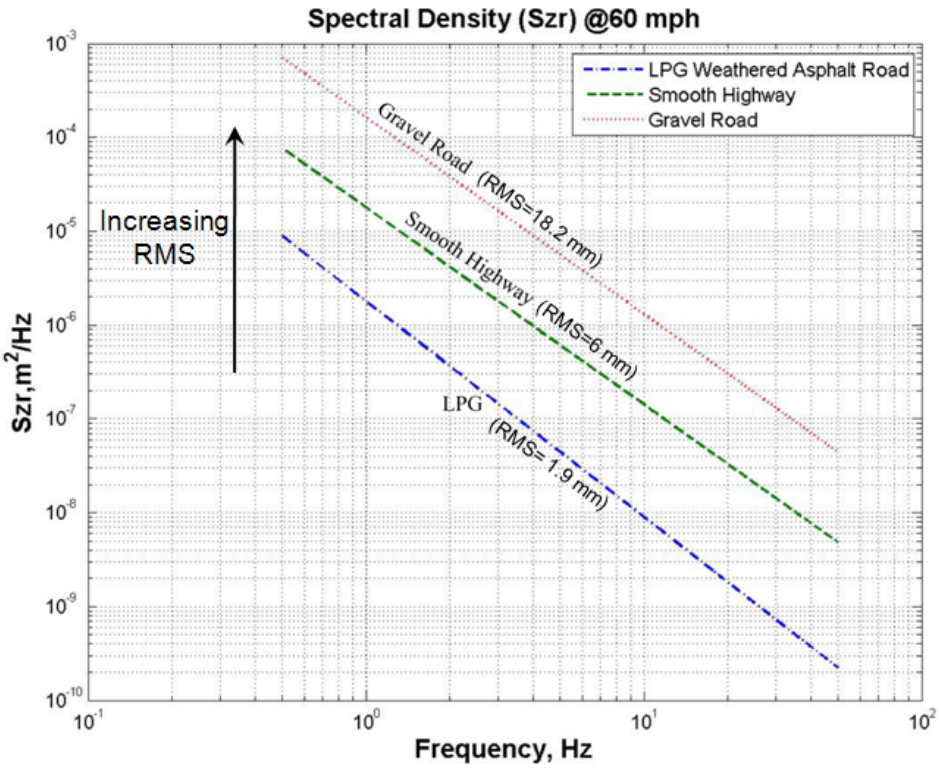


Figure 4.13: Spectral Density for Roads with Increasing RMS Roughness

Table 4.17 and Figure 4.14 show results of the simulations for this part of the study. As compared to the WA-LPG road, all the TWEELs™ and the OE tire have longer stopping distances on the "Smooth Highway". This is due to the relatively larger RMS roughness of the "Smooth Highway" which induces larger dynamic tire-to-road forces. No significant improvement in stopping distance was gained by selecting TWEELs™ over the OE tire on the "Smooth Highway". With the greater RMS roughness of the "Gravel Road", there are significant increases in the stopping distance for TWEELs™ and the OE tire as compared to either the results for the "Smooth Highway" or the WA-LPG road. The "softer" TWEELs™ now perform better than the OE Tire with the former showing about

5-6 % (for TWEEL™ $\delta_{max} = 15mm\, N = 0.6$) improvement in stopping distance over the latter. A study to investigate this result is also presented in this section.

| | Smooth Highway (RMS= 6.00 mm) | Gravel (RMS= 18.2 mm) | WA-LPG (RMS= 1.9 mm) |
|---|---|---|---|
| $\delta_{max} = 15mm$, $N = 0.4$ | 138.8 $ft$ | 144.7 $ft$ | 136 $ft$ |
| $\delta_{max} = 15mm$, $N = 0.6$ | 139.9 $ft$ | 155.2 $ft$ | 136 $ft$ |
| $\delta_{max} = 15mm$, $N = 0.8$ | 139.3 $ft$ | 164.4 $ft$ | 136 $ft$ |
| $\delta_{max} = 15mm$, $N = 1$ | 139.0 $ft$ | 163.7 $ft$ | 136 $ft$ |
| OE Tire | 138.8 $ft$ | 163.9 $ft$ | 136 $ft$ |

Table 4.17: Stopping Distance on Real Roadways (Brake from 60 mph, C+D Configuration)

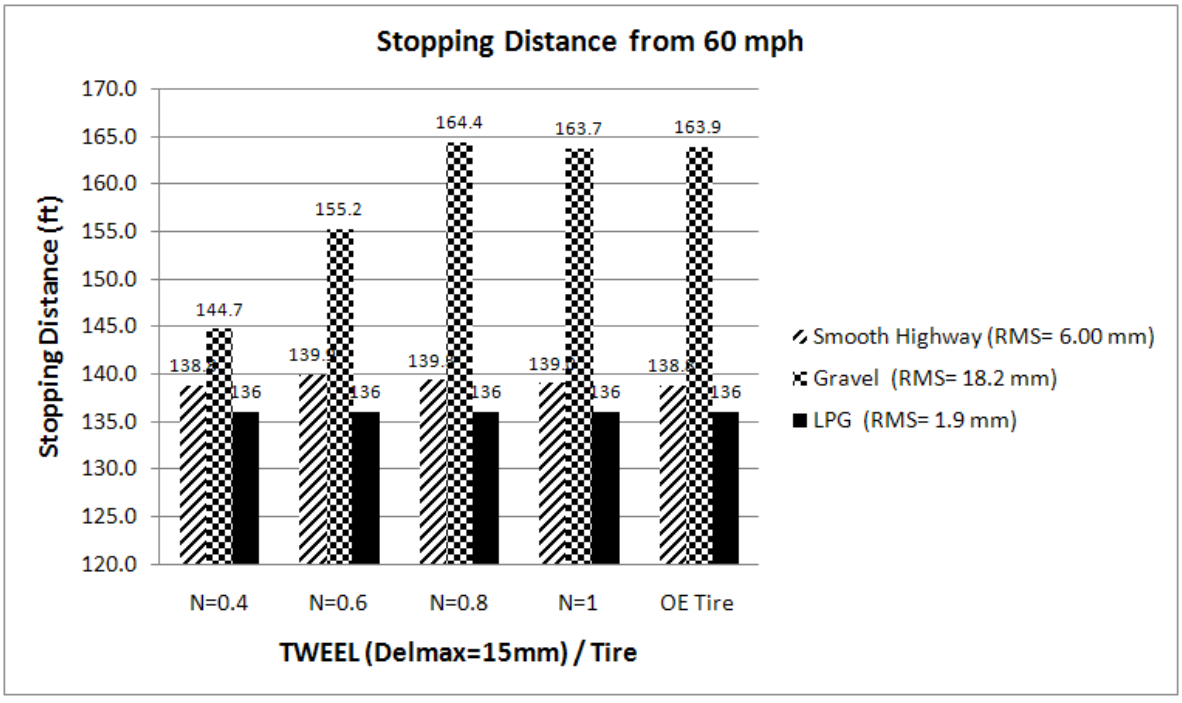


Figure 4.14: Stopping Distance on Real Roadways (C+D Configuration)

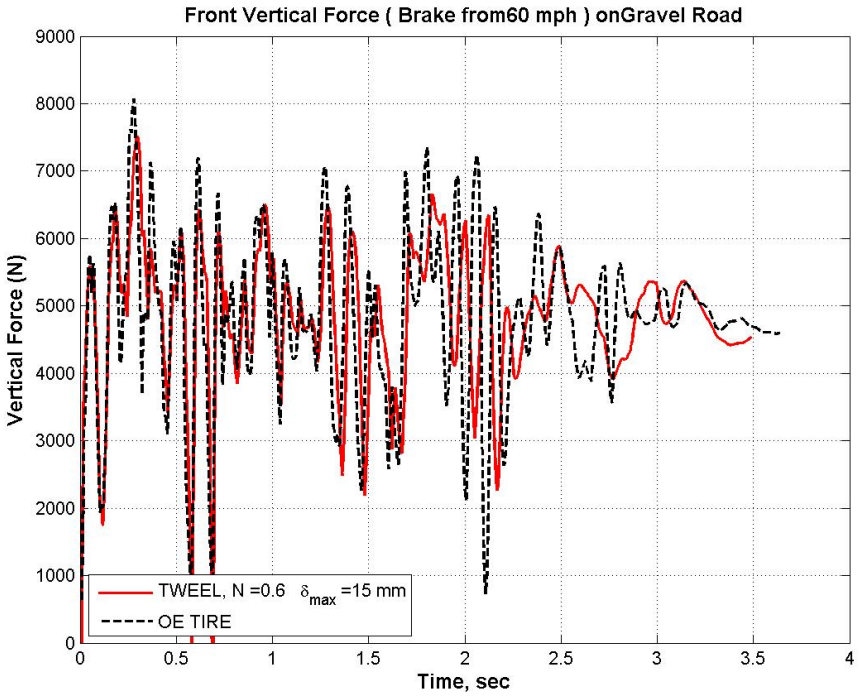


(a) Front Tire Vertical Load (per wheel)

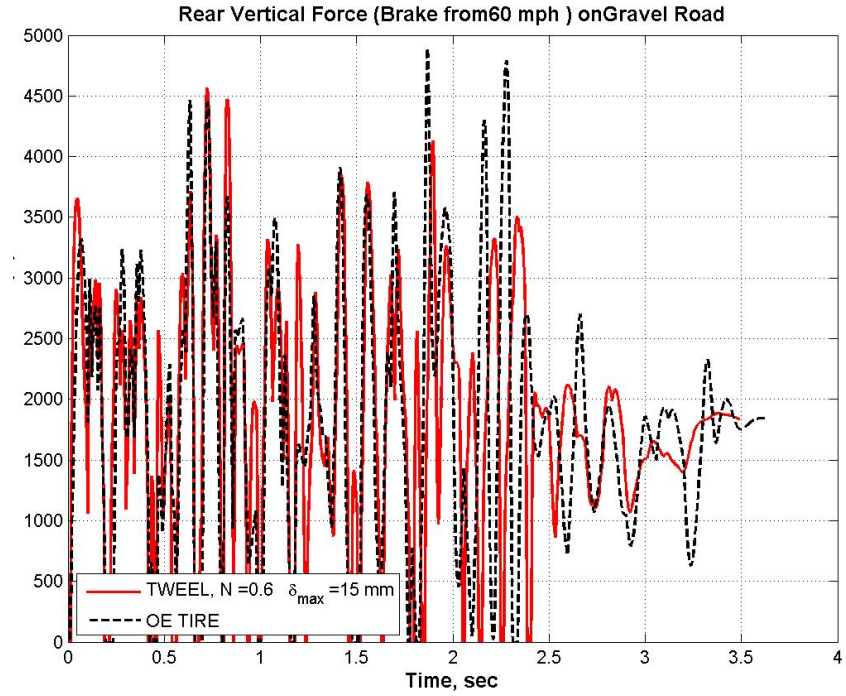


(b) Rear Tire Vertical Load (per wheel)

Figure 4.15: Vertical Response on Gravel Road (C+D, Brake from 60 mph)

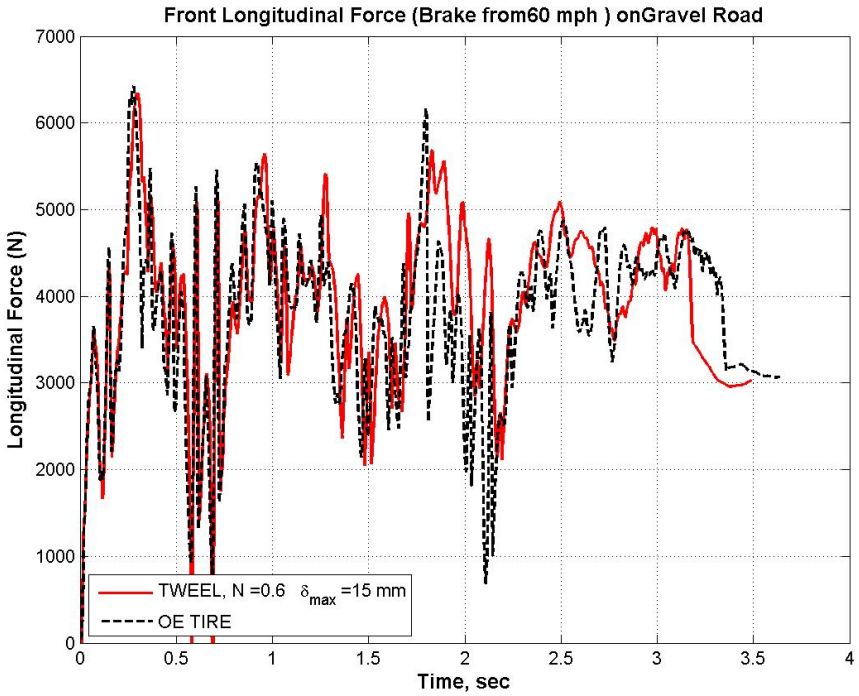


(a) Front Tire Longitudinal Force (per wheel)

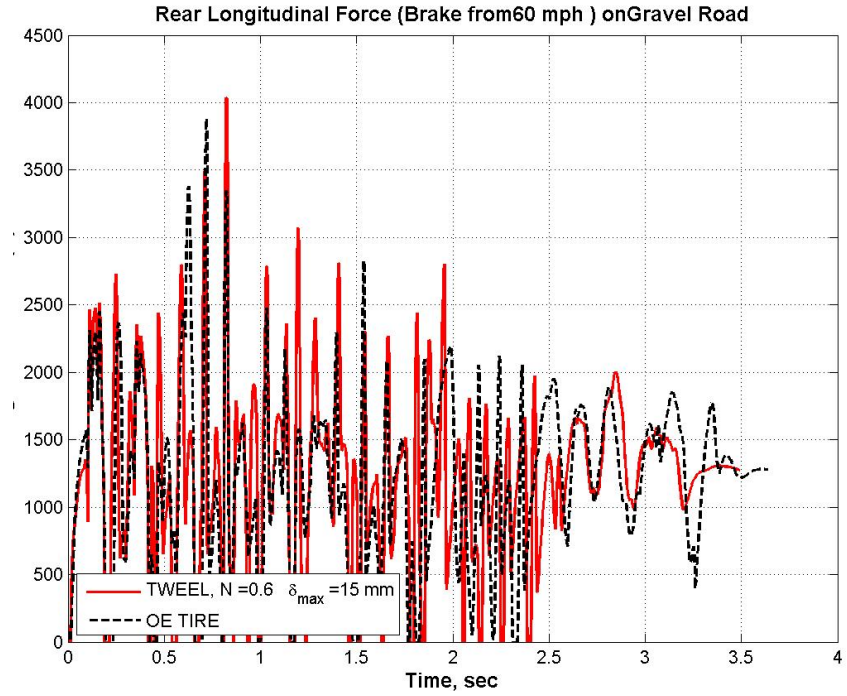


(b) Rear Tire Longitudinal Force (per wheel)

Figure 4.16: Longitudinal Tire Forces on Gravel Road (C+D, Brake from 60 mph)

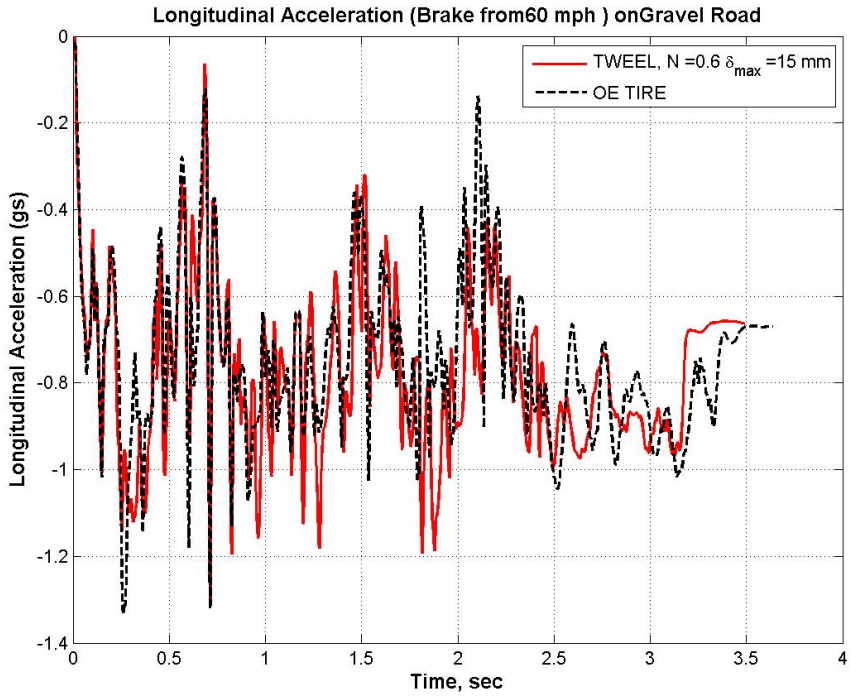


(a) Longitudinal Acceleration

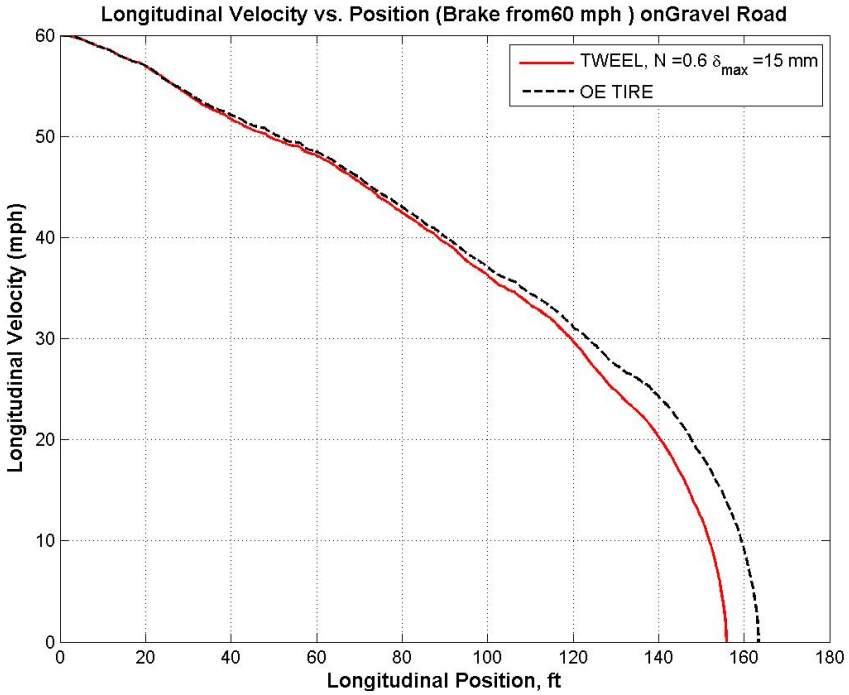


(b) Longitudinal Velocity vs. Position

Figure 4.17: Response on the Gravel Road (C+D, Brake from 60 mph)

Figures 4.15 and 4.16 show the time histories for vertical and longitudinal forces respectively when braking was simulated on the "Gravel Road". Figures 4.4 and 4.5 show corresponding plots for the WA-LPG road. Note that, on the WA-LPG road, the change in vertical force due to road roughness is relatively small, compared to the weight shift. The effect of road roughness is much more pronounced on the "Gravel Road". Also, note that the vertical load is zero at time t = zero second. This can be attributed to the simulation being started from a position on road which has a dip.

Table 4.18 shows the results from the braking simulation on the "Gravel Road" and the WA-LPG road. Note that on the "Gravel Road", performance of the TWEEL™ is much better than the OE tire. The RMS values of Fz are larger at front and smaller at rear for the TWEEL™. Recall that during braking, load increases at front and decreases from rear. Larger Fz values typically mean larger Fx values. Recall that RMS value of Fz includes components from weight shift and road roughness. Also, higher deceleration levels are achieved with the TWEEL™. This explains the shorter stopping distances achieved by the vehicle equipped with TWEEL™ on "Gravel Road".

| | RMS Front Fz (N) | RMS Front Fx (N) | RMS Rear Fz (N) | RMS Rear Fx (N) | RMS Longitudinal Deceleration (g's) |
|---|---|---|---|---|---|
| TWEEL™ $\delta_{max} = 15\,mm, N = 0.6$ "Gravel Road" | 1024.5 | 4349.2 | 639.07 | 1458.8 | 0.88 |
| OE Tire "Gravel Road" | 671.03 | 4016.5 | 1077 | 1232 | 0.79 |
| TWEEL™ $\delta_{max} = 15\,mm, N =$ 0.6"WA-LPG Road" | 1050 | 4351.2 | 1114.9 | 1425.5 | 0.89 |
| OE Tire "WA-LPG Road" | 1082 | 4453.2 | 1065.8 | 1474.9 | 0.91 |

Table 4.18: Results of Simulation on (Brake from 60 mph, C+D Configuration) TWEEL™ vs. OE Tire

Tables 4.19 and 4.20 show the corresponding tire and TWEEL™ stiffnesses for front and rear wheels on the "Gravel Road" and the WA-LPG road. The stiffness for the front TWEEL™ does not change significantly between the two simulations. However, during unloading (at garage load - RMS vertical load), the rear TWEEL™ is "softer" on "Gravel Road" as compared to rear TWEEL™ on the WA-LPG road.

| Stiffness $\left(\frac{N}{m}\right)$ | At Garage Load (3894.6 N) | At Garage Load + RMS Vertical Load |
|---|---|---|
| TWEEL™ ($\delta_{max} = 15\,mm, N = 0.6$) "Gravel Road" | 183.51 $e3$ | 157.03 $e3$ |
| OE Tire "Gravel Road" | 232.02 $e3$ | 232.02 $e3$ |
| TWEEL™ ($\delta_{max} = 15\,mm, N = 0.6$) "WA-LPG Road" | 183.51 $e3$ | 156.36 $e3$ |
| OE Tire "WA-LPG Road" | 232.02 $e3$ | 232.02 $e3$ |

Table 4.19: TWEEL™ and OE Tire Stiffness (per Wheel) (C+D, at Front Wheel when Braked from 60 mph)

| Stiffness $\left(\frac{N}{m}\right)$ | At Garage Load (2599.7 N) | At Garage Load - RMS Vertical Load |
|---|---|---|
| TWEEL™ ($\delta_{max} = 15\,mm, N = 0.6$) "Gravel Road" | 240.26 $e3$ | 290.18 $e3$ |
| OE Tire "Gravel Road" | 232.02 $e3$ | 232.02 $e3$ |
| TWEEL™ ($\delta_{max} = 15\,mm, N = 0.6$) "WA-LPG Road" | 240.26 $e3$ | 349.2 $e3$ |
| OE Tire "WA-LPG Road" | 232.02 $e3$ | 232.02 $e3$ |

Table 4.20: TWEEL™ and OE Tire Stiffness (per Wheel) (C+D, at Rear Wheel when Braked from 60 mph)

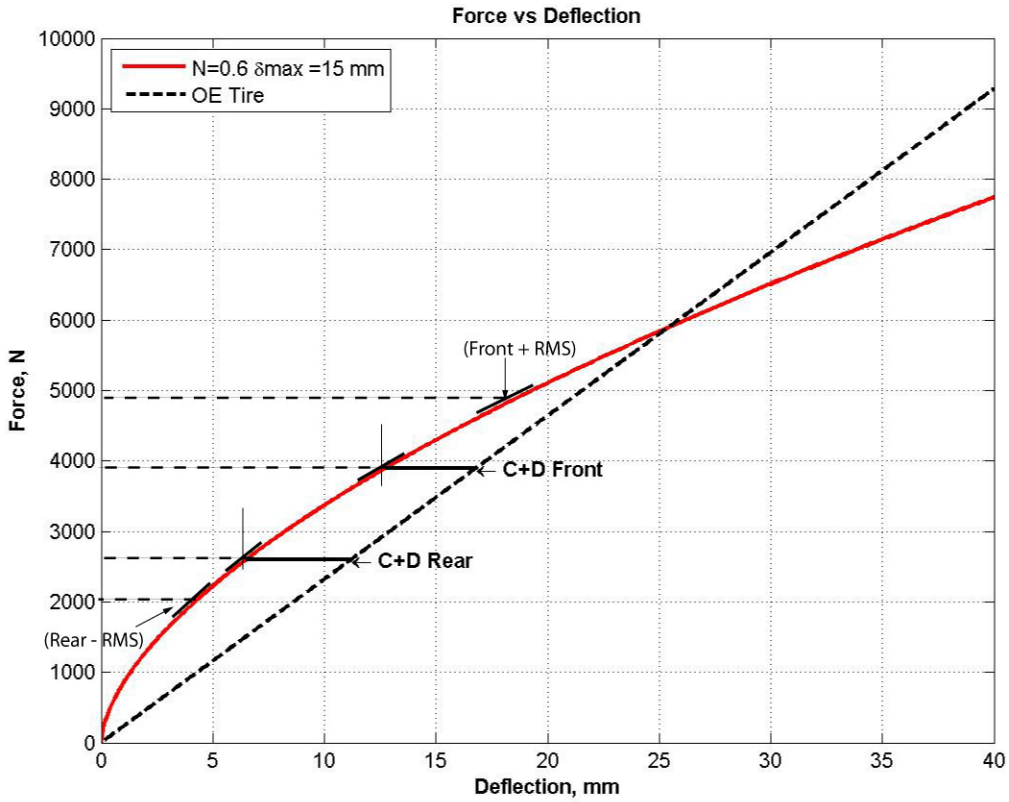


Figure 4.18: Force vs. Deflection Curve

Table 4.21 shows the mean vertical load and the standard deviation for the TWEEL™ and the tire for simulation on the "Gravel Road". Table 4.22 shows corresponding values for simulation on the WA-LPG road. Notice the much higher standard deviation on the "Gravel Road". This is due to the increased roughness of the "Gravel Road". Also, notice that on the "Gravel Road" the rear TWEEL™ has larger standard deviation than the OE tire. Figures 4.19 and 4.20 show the probability density function (PDF) for the simulation on the "Gravel Road" and the WA-LPG road. Notice the larger mean vertical loads for the front and the rear TWEEL™ as compared to the OE tire on the "Gravel Road". Also, note that the PDF for TWEEL™ is more towards right than the PDF for the OE tire, indicating higher vertical loads. Since the adhesion coefficient is not changing, the longitudinal force is largely dependent on the vertical load. This explains the larger RMS longitudinal forces and the shorter stopping distance for the TWEEL™ on the "Gravel Road".

| Variable | Mean (N) | Standard Deviation (N) |
|---|---|---|
| Front TWEEL™ ($\delta_{max} = 15\,mm$, $N = 0.6$) | 4846.2 | 816.88 |
| Front OE Tire | 4486.9 | 818.78 |
| Rear TWEEL™ ($\delta_{max} = 15\,mm$, $N = 0.6$) | 1690.7 | 983.49 |
| Rear OE Tire | 1343.4 | 706.95 |

Table 4.21: Post-processing of Vertical Force data on Gravel Road (C+D Configuration, Brake from 60 mph)

| Variable | Mean (N) | Standard Deviation (N) |
|---|---|---|
| Front TWEEL™ ($\delta_{max} = 15\,mm$, $N = 0.6$) | 4840.2 | 205.1 |
| Front OE Tire | 4978.7 | 165.0 |
| Rear TWEEL™ ($\delta_{max} = 15\,mm$, $N = 0.6$) | 1470.2 | 170.2 |
| Rear OE Tire | 1524.6 | 119.2 |

Table 4.22: Post-processing of Vertical Force Data on the WA-LPG road (C+D Configuration, Brake from 60 mph)

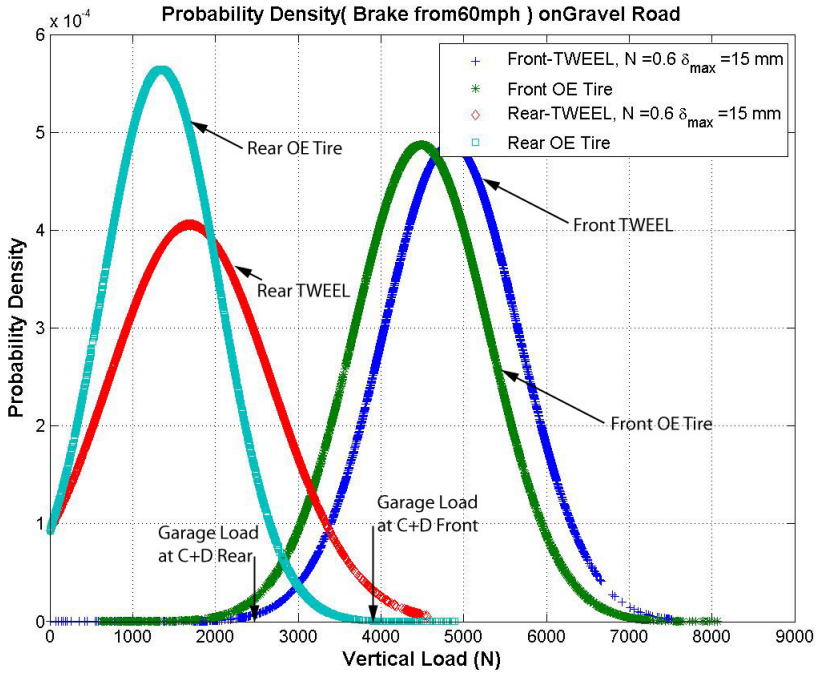


Figure 4.19: Probability Density Function on Gravel Road (C+D Configuration, Brake from 60 mph)

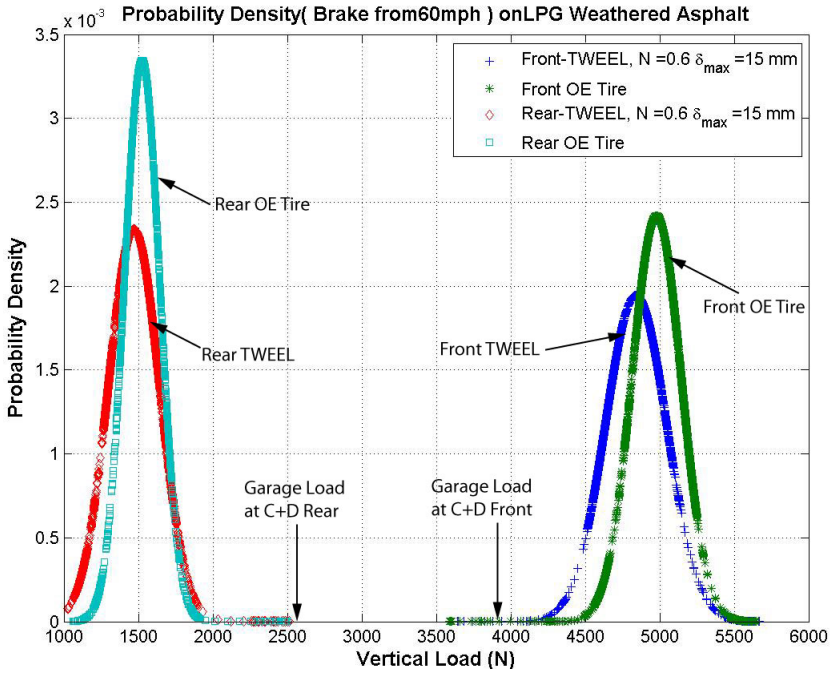


Figure 4.20: Probability Density Functions on the WA-LPG road (C+D Configuration, Brake from 60 mph)

### 4.3.3 Sensitivity to Shock Damping

Automobile manufacturers often tune the shock absorbers in order to get the desired ride and handling characteristics from a given vehicle and tire combination. This helps in keeping the overall development cost down while achieving the desired characteristics from the combination. Law [36] modified shock damping to investigate the effect on ride characteristics and RMS tire-to-road forces. He used linear damping coefficients at front and the rear in C+D configuration for the BMW Mini. He found out that increasing shock damping at front and reducing it at the rear improved the ride characteristics and also reduced the RMS tire-to-road forces. In [17], Law evaluated the effect of shock absorber damping on the ride characteristics of a quarter vehicle model. He examined the effects of variation in shock damping on sprung and unsprung mass heave, sprung mass vertical acceleration and dynamic tire-to-road force. He concluded that, by increasing shock damping :

1. Dynamic tire-to-road force decreased at both the body mode and the wheel hop mode. It also decreased for frequencies above the wheel hop mode.

2. For frequencies between the body mode and wheel hop mode, the dynamic tire-to-road force increased.

Recall that greater dynamic tire-to-road force means more variation from the static loading conditions and possibly longer stopping distances. Hazare and Law [13] evaluated the "best" shock configuration for the current vehicle equipped with the TWEEL™ ($\delta_{max} = 15\,mm, N = 0.6$), with respect to ride acceleration and the RMS values of Fz at the front and rear. They approximated various shock characteristics (softer to firmer) by scaling the experimentally measured shock force vs. velocity curves (refer to section 3.3) and used the OE tire as a benchmark to compare the results with TWEEL™. According to their findings, a "soft" setting on both front and rear shocks yielded lower RMS values of the front tire-to-road Fz but slightly higher RMS values of the rear Fz compared to those of the OE tire, while "softer" shocks at front and "stock" shocks at rear give better results at both ends. This section will carry forward the work by Hazare and Law by evaluating the

effect of these shock settings on braking performance. In addition to evaluating different TWEELs™, the effect of changing shock damping on different roads will also be discussed.

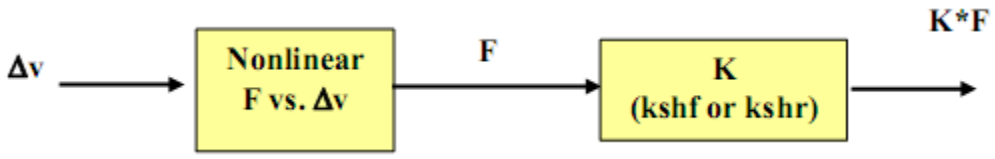


Figure 4.21: Scaling Shock Force vs. Velocity Curve ([13])

Recall from Section 3.8 that the nonlinear shock force vs. velocity curves are incorporated in Simulink using look up tables. A gain block was added to the output of the look up table in Simulink to vary the shock characteristics. This approach is similar to the one used by Hazare and Law in [13]. Figure 4.21 shows this scheme. $K_{shf}$ and $K_{shr}$ are gains for the front and the rear shocks respectively. Table 4.23 shows the range of gains used for this study. Figure 4.22 shows the corresponding shock force vs. velocity curves.

| $K_{shf}$ / $K_{shr}$ | Setting |
|---|---|
| 1 | Stock |
| 0.5 | Soft |
| 1.5 | Firm |

Table 4.23: Scaling Factor for Shocks

From [35] and conclusions by Paradiso [15], the $\delta_{max} = 15\,mm$, $N = 0.6$ TWEEL™ offered the best performance for ride under the various constraints on $\delta_{max}$ and $N$ values. Only the performance of this TWEEL™ is compared to the OE tire. Four different shock combinations were run on two different roads for this sensitivity study, two of which are recommendations by Hazare and Law [13]. All the shock combinations are enlisted in Table 4.24. The roads chosen for this part were the “Smooth Highway” and the “Gravel Road”.

| Combination | Front/Rear |
|---|---|
| $K_{shf} = 0.5$ , $K_{shr} = 0.5$ | Soft / Soft |
| $K_{shf} = 0.5$ , $K_{shr} = 1$ | Soft / Stock |
| $K_{shf} = 1$ , $K_{shr} = 1$ | Stock / Stock |
| $K_{shf} = 1.5$ , $K_{shr} = 1.5$ | Firm / Firm |

Table 4.24: Combination of Shock Absorber Damping

The stopping distance for each case was then normalized with respect to the stopping distance for OE tire with stock shock absorbers. For example, a normalized stopping distance of 0.99 for "Case A" , 1.01 for "Case B" and 1 for "Case C" would mean that there is 1 % improvement in stopping distance for "Case A", vice-versa for "Case B" and no improvement for "Case C" (all compared to OE tire with stock shocks at front and rear).

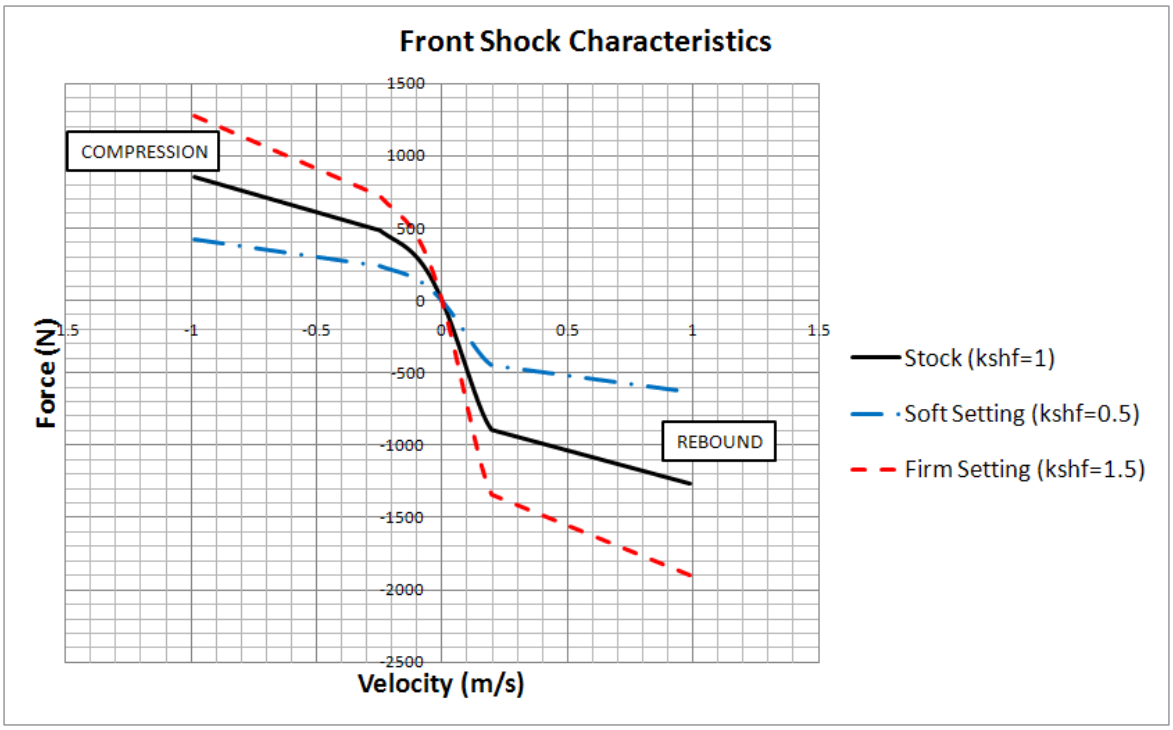


(a) Front Shock

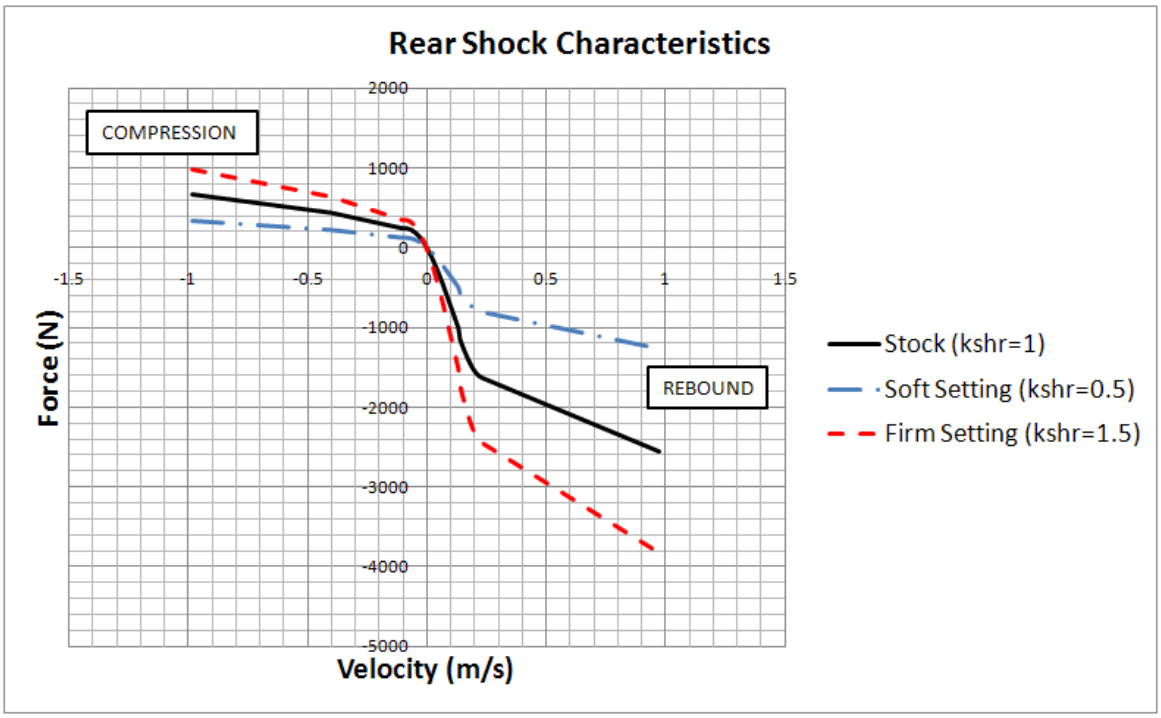


(b) Rear Shock

Figure 4.22: Scaled Shock Characteristics

When simulated on the WA-LPG road, there was no effect of changing shock configuration on stopping distance. Figure 4.23 and Table 4.26 show the results for braking on the "Smooth Highway" with all the shock configurations. Note that (relative to OE tire with stock shocks) there is a degradation in stopping distance with every shock configuration simulated both for the TWEEL™ and the OE tire with the latter faring better than the former. Note also that, the *maximum* increase in stopping distance is of the order of 1.6 % (TWEEL™ in Case 2). If looked at in absolute terms, this number is statistically insignificant. Therefore, it can be said that on the "Smooth Highway", changing shock absorber damping has no significant effect on braking performance.

| | $K_{shf} = 0.5$ $K_{shr} = 0.5$ (Case 1) | $K_{shf} = 0.5$ $K_{shr} = 1$ (Case 2) | $K_{shf} = 1$ $K_{shr} = 1$ (Case 3) | $K_{shf} = 1.5$ $K_{shr} = 1.5$ (Case 4) |
|---|---|---|---|---|
| $\delta_{max} = 15\,mm$, $N = 0.6$ | 1.005 | 1.016 | 1.008 | 1.010 |
| OE Tire | 1.001 | 1.005 | 1.000 | 1.011 |

Table 4.26: Normalized Stopping Distance with Different Shock Characteristics on "Smooth Highway"

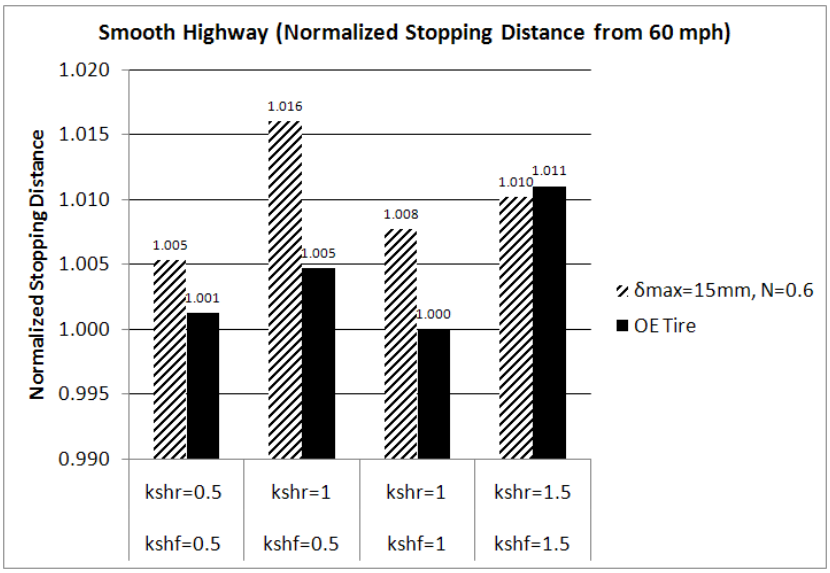


Figure 4.23: Normalized Stopping Distance with Different Shock Characteristics on "Smooth Highway"

On the "Gravel Road", the TWEEL™ ($\delta_{max} = 15\,mm$, $N = 0.6$) was always superior to the OE tire with stopping distance smaller by about 5 to 6 % over the OE tire for all the simulated shock configurations. Note that for the Cases 1 and 2 the braking performance of the TWEEL™ deteriorates by approximately 0.5 to 1.3 %, which is lower than the 7 to 8 % deterioration for the OE tire. In stock setting, the TWEEL™ registers an improvement of about 5.3 % over the OE tire. Also, with Case 4, both the TWEEL™ and the OE tire register improvements of about 7.4 % and 2.2 % respectively over the OE tire with stock shocks.

| | $K_{shf} = 0.5$<br>$K_{shr} = 0.5$<br>(Case 1) | $K_{shf} = 0.5$<br>$K_{shr} = 1$<br>(Case 2) | $K_{shf} = 1$<br>$K_{shr} = 1$<br>(Case 3) | $K_{shf} = 1.5$<br>$K_{shr} = 1.5$<br>(Case 4) |
|---|---|---|---|---|
| $\delta_{max} = 15\,mm$, $N = 0.6$ | 1.005 | 1.013 | 0.947 | 0.926 |
| OE Tire | 1.073 | 1.084 | 1.000 | 0.978 |

Table 4.28: Normalized Stopping Distance with Different Shock Characteristics on "Gravel Road"

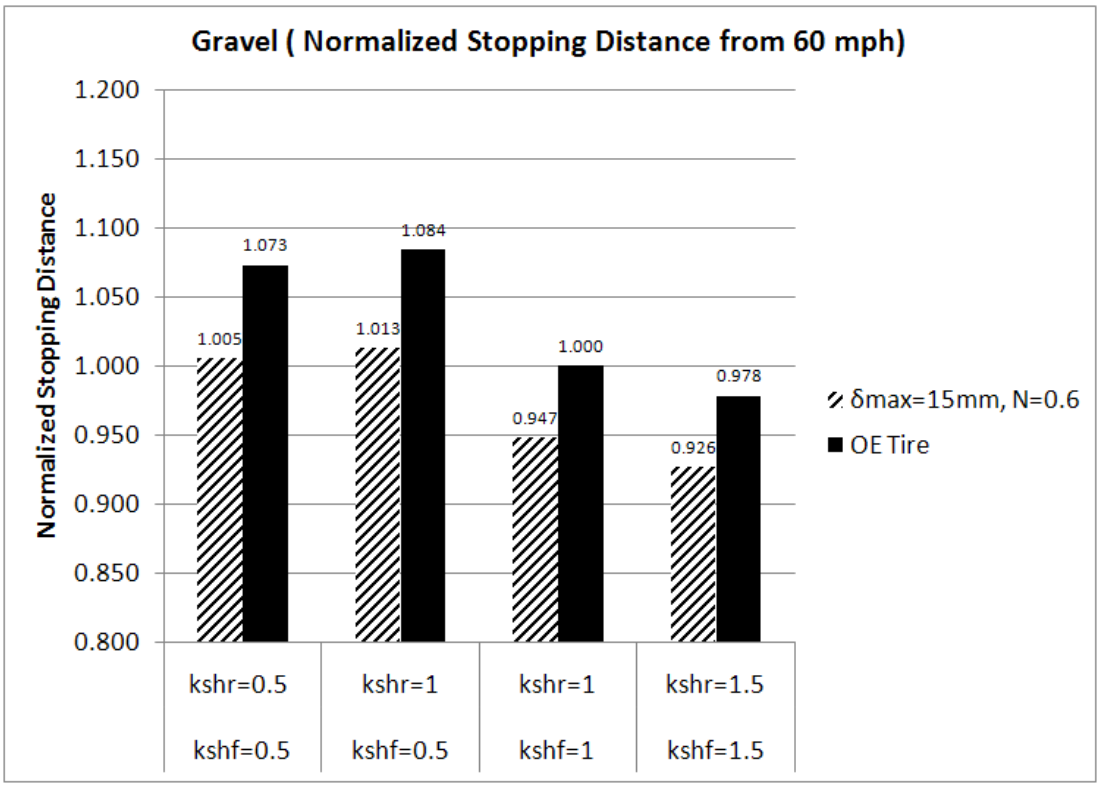


Figure 4.24: Normalized Stopping Distance with Different Shock Characteristics on "Gravel Road"

Figure 4.25 shows the power spectral density of the front tire-to-road force when traveling at a constant speed of 60 mph on the "Gravel Road". Note the increased response around the body mode (1-2 Hz) and the wheel hop mode (9-11 Hz) due to reduced shock damping. This explains the shorter stopping distances for the "Firm" setting (Case 4) as compared to other relatively "Soft" settings (Cases 1, 2, and 3). It is worth mentioning that with "Firm" settings on the shocks, the ride acceleration will increase and relatively uncomfortable ride characteristics should be expected.

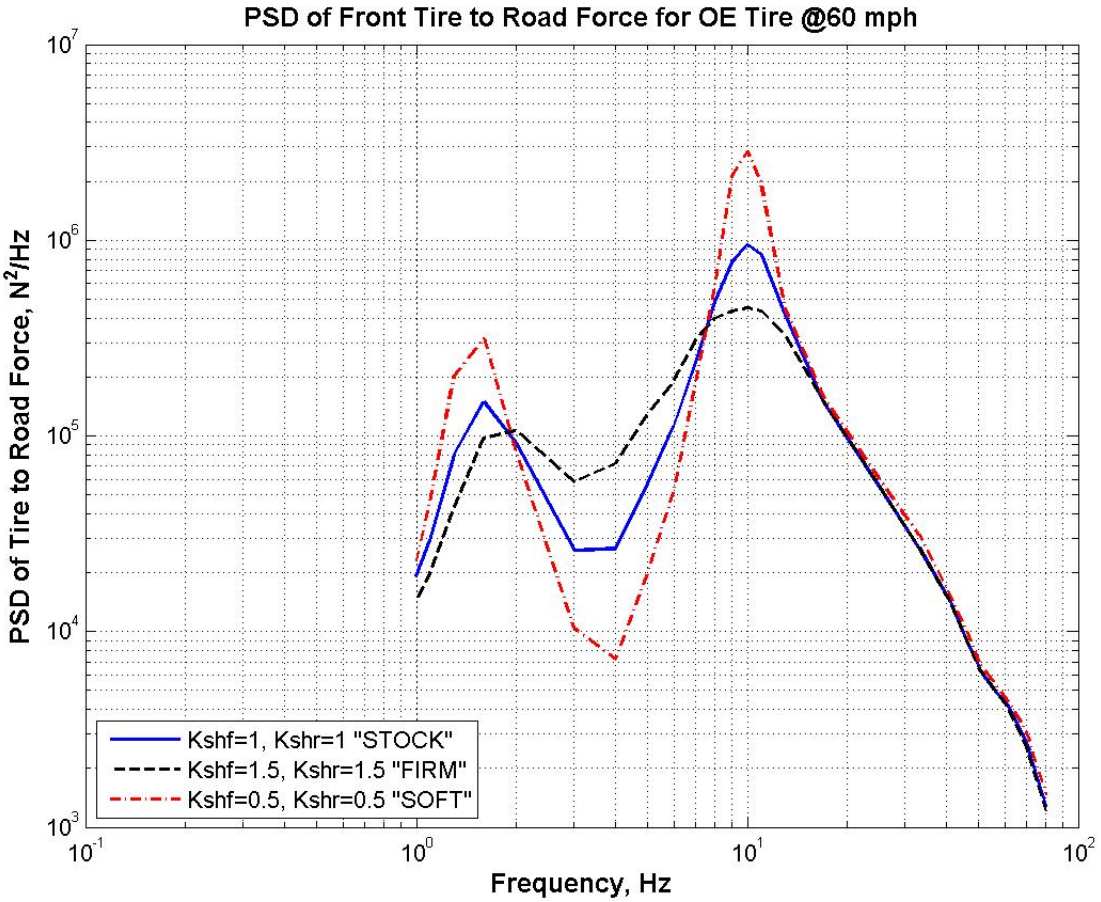


Figure 4.25: PSD of Front tire-to-road Force on "Gravel Road" for OE Tire

# Chapter 5

# Conclusions

## 5.1 Introduction

An eight degree of freedom vehicle model of the 2007 BMW Mini in C+D configuration was utilized to study the effect of nonlinear tire stiffness, road vertical profile, and shock absorber damping on braking performance. The vehicle model included vertical and longitudinal dynamics and only in-plane motions were considered. Stopping distance was used as a performance metric. The vehicle model was realized in Matlab/Simulink environment. This helped the realization of nonlinear force vs. velocity curves for the shock absorbers and tire force vs. deflection curves. The Pacejka formulation was used for calculating longitudinal tire forces. A simplified brake system was also modeled; it uses an idealized anti-lock system to avoid wheel lock during limit braking.

Different road profiles were artificially generated for simulation purposes. A hard braking test was simulated from an initial speed of 60 mph to a complete stop. Various hypothetical TWEELs™ were evaluated for braking performance on the simulated road profile similar to the WA-LPG road. Road profiles of varying roughness amplitude and frequency content were also used in evaluating their effects on stopping distance. Finally, different shock absorber damping values were chosen and resulting vehicles were evaluated for braking performance.

## 5.2 Braking Performance

As long as the brake torque was enough to activate ABS, stopping distance for the car with OE tires was largely unaffected by the peak value or distribution of the brake torque. On the WA-LPG road, stopping distance was unaffected by tire or TWEEL™ choice. Thus the choice of tires does not affect braking performance on roads as "smooth" as the WA-LPG road. When simulated on roads with similar RMS roughness, the stopping distances increased on the road with greater roughness in the vicinity of wheel hop modes. In this case, the stopping distance for every TWEEL™ and the OE tire increased, but not significantly. The "softer" TWEEL™ performed marginally better or on a par with the OE tire. This indicates the effect of wheel hop modes on grip and hence braking performance.

On the other hand, when the RMS roughness of the road profile was increased, the stopping distances increase and the "softer" TWEELs™ perform consistently better than the OE tire on the simulated "Gravel Road". This substantiates the advantage of TWEEL™ design on "rougher" roads. The sensitivity study for shock absorbers revealed that on "smooth" roads changing shocks was ineffective; "firmer" dampers proved to be advantageous in braking on the simulated "Gravel Road" by reducing stopping distances. It is to be recalled that "firm" dampers yield poor ride and hence a compromise must be made.

## 5.3 Recommendations

The results of this study clearly indicate that there is a gain in braking performance with the adoption of the TWEEL™ on "rougher" road profiles. Thus no braking performance would be lost by adopting the TWEEL™ on roads as "smooth" as the WA-LPG road and there would be performance gains on rougher roads. For the sensitivity study with shock absorber damping, softening the shocks at either the front and/or rear did not present any improvements in stopping distance. Firmer shocks at the front and rear, however, registered decrease in stopping distances. It must be kept in mind that firmer shocks

lead to a somewhat uncomfortable ride. It would be up to the manufacturer to determine the compromise between ride and braking performance due to the switch to firmer shocks.

For the future, this work can be further extended by:

1. Once manufactured, physical test data like vertical stiffness, longitudinal and lateral force data from the TWEELs™ should be used for more accurate simulation results.

2. Hard braking tests in the field would provide data to help validate the model and the results from the sensitivity studies.

3. Simulation of the GVW (gross vehicle weight) configuration should be performed as the stiffness of a TWEEL™ is strong function of loading.

4. Simulation and tests of a brake-in-turn maneuver would exercise the TWEEL™ in both the longitudinal and the lateral directions. This would help to determine handling ability of the TWEEL™ under braking.

5. Simulation shows a potential increase in braking performance with firmer shocks. It would be worthwhile to get opinions of subjective test drivers about ride "comfort" with this shock configuration while evaluating its effect on stopping distance.

# APPENDICES

# Appendix A

# Derivation of Equations of Motion

Figure A.1 shows the vehicle model for longitudinal and vertical dynamics. The equations were derived using the Newton-Euler approach and solved using numerical integration in Simulink. This section describes detailed step by step derivation of these equations. Figure A.1 shows the vehicle model used in this study. The degrees of freedom are:

$$
\begin{aligned}
z_s &= Sprung\,Mass\,CG\,Heave \\
theta &= Sprung\,Mass\,Pitch \\
z_{tf} &= Front\,Axle\,Heave \\
z_{tr} &= Rear\,Axle\,Heave \\
z_e &= Engine\,Heave \\
\nu &= Longitudinal\,Velocity \\
\omega_f &= Front\,Wheel\,Angular\,Velocity \\
\omega_r &= Rear\,Wheel\,Angular\,Velocity
\end{aligned}
$$

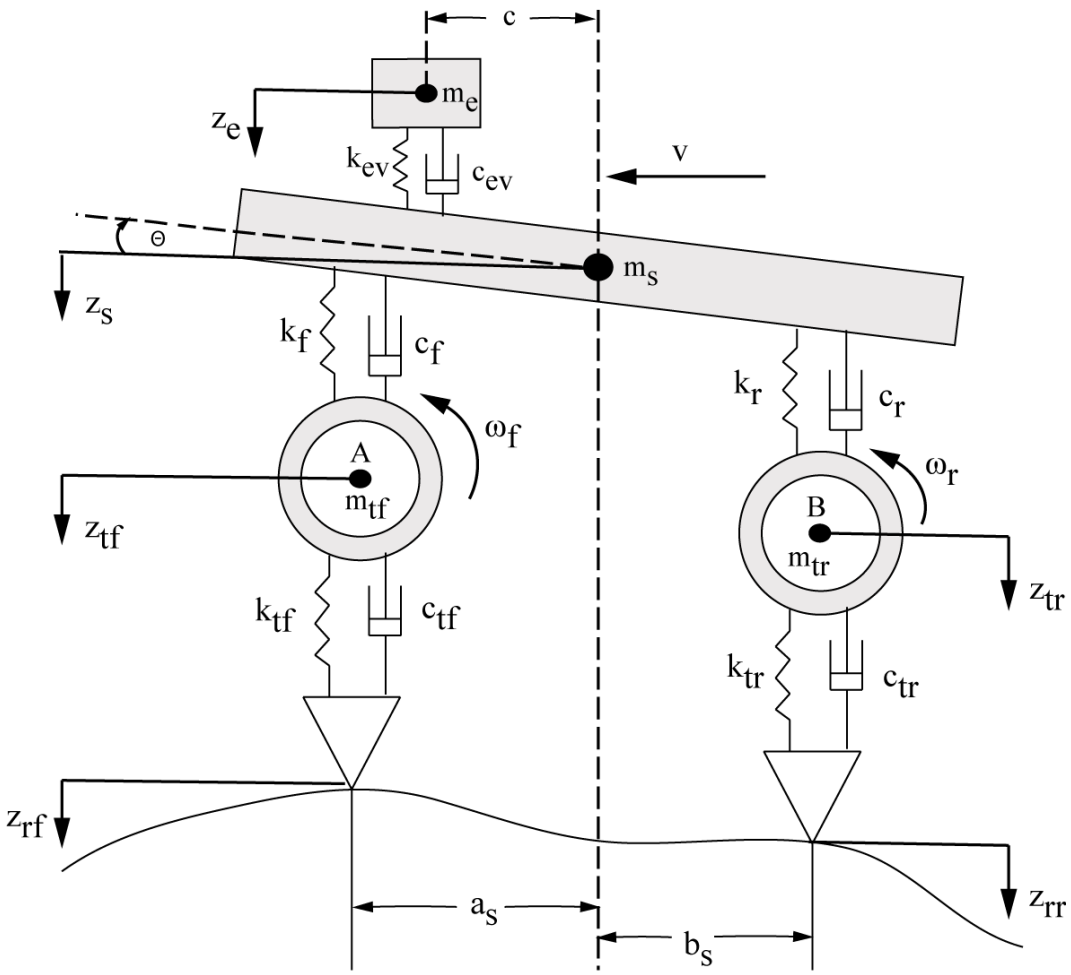


Figure A.1: 8 degree of freedom model

Figure A.2 shows the free body diagram with both static and dynamic forces on the sprung mass. Recall that the sprung mass is modeled as a rigid body. Note that points A and B mark the location of front and rear wheel centers respectively.

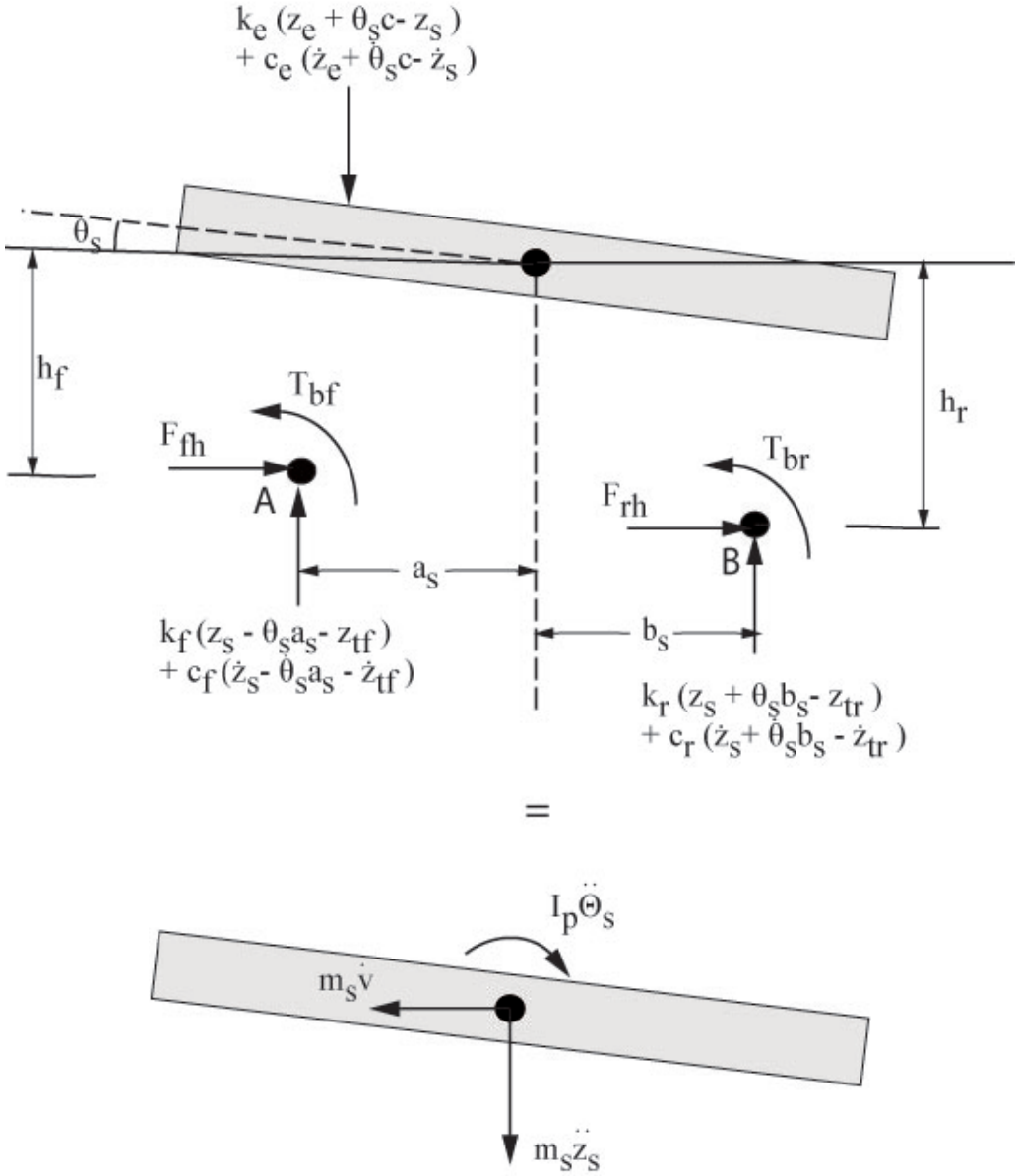


Figure A.2: Sprung Mass Free Body Diagram

Summing the vertical forces on both sides we have,

$$\begin{aligned} m_s\ddot{z}_s &= -k_f\left(z_s-\theta_s a_s-z_{tf}\right)-c_f\left(\dot{z}_s-\dot{\theta}_s a_s-\dot{z}_{tf}\right) \\ &\quad -k_r\left(z_s+\theta_s b_s-z_{tr}\right)-c_r\left(\dot{z}_s+\dot{\theta}_s b_s-\dot{z}_{tr}\right) \\ &\quad +k_e\left(z_e+\theta_s c-z_s\right)+c_e\left(\dot{z}_e+\dot{\theta}_s c-\dot{z}_s\right) \end{aligned} \tag{A.1}$$

Summing the moments about CG,

$$\begin{aligned} Ip\ddot{\theta}_s &= \left[k_f\left(z_s-\theta_s a_s-z_{tf}\right)+c_f\left(\dot{z}_s-\dot{\theta}_s a_s-\dot{z}_{tf}\right)\right]a_s \\ &\quad -\left[k_r\left(z_s+\theta_s b_s-z_{tr}\right)+c_r\left(\dot{z}_s+\dot{\theta}_s b_s-\dot{z}_{tr}\right)\right]b_s \\ &\quad -\left[k_e\left(z_e+\theta_s c-z_s\right)+c_e\left(\dot{z}_e+\dot{\theta}_s c-\dot{z}_s\right)\right]c \\ &\quad -F_{fh}h_f-F_{rh}h_r-T_{bf}-T_{br} \end{aligned} \tag{A.2}$$

where

$$\begin{aligned} h_f &= h_{wc}-\left(z_s-\theta_s a_s-z_{tf}\right) \\ h_r &= h_{wc}-\left(z_s+\theta_s b_s-z_{tr}\right) \\ h_{wc} &= Height\,of\,Sprung\,Mass\,CG\,above\,Wheel\,Center \end{aligned}$$

Note that $c_f\left(\dot{z}_s-\dot{\theta}_s a_s-\dot{z}_{tf}\right)\&\,c_r\left(\dot{z}_s+\dot{\theta}_s b_s-\dot{z}_{tr}\right)$ are the nonlinear shock forces. From Equations A.5 and A.2, sprung mass heave and pitch acceleration respectively are,

$$\begin{aligned} \ddot{z}_s &= \frac{1}{m_s}\{-k_f\left(z_s-\theta_s a_s-z_{tf}\right)-c_f\left(\dot{z}_s-\dot{\theta}_s a_s-\dot{z}_{tf}\right) \\ &\quad -k_r\left(z_s+\theta_s b_s-z_{tr}\right)-c_r\left(\dot{z}_s+\dot{\theta}_s b_s-\dot{z}_{tr}\right) \\ &\quad +k_e\left(z_e+\theta_s c-z_s\right)+c_e\left(\dot{z}_e+\dot{\theta}_s c-\dot{z}_s\right)\} \end{aligned} \tag{A.3}$$

$$\begin{aligned}
\ddot{\theta}_s &= \frac{1}{Ip}\{[k_f(z_s-\theta_s a_s-z_{tf})+c_f(\dot{z}_s-\dot{\theta}_s a_s-\dot{z}_{tf})]a_s \\
&\quad -[k_r(z_s+\theta_s b_s-z_{tr})+c_r(\dot{z}_s+\dot{\theta}_s b_s-\dot{z}_{tr})]b_s \\
&\quad -[k_e(z_e+\theta_s c-z_s)+c_e(\dot{z}_e+\dot{\theta}_s c-\dot{z}_s)]c \\
&\quad -F_{fh}h_f-F_{rh}h_r-T_{bf}-T_{br}\} \qquad \text{(A.4)}
\end{aligned}$$

Figure A.3 shows the free body diagram of the engine. Equation A.5 shows the corresponding equation of motion.

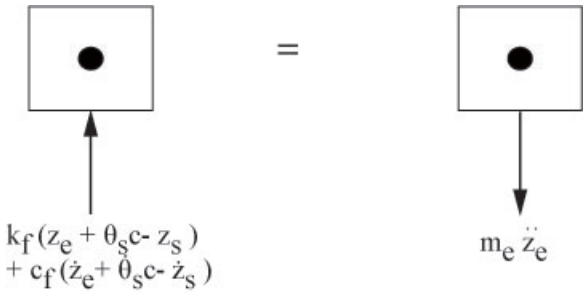


Figure A.3: Engine Free Body Diagram

$$\begin{aligned}
m_e\ddot{z}_e &= - \quad k_e(z_e+\theta_s c-z_s)-c_e(\dot{z}_e+\dot{\theta}_s c-\dot{z}_s) \\
\ddot{z}_e &= \quad \frac{1}{m_e}[k_e(z_e+\theta_s c-z_s)+c_e(\dot{z}_e+\dot{\theta}_s c-\dot{z}_s)] \qquad \text{(A.5)}
\end{aligned}$$

Figure A.4 shows the free body diagram of the front wheel under braking. The free body diagram for the rear wheel is similar. Both static and dynamic forces are shown for vertical and longitudinal motions. Moments acting on the wheel during braking are also shown.

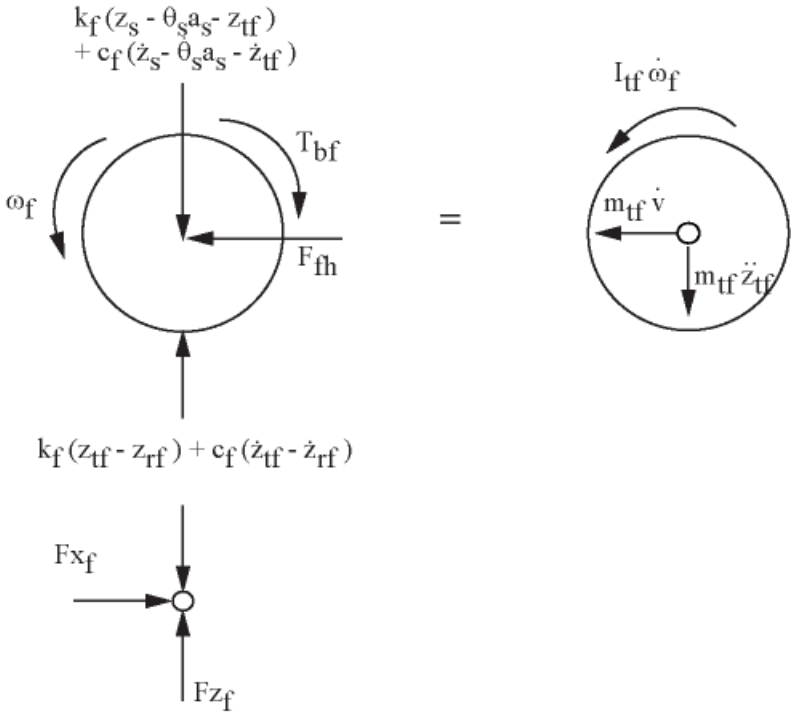


Figure A.4: Wheel Free Body Diagram

Summing the vertical forces on the wheel, the vertical acceleration can be found out as,

$$\begin{aligned} m_{tf}\ddot{z}_{tf} &= [k_f(z_s - \theta_s a_s - z_{tf}) + c_f(\dot{z}_s - \dot{\theta}_s a_s - \dot{z}_{tf})] \\ &\quad -[k_{tf}(z_{tf} - z_{rf}) + c_{tf}(\dot{z}_{tf} - \dot{z}_{rf})] \\ \ddot{z}_{tf} &= \frac{1}{m_{tf}}\{[k_f(z_s - \theta_s a_s - z_{tf}) + c_f(\dot{z}_s - \dot{\theta}_s a_s - \dot{z}_{tf})] \\ &\quad -[k_{tf}(z_{tf} - z_{rf}) + c_{tf}(\dot{z}_{tf} - \dot{z}_{rf})]\} \end{aligned} \tag{A.6}$$

The equation for angular acceleration is,

$$\begin{aligned} -I_{tf}\dot{\omega}_f &= T_{bf} - F_{xf} r_f \\ \dot{\omega}_f &= \frac{1}{I_{tf}} \{F_{xf} r_f - T_{bf}\} \end{aligned}$$

where $$r_f = Front\, Rolling\, Radius$$

$$k_{tf}\,(z_{tf} - z_{rf}) = Non\, Linear\, TWEEL\, Force$$

The longitudinal equation of motion is,

$$\begin{aligned} m_{tf}\dot{v} &= F_{fh} - F_{xf} \\ F_{fh} &= m_{tf}\dot{v} + F_{xf} \end{aligned} \tag{A.7}$$

Similarly for rear wheel, the vertical, rotational, and longitudinal equations are,

$$\begin{aligned} \ddot{z}_{tr} &= \frac{1}{m_{tr}} \{[k_r\,(z_s + \theta_s b_s - z_{tr}) + c_r\,(\dot{z}_s - + \dot{\theta} b_s - \dot{z}_{tr})] \\ &\quad -[k_{tr}\,(z_{tr} - z_{rr}) + c_{tr}\,(\dot{z}_{tr} - \dot{z}_{rr})] \end{aligned} \tag{A.8}$$

$$\dot{\omega}_r = \frac{1}{I_{tr}} \{F_{xr} r_r - T_{br}\} \tag{A.9}$$

where $$r_r = Rear\, Rolling\, Radius$$

$$k_{tr}\,(z_{tr} - z_{rr}) = Non\, Linear\, TWEEL\, Force$$

$$\begin{aligned} m_{tf}\dot{v} &= F_{fh} - F_{xf} \\ F_{fh} &= m_{tf}\dot{v} + F_{xf} \end{aligned} \tag{A.10}$$

The longitudinal equation of motion for the complete car is given as,

$$m_{total}\dot{v} = F_{xf} + F_{xr} \tag{A.11}$$

where $$m_{total} = m_s + m_{tf} + m_{tr}$$

The longitudinal reactions $F_{fh} \& F_{rh}$ at wheel center can be eliminated from Equation A.4 using Equations A.7 and A.10. There are 8 differential equations with 8 unknowns. The unknowns are $z_s, z_{tf}, \theta_s z_{tr}, z_e, \nu, \omega_f, \& \omega_r$ . The inputs to the model are $z_{rf}, z_{rr}, \dot{z}_{rf}, \dot{z}_{rr}, T_{bf}, \& T_{bf}$. This can be solved using numerical integration techniques in Simulink.

# Appendix B

# Vehicle Model Parameters

The input parameters for the BMW Mini in C + D configuration were selected from [19] and are as below :

| Symbol | Description, (unit) | Value |
|---|---|---|
| $L$ | Wheelbase, $(m)$ | 2.468 |
| $r_f$ | Front Rolling Radius $(m)$ | 0.29 |
| $r_r$ | Rear Rolling Radius $(m)$ | 0.296 |

Table B.1: Geometric Parameters

s

| Symbol | Description, (unit) | Value |
|---|---|---|
| $k_f$ | Front Suspension Stiffness (Per Axle), $\frac{kN}{m}$ | 66.3 |
| $k_r$ | Rear Suspension Stiffness (Per Axle), $\frac{kN}{m}$ | 50.6 |
| $k_{tf}$ | Front Tire Stiffness (Per Axle), $\frac{kN}{m}$ | 464.04 |
| $k_{tr}$ | Rear Tire Stiffness (Per Axle), $\frac{kN}{m}$ | 464.04 |
| $c_f$ | Front Suspension Damping (Per Axle), $\frac{N}{\frac{m}{s}}$ | 7839 |
| $c_r$ | Rear Suspension Damping (Per Axle), $\frac{N}{\frac{m}{s}}$ | 5180 |
| $c_{tf}$ | Front Tire Damping (Per Axle), $\frac{N}{\frac{m}{s}}$ | 93.6 |
| $c_{tr}$ | Rear Tire Damping (Per Axle), $\frac{N}{\frac{m}{s}}$ | 93.6 |

Table B.2: Suspension and Tire Parameters

| Symbol | Description, (unit) | Value |
|---|---|---|
| $m$ | Car (total) Mass, kg | 1323 |
| $W$ | Car (total) Weight (Calculation, W=m*g), kN | 12.979 |
| $m_{tf}$ | Front Unsprung Mass (includes wheels and tires ), kg | 141 |
| $m_{tr}$ | Rear Unsprung Mass (includes wheels and tires ), kg | 111 |
| $m_e$ | Engine + Transmission Mass, kg | 272 |
| $m_{sc}$ | Chassis + Engine Mass, kg | 1071 |
| $m_s$ | Sprung Mass, kg | 799 |
| $F/R$ | Front to Rear Weight Distribution | 60/40 |
| $a$ | Longitudinal Distance from Total CG to Front Wheels, m | 0.987 |
| $b$ | Longitudinal Distance from Total CG to Rear Wheels, m | 1.481 |
| $a_s$ | Longitudinal Distance from CG of Sprung Mass to Front Wheels, m | 1.3443 |
| $b_s$ | Longitudinal Distance from CG of Sprung Mass to Rear Wheels, m | 1.1237 |
| $h$ | Height of Car (total) CG above Ground, adjusted for CG of seated humans, m | 0.517 |
| $h_s$ | Height of Sprung Mass CG above Ground, m | 0.602 |
| $h_e$ | Height of CG of Engine + Transmission above Front Axle, m | 0.1397 |
| $d_e$ | Longitudinal Distance of CG of Engine + Transmission behind the Front Wheels, m | -0.157 |
| $I_z$ | Centroidal Pitch Inertia of Sprung Mass, $kg \cdot m^2$ | 680.4 |

Table B.3: Inertial Parameters and CG Locations

| Symbol | Description, (unit) | Value |
|---|---|---|
| $T_b$ | Full Brake Torque, $N-m$ | 6000 |
| $K_b$ | Brake Distribution (Front:Rear) | 70:30 |
| $\kappa_{high}$ | High Limit of ABS Controller | 0.15 |
| $\kappa_{low}$ | Low Limit of ABS Controller | 0.11 |
| $v_{cut}$ | ABS Cut-off Velocity (mph) | 5 |

Table B.4: Brake and ABS System Parameters

# Appendix C

# Simulink Models

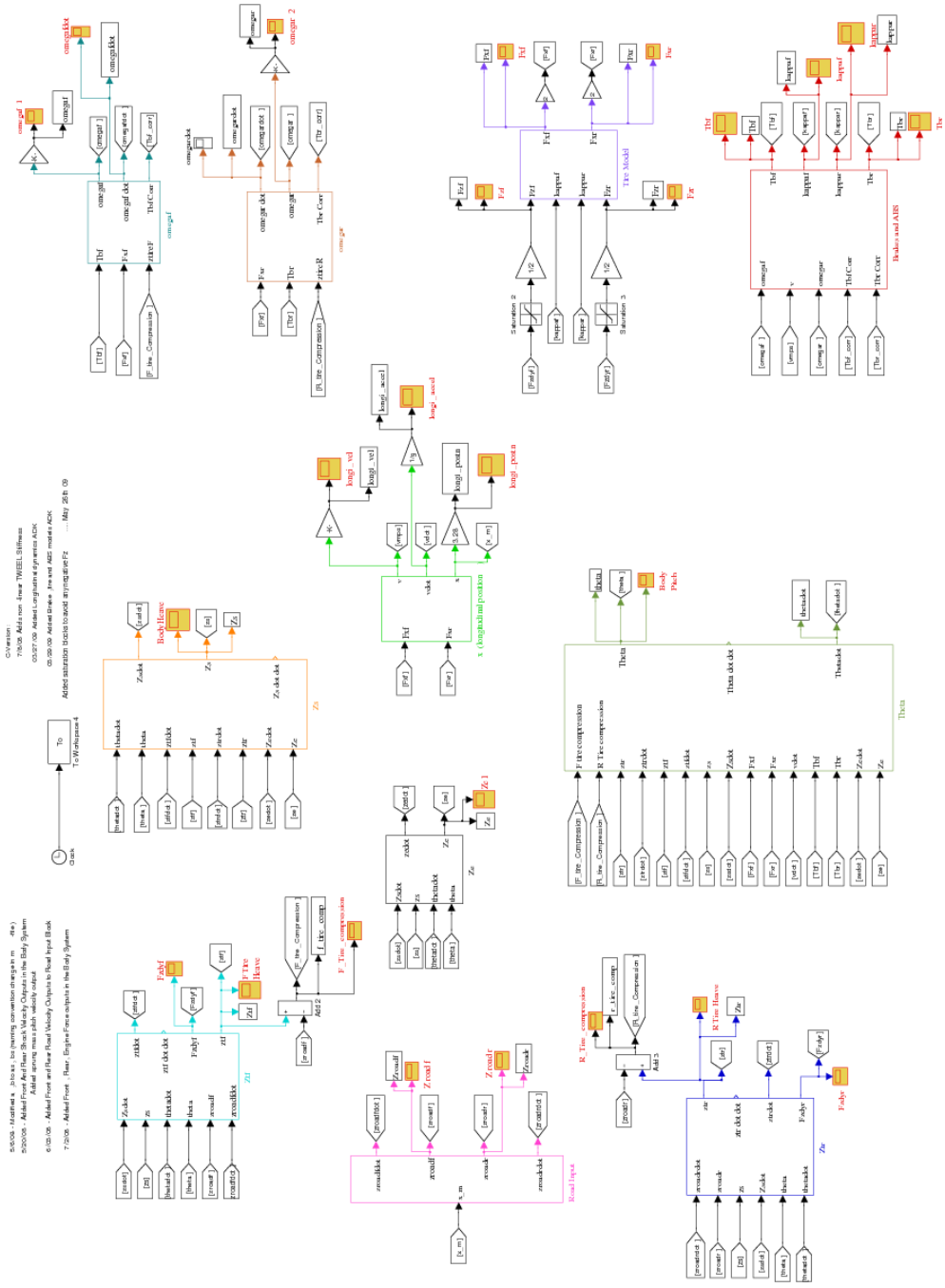

Figure C.1: Top Level Diagram

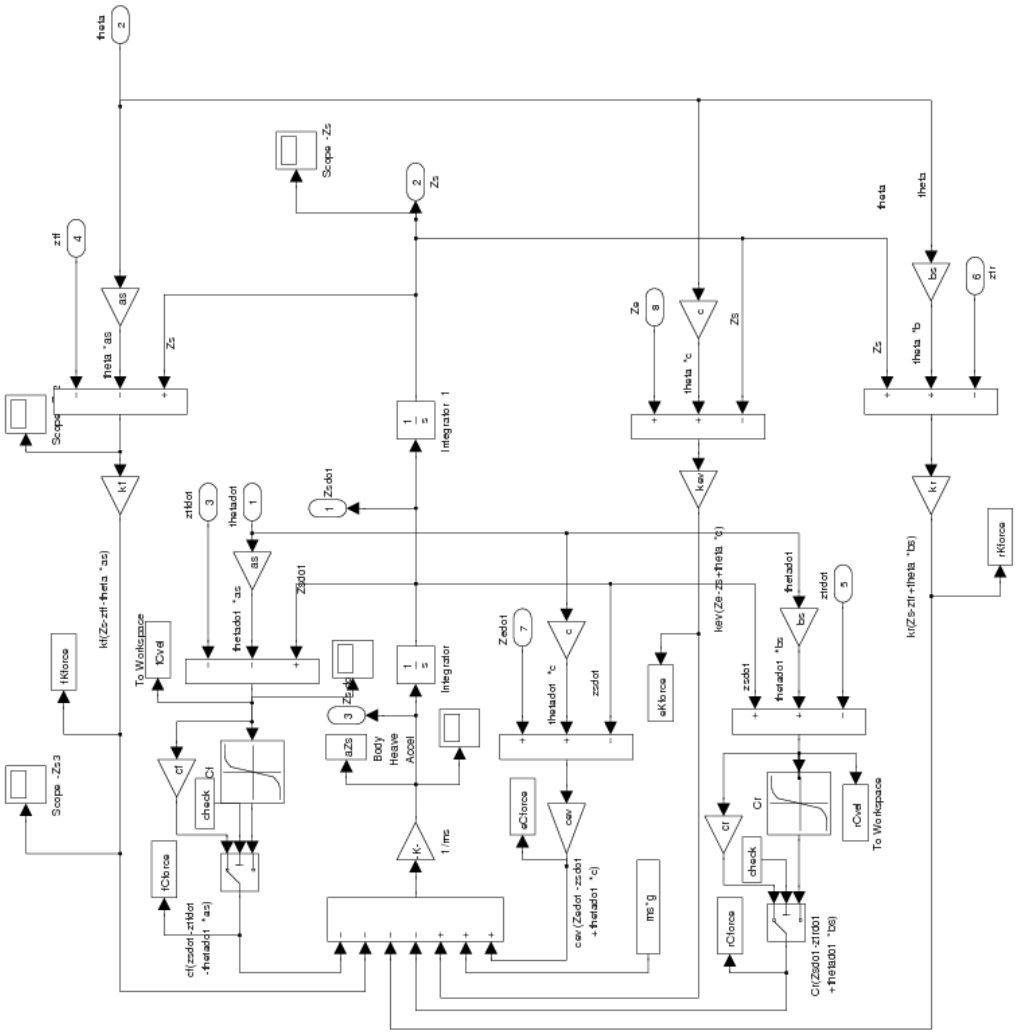


Figure C.2: Sprung Mass Heave

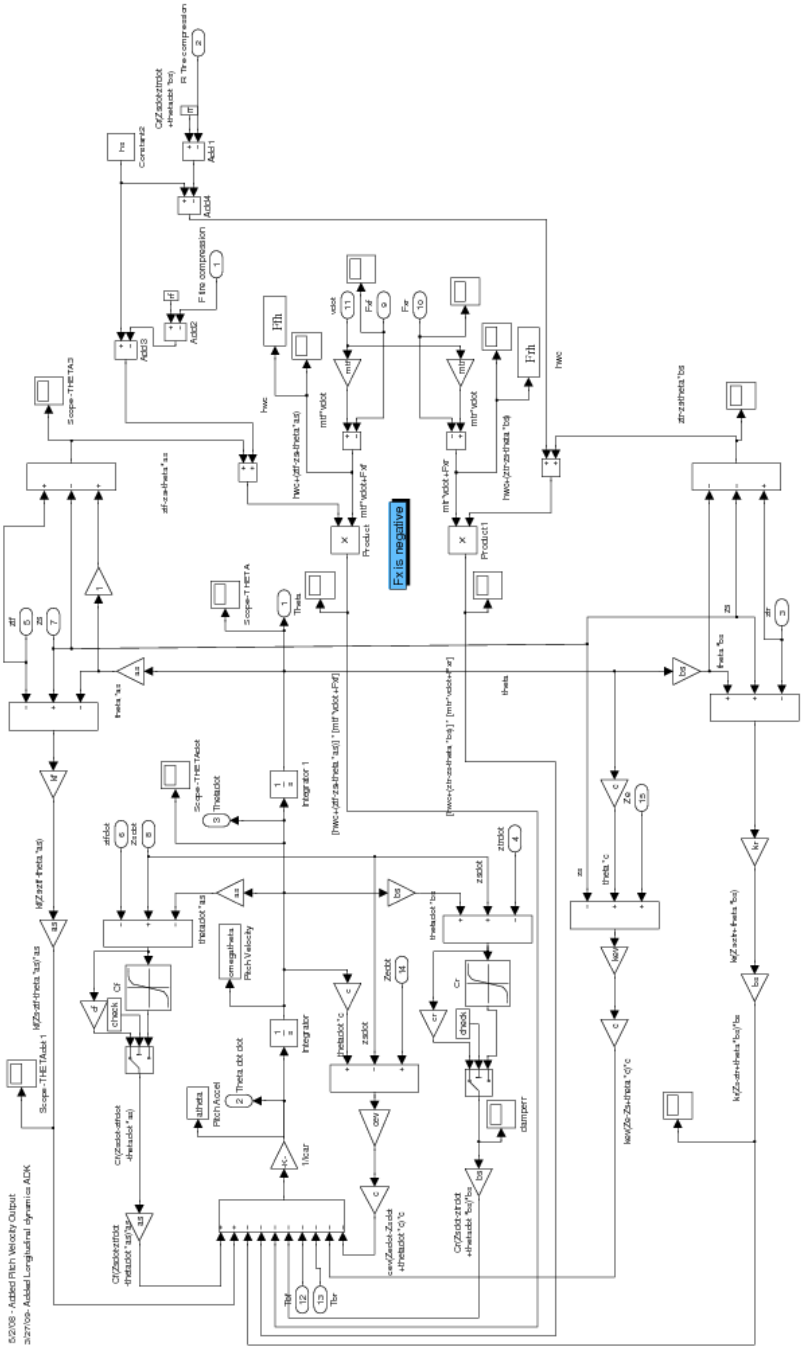


Figure C.3: Sprung Mass Pitch

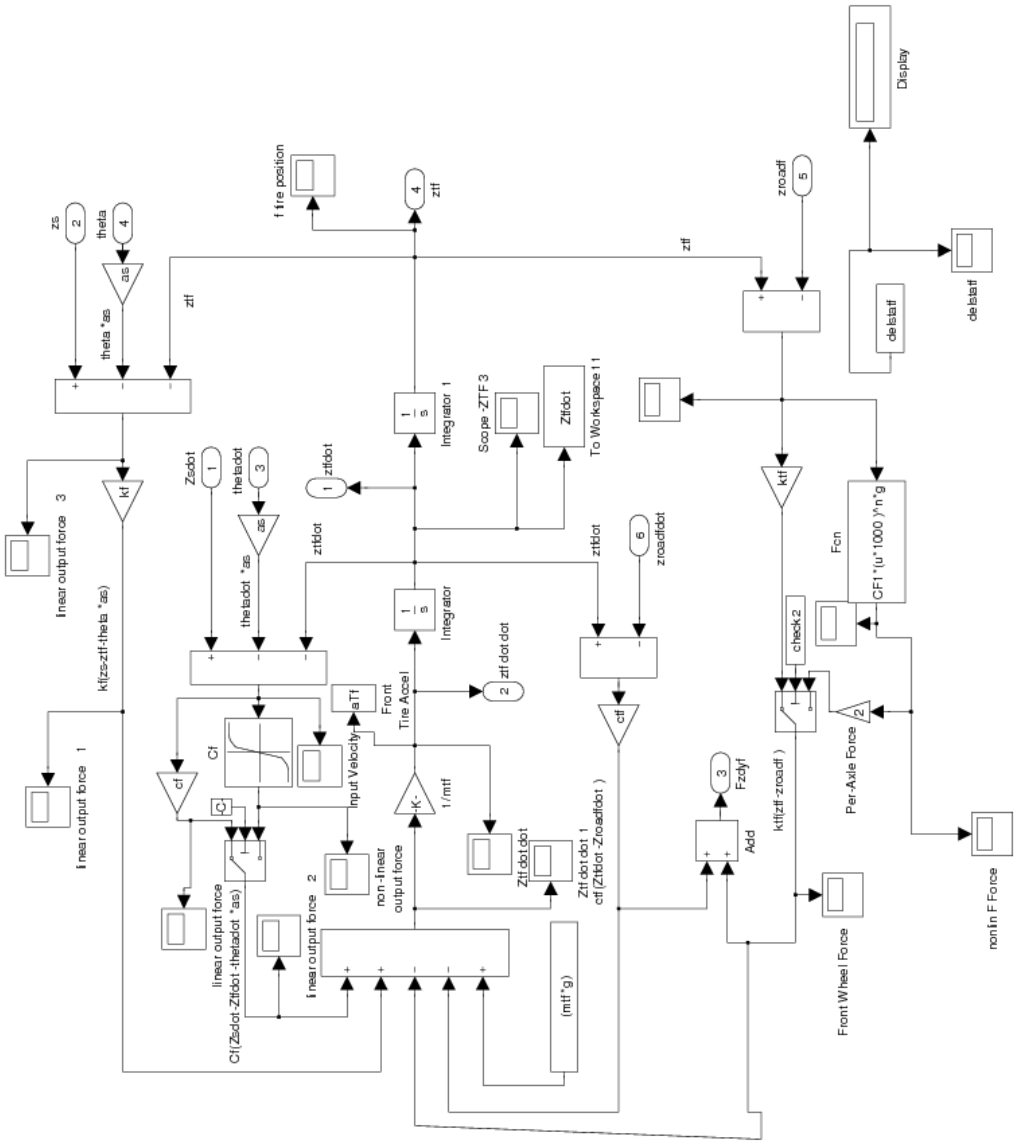


Figure C.4: Front Axle Heave

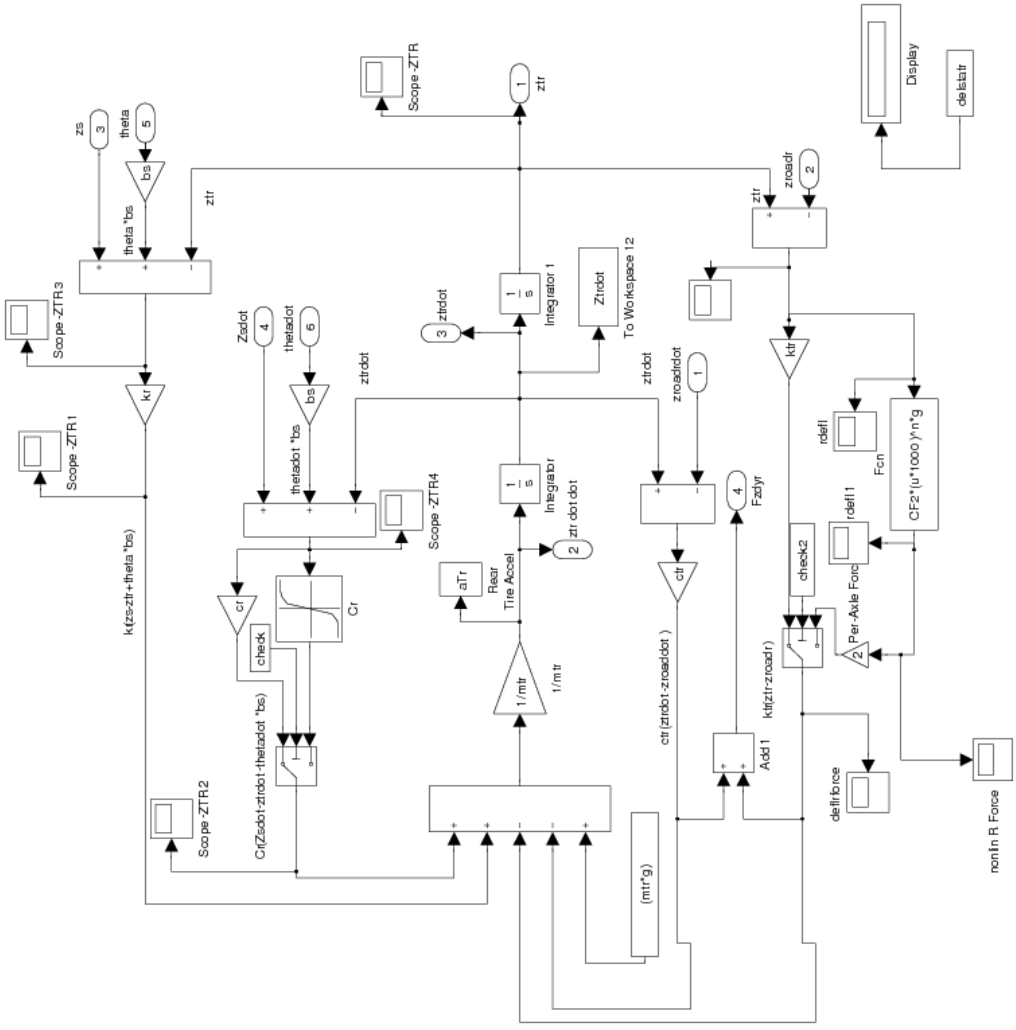


Figure C.5: Rear Axle Heave

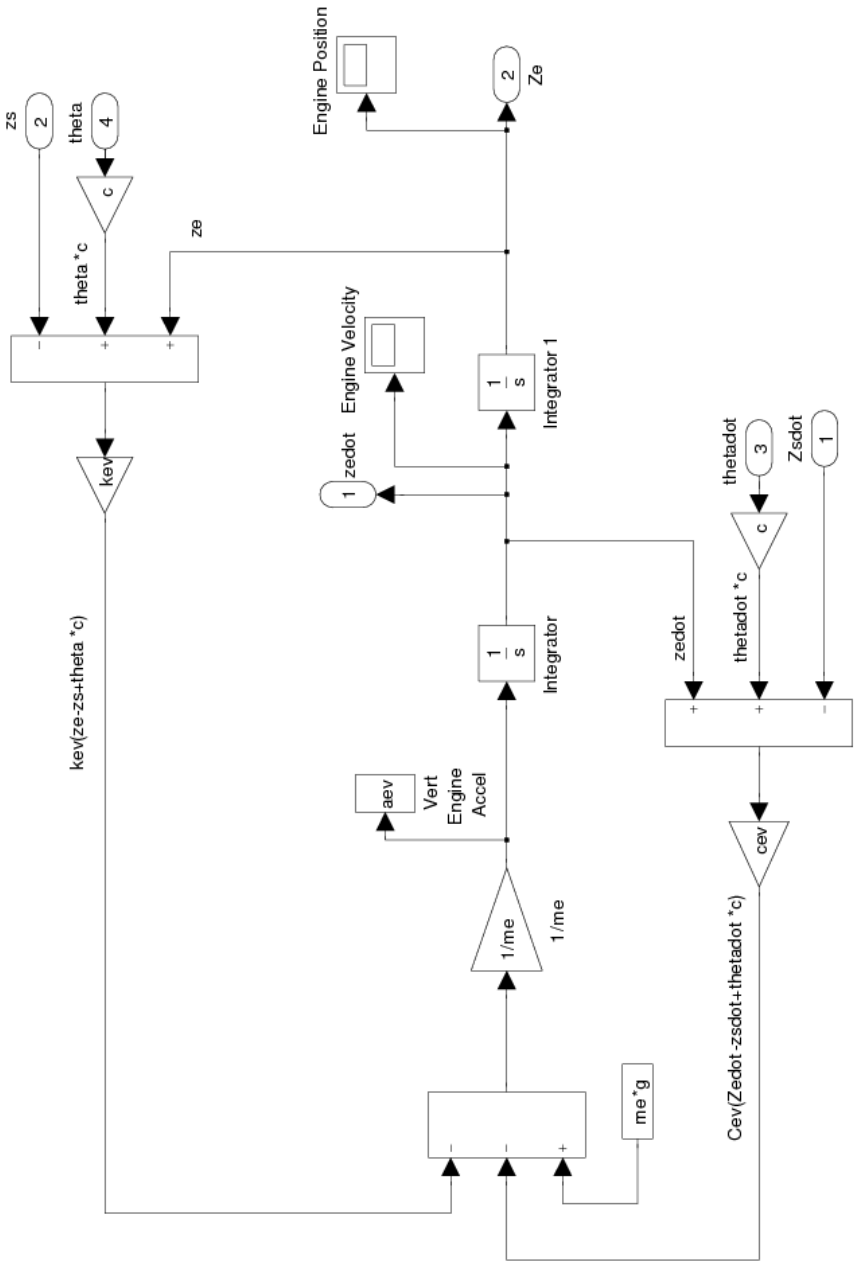


Figure C.6: Engine Heave

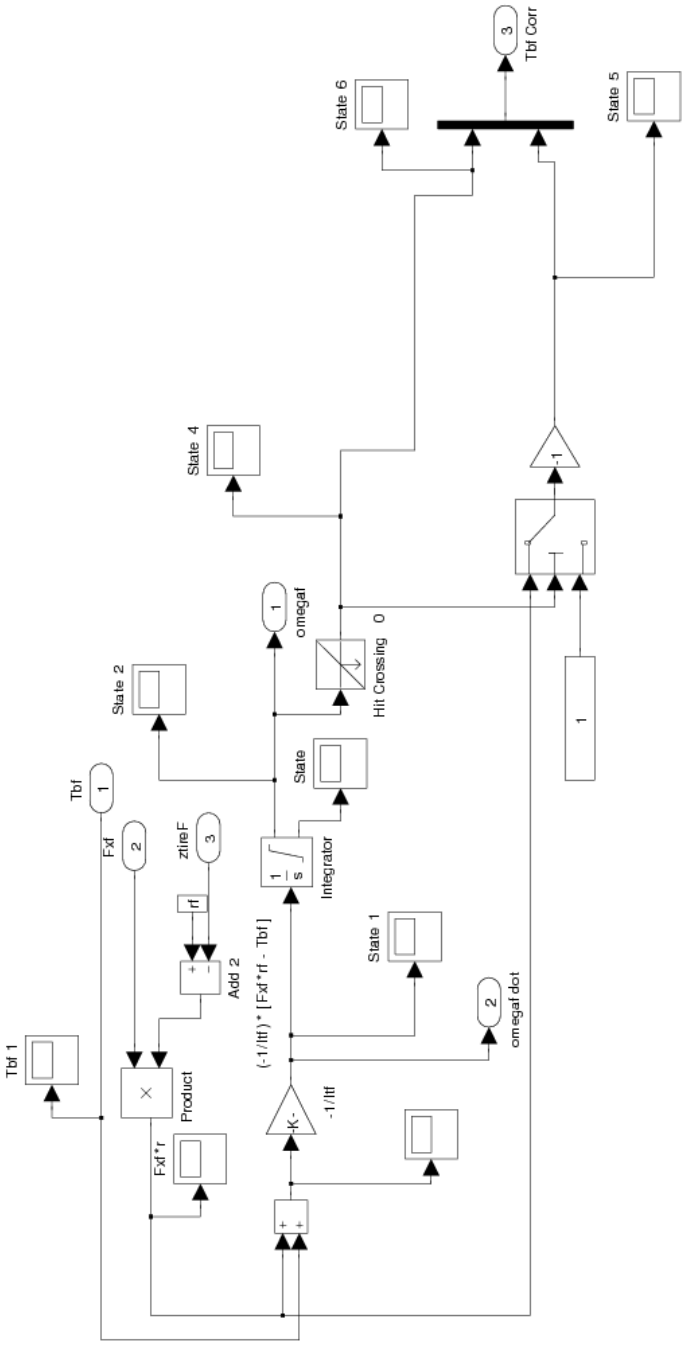


Figure C.7: Angular Velocity at Front

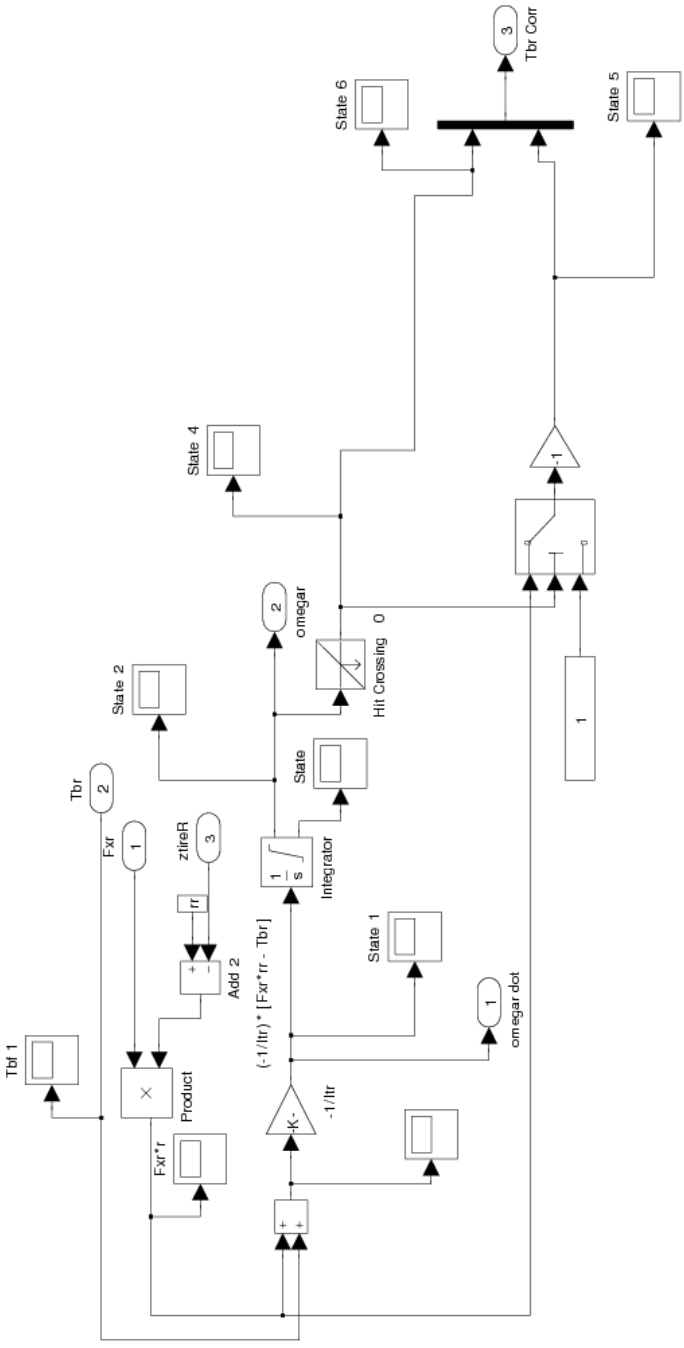


Figure C.8: Angular Velocity at Rear

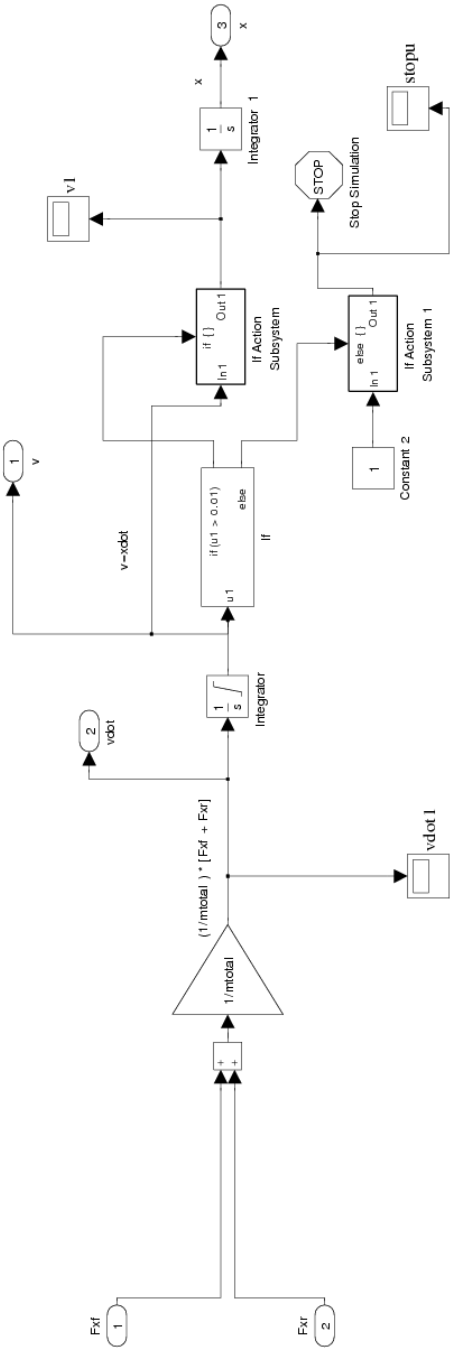


Figure C.9: Longitudinal Velocity of the Car

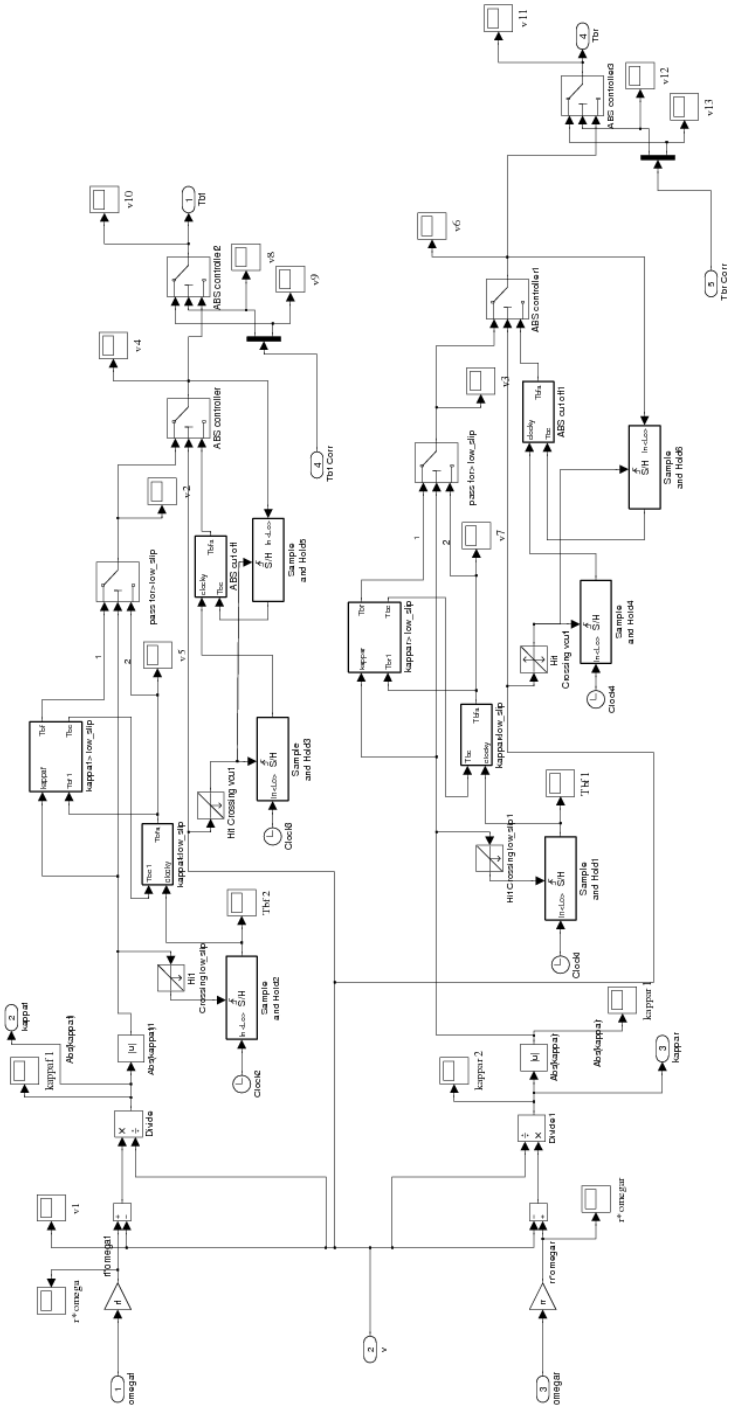


Figure C.10: Brakes and Anti-Lock System

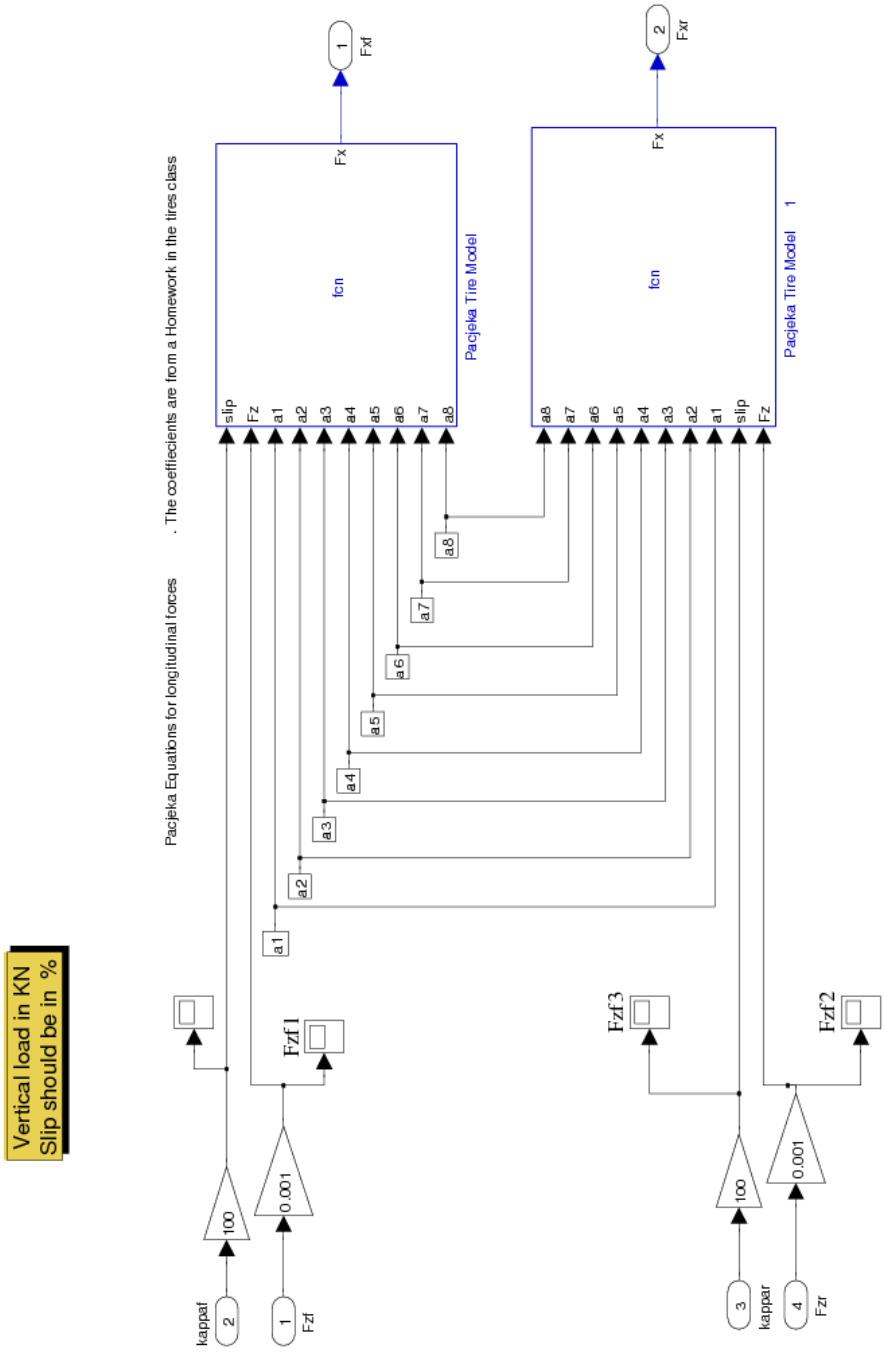


Figure C.11: Tire Model

# Appendix D

# Matlab Programs

## D.1 Shockdata.m

```
%%%%%%%%%%%%%%%%%%%%%%%%%%%%%%%%%%%%%%%%%%%%%%%%%%%%%%%%%%%%%%%%%%%%%%%%%%%%%%%
% shockdata.m %
% creates the lookup table parameters needed to use the shock dyno data in
% the Simulinkprograms. Note that the data is multiplied by two since
% this is a per axle force,and not a per corner force.
% % Created by MAP 5/22/08
%%%%%%%%%%%%%%%%%%%%%%%%%%%%%%%%%%%%%%%%%%%%%%%%%%%%%%%%%%%%%%%%%%%%%%%%%%%%%%%
%  Create Lookup Tables for Dampers
%  Equations from Excel Data Regression
velshock.f1=-1:.01:-.25;
velshock.f2=-.24:.01:.2;
velshock.f3=.21:.01:1;
frontforce1=(-497.52*velshock.f1+358.48)*2;
frontforce2=(88768*velshock.f2.^5+110931*velshock.f2.^4
+14449*velshock.f2.^3-10290*velshock.f2.^2-4031.1*velshock.f2)*2;
```

```
frontforce3=(-468.75*velshock.f3-801.25)*2;
frontforce=fliplr([frontforce1 frontforce2 frontforce3]);
velshock.r1=-1:.01:-.4;
velshock.r2=-.39:.01:-.1;
velshock.r3=-.09:.01:.13;
velshock.r4=.14:.01:.22;
velshock.r5=.23:.01:1;
rearforce1=(-391.7*velshock.r1+273.3)*2;
rearforce2=(-649.8*velshock.r2+170.1)*2;
rearforce3=(208662*velshock.r3.^4+39380*velshock.r3.^3-
26550*velshock.r3.^2-5177.8*velshock.r3)*2;
rearforce4=(208662*velshock.r4.^4+39380*velshock.r4.^3
-26550*velshock.r4.^2-5177.8*velshock.r4-88)*2;
rearforce5=(-1237.3*velshock.r5-1339.8)*2;
rearforce=fliplr([rearforce1 rearforce2 rearforce3 rearforce4 rearforce5]);
velshock=-1:.01:1;
ff=1;   %Fudge Factor For Rear Damping Curve
```

## D.2 Longitudinal_tire_force_estimation.m

```
%%
clear all
close all
clc
load Runny
load Carsim
%Longitudinal Tire force estimation
%Longitudinal Force Symbol = X, Units = N
%Slip Angle Symbol = delta, Units = deg
%Vertical Load Symbol = Z, Units = kN
%Camber Angle Symbol = gamma, Units = deg
%Pajecka coefficients taken from Dr. Rhyne's AuE 829 HW 8 and using that
%Pajecka formula will try to find a suitable solution for longitudinal
%force
%Some have been modified from what was originally given to give the curve
%wanted
a1=-21.3;
a2=1009;
a3=49.6;
a4=226;
a5=0.069;
a6=-0.001;
a7=0.056;
a8=0.486;
%%
%Pacjeka Magic Formula for longitudinal force
```

```
%This is intended purely as an estimation of the longitudinal force since
%no data actually exists.Some of this will be based off the Pacejka data
%for lateral force the other parts will be guesses based on what the curve
%should approximately look like. The goal is to have the peak Fx at 10%
%slip with mu at the same for lateral force,then at steady state have it
%drop off to 70% off peak for large slip ratio
%
Z=1.0:0.5:6.5; % range of vertical loads in kN
ZN=Z*1000; %vertical load in N
g=0:0.5:100; %slip ratio
trang=g'/100;
X=zeros(length(g),length(Z)); %preallocate
for i=1:length(g)
for k=1:length(Z)
D=a1*Z(k)^2+a2*Z(k);
C=1.615;
B=(a3*Z(k)^2+a4*Z(k))/(C*D*exp(a5*Z(k)));
E=a6*Z(k)^2+a7*Z(k)+a8;
theta=(1-E)*g(i)+(E/B)*atan(B*g(i));
X(i,k)=D*sin(C*atan(B*theta));
end
end
figure(1)
plot(g,X(:,1),g,X(:,2),g,X(:,3),g,X(:,4),g,X(:,5),g,X(:,6),g,X(:,7),g,X(:,8)...
,g,X(:,9),g,X(:,10),g,X(:,11),g,X(:,12),'linewidth',1.5)
ylabel('Longitudinal Force, kN','fontweight','bold','fontsize',12)
xlabel('Slip Ratio (%) ','fontweight','bold','fontsize',12)
title('Longitudinal Force vs. Slip Ratio','fontweight','bold','fontsize',12)
```

```
legend('1.0 kN','1.5 kN','2.0 kN','2.4 kN', '3.0 kN', '3.5 kN', '4.0 kN','4.5 kN'
,'5.0 kN','5.5 kN','6.0 kN','6.5 kN','Location','best')
grid on
saveas(gcf,'Longitudinal Force vs. Slip Ratio', 'ai')
figure
plot(g,X(:,1)./ZN(1),g,X(:,2)./ZN(2),g,X(:,3)./ZN(3),g,X(:,4)./ZN(4)...
,g,X(:,5)./ZN(5),g,X(:,6)./ZN(6),g,X(:,7)./ZN(7),g,X(:,8)./ZN(8)...
,g,X(:,9)./ZN(9),g,X(:,10)./ZN(10),g,X(:,11)./ZN(11),g,X(:,12)./ZN(12)
,'linewidth',1.5)
legend('1.0 kN','1.5 kN','2.0 kN','2.4 kN', '3.0 kN', '3.5 kN',
'4.0 kN','4.5 kN','5.0 kN','5.5 kN','6.0 kN',
'6.5 kN','7 kN','Location','best')
hold on
% plot(-kappaf*100,-Fxf./Fzf,':k','linewidth',4)
ylabel('Mu = Fx/Fz','fontweight','bold','fontsize',12)
xlabel('Slip Ratio (%)','fontweight','bold','fontsize',12)
title('Mu vs. Slip Ratio','fontweight','bold','fontsize',12)
grid on
saveas(gcf,'Mu vs. Slip Ratio', 'ai')
figure
plot(g,X(:,1)./ZN(1),g,X(:,2)./ZN(2),g,X(:,3)./ZN(3),g,X(:,4)./ZN(4)...
,g,X(:,5)./ZN(5),g,X(:,6)./ZN(6),g,X(:,7)./ZN(7),g,X(:,8)./ZN(8)...
,g,X(:,9)./ZN(9),g,X(:,10)./ZN(10),g,X(:,11)./ZN(11),
g,X(:,12)./ZN(12),'linewidth',1.5) legend('1.0 kN','1.5 kN',
'2.0 kN','2.4 kN', '3.0 kN', '3.5 kN', '4.0 kN','4.5 kN'
,'5.0 kN','5.5 kN','6.0 kN','6.5 kN','7 kN','Location','best')
hold on plot(-kappaLF*100,-Fx_front./Fz_front,':k','linewidth',4)
ylabel('\mu = Fx/Fz','fontweight','bold','fontsize',12)
```

```
xlabel('Slip Ratio (%) ','fontweight','bold','fontsize',12)
title('\mu versus Slip Ratio','fontweight','bold','fontsize',12)
grid on
nend1=size(X);  % gets index of last value nend=nend1(1);
longss=X(nend); % steady state longitudinal force at high slip
peak=max(X(:,1));
ratio=longss/peak;
fprintf('Percentage of steady state to max force %.3f \n',ratio) disp('  ')
%% %find the coefficient of friction for longitudinal slip
mu1=max(X(:,1))/ZN(:,1);
mu2=max(X(:,2))/ZN(:,2);
mu3=max(X(:,3))/ZN(:,3);
mu4=max(X(:,4))/ZN(:,4);
mu5=max(X(:,5))/ZN(:,5);
mu6=max(X(:,6))/ZN(:,6);
mu7=max(X(:,7))/ZN(:,7);
mu8=max(X(:,8))/ZN(:,8);
mu9=max(X(:,9))/ZN(:,9);
mu10=max(X(:,10))/ZN(:,10);
mu11=max(X(:,11))/ZN(:,11);
mu12=max(X(:,12))/ZN(:,12);
mu=[mu1 mu2 mu3 mu4 mu5 mu6 mu7 mu8 mu9 mu10 mu11 mu12];
muavg=mean(mu);
fprintf('Mu, Fy/Fz        %.3f \n',muavg) disp('  ')
```

## D.3 DOF8_Straight_Line_Braking.m

```
%%%%%%%%%%%%%%%%%%%%%%%%%%%%%%%%%%%%%%%%%%%%%%%%%%%%%%%%%%%%%%%%%%%%%%%%%%%%
%
% rh5psd5D.m   DEVELOPED BY EHL 2-25-93 (psd6.m) and MODIFIED 9-23-96
% CALCULATES PSDs OF 5 DOF CAR with TWEELs -
%
% Edited by ADK in April 09 to add longitudinal degrees of
% freedom to the existing ride model.
%
%
% The Degrees of Freedom are:
%       x1=z            car body vertical, positive down
%       x2=theta        car body pitch, positive nose up
%       x3=zf           front axle vertical, positive down
%       x4=zr           rear axle vertical, positive down
%       x5=ze           Engine Heave, positive down
%       x6=v            Longitudinal Velocity of car, SAE convention
%       x7=wf           Rotational velocity of Front Wheel, +ve Clockwise
%       x8=wr           Rotational Velocity of Rear Wheel, +ve Clcokwise
% Engine DOF added May 2007, EHL
%
% Choice of configurations added, Dec. 29, 2007, EHL
%
% Includes TWEEL stiffness and damping values, Jan 3, 2008
%
% Code rewritten to Work with Simulink 5 DOF model, May 22, 2008
%
```

```
% Code rewritten to Work with Simulink 8 DOF model, June 15, 2009
%
% Includes TWEEL nonlinear Stiffness, July 12, 2008
%
% Select the ode45 solver with following parameters to run the cases
since ode1 creates problems with
% stiffer TWEELs.
%
% Max Step size------------0.005
% Min Step size-------------auto
% Initial Step size---------0.002
% Relative tolerance--------1e-6
% Absolute tolerance--------auto
%%%%%%%%%%%%%%%%%%%%%%%%%%%%%%%%%%%%%%%%%%%%%%%%%%%%%%%%%%%%%%%%%%%%%%%
clc
clear
close all
clear all
format short g
format compact
disp('  ')
disp('         %%%%%%%%%%     %%%%%       %%%%     %%%%%%%%%%%%%   ')
disp('         %%%%%%%%%%     %%%%%%    %%%%%%     %%%%        %%%%')
disp('            %%%         %%%% %%%%% %%%%     %%%         %%%%')
disp('            %%%         %%%%  %%%  %%%%     %%%%        %%%%' )
disp('            %%%         %%%%        %%%%     %%%%%%%%%%%%    ')
disp('            %%%         %%%%        %%%%     %%%                ')
disp('         %%%%%%%%%%     %%%%        %%%%     %%%              %%%%')
```

```
disp('          %%%%%%%%%%      %%%%        %%%%      %%%             %%%%')
disp('  ')
disp('  ')
disp('  ')
disp('*****************************************************************
*************************************')
disp('*****THE INITIAL CONDITIONS FOR Zs, Ztf, Ztr, theta MUST BE
CALCULATED BY RUNNING THE RIDE MODEL ******')
disp('*****************************************************************
*************************************')
disp('  ')
disp (' Static Fz Front = 3895.1 N ' )
disp (' Static Fz Rear = 2594.25 N ' )
% read in parameters in SI units
vmph=input('Input speed in mph, Speed =  ');
vmps=vmph*0.4469;   % speed, meters/sec
weightchoice=input('Which Configuration do you want to analyze?
\n 1. Curb + Driver, tested at LPG \n 2. Curb + 2 Passengers \n
3. GVW \n >>');
if weightchoice==1
    Param_Curb_Driver_ADK
%     Param_Carsim
    param= char('C+D');
    KTF=[2*156.8e3,2*156.8e3,2*156.8e3,2*156.8e3,ktf];
%TWEEL front Stiffness, N/m, per axle
    KTR=[2*186.53e3,2*186.53e3,2*186.53e3,2*186.53e3,ktr];
%TWEEL Rear Stiffness, N/m, per axle
%     CTF=[400,400,400,400,ctf];           %Front TWEEL/Tire damping,
```

```
N/(m/s) (per axle)
%     CTR=[400,400,400,400,ctr];           %Rear TWEEL/Tire damping,
N/(m/s) (per axle)
    CTF=[0,0,0,0,ctf];                %Front TWEEL/Tire damping,
N/(m/s) (per axle)
    CTR=[0,0,0,0,ctr];                %Rear TWEEL/Tire damping,
N/(m/s) (per axle)
elseif weightchoice==2
    Param_Curb_2Front          % This is not really used since
only C+D and GVW is focused on..note the different format than other
files
elseif weightchoice==3
    Param_GVW_ADK
    param= char('GVW');
     KTF=[2*150.39e3,2*150.39e3,2*150.39e3,2*150.39e3,ktf];
%TWEEL/Front tire Stiffness, N/m, per axle
    KTR=[2*166.79e3,2*166.79e3,2*166.79e3,2*166.79e3,ktr];
%TWEEL/Rear tire Stiffness, N/m, per axle
    CTF=[400,400,400,400,ctf];                %Front TWEEL/Tire damping,
N/(m/s) (per axle)
    CTR=[400,400,400,400,ctr];                %Rear TWEEL/Tire damping,
N/(m/s) (per axle)
end
% t2=L/vmps;
%% Brake Torque definition
Tb_full=6000;                         %Total brake torque in N-m
% Tb_full=0;                          %Total brake torque in N-m
distri=0.70;                          % Desired distribution on front axle.
```

```
Tb_full_front=(distri*Tb_full);
Tb_full_rear=((1-distri)*Tb_full);
low_slip=0.11;                  %The low range of slip for ABS controller
high_slip=0.15;                 %The high range of slip for ABS controller
vcut=65;                        % disable ABS at this velocity in mph
vcut=vcut*0.4469 ;              %vcut in mps
%% Pacjeka coefficients (THIS SECTION NOT BEING USED IN THIS VERSION OF CODE)
%Longitudinal Tire force estimation
%Longitudinal Force Symbol = X, Units = N
%Slip Angle Symbol = delta, Units = deg
%Vertical Load Symbol = Z, Units = kN
%Camber Angle Symbol = gamma, Units = deg
%Pajecka coefficients taken from Dr. Rhyne's AuE 829 HW 8 and using that
%Pajecka formula will try to find a suitable solution for longitudinal force.
%Some have been modified from what was originally given to give the
desired curve.
a1=-21.3;
a2=1009;
a3=49.6;
a4=226;
a5=0.069;
a6=-0.001;
a7=0.056;
a8=0.486;
%% Define Road Profile
% Depending on the road type generated in the Anup_PSD file change the
% labels used in this part of the code.
% road1= constant RMS road 1
```

```
% road2= constant RMS road 2
% road3= constant N road 1
% road4= constant N road 2
% road5= Rough Runway
% road6= Gravel
% road7= LPG weathered asphalt
% road8= FLAT
% road9= BUMP
% Make your choice of road by choosing the appropriate mat file.
roadchoice=input('Which Road do you want? \n 1. Road Const RMS # 1
\n 2. Road Const RMS # 2   \n 3. Road Const N # 1  \n 4. Road Const N # 2
\n 5. Smooth Highway \n 6. Gravel Road  \n 7. LPG Weathered Asphalt
\n 8. FLAT \n 9. Bump \n >>');
roadtypes=char('Road 1','Road 2','Road Const N # 1','Road Const N # 2',
'Smooth Highway','Gravel Road','LPG Weathered Asphalt','FLAT','Bump');
% filename= strcat('road',num2str(roadchoice));
% load filename
roadtype=roadtypes(roadchoice,:);
if roadchoice==1
    load road_const_RMS1
    road=road1;
elseif roadchoice==2
    load road_const_RMS2
    road=road2;
elseif roadchoice==3
    load road_const_N_1
    road=road3;
elseif roadchoice==4
```

```
    load road_const_N_2
    road=road4;
elseif roadchoice==5
    load Smooth_Highway
    road=road5;
elseif roadchoice==6
    load Gravel
    road=road6;
elseif roadchoice==7
    load LPG
    road=road7;
elseif roadchoice==8
    load road8
    road=road8;
elseif roadchoice==9
    load bump30
    road=bump30;
else

end
% The time t below corresponds to a time vector in
"Braking_Road_PSD.m" file. This file was used to
% generate this road profile assuming a velocity of 60 mph. We are using
% the same time in here to match the array sizes.
The simulink model "derivative.mdl" calculates the input
% road velocities to the model from the input road profile.
% it does not matter what time step we use here since we use x vs z tables
% in the main simulation. However, it would matter what step size we use
```

```
% when we do a derivative on the road data obtained
from "Braking_Road_PSD.m". Hence
% this exercise.
% Take over if bump is used
if roadchoice==9
    load dbumpdt30
    road_vel=dbumpdt30;
else
t=(0:0.01:20)';
sample=diff(t);
options=simset('Solver','ode1','FixedStep',(t(2)-t(1)));
sim('derivative',t(end),options);
% derivative model gives a file road_vel with time and velocity values for
% the road input.
load road_vel
road_vel=road_vel';
end
%% Damper Data
% load Damper lookup curves
% updated MAP 12/08
shockdata       % Changed to take in full non linear shock data for
larger velocities....edited ADK
load springs
%%
%%%%%%%%%%%%%%%%%%%%%%%%%%%%%%%%%%
% Begin Main Loop
%%%%%%%%%%%%%%%%%%%%%%%%%%%%%%%%%%
Del_static1=15;         % Max Static Defelection in mm
```

```
np=[0.4 0.6 0.8 1];
for eee=1:length(Del_static1)
for sss=1:5;

        if sss==1,
        check2=0;
        Del_static=Del_static1(eee);
        disp('-----------------------------------------------------
-----------------------------------')
        fprintf('\n****** delta max =%3.0f mm NONLINEAR TWEEL
STIFFNESS VALUE ********\n',Del_static)
        disp('-----------------------------------------------------
-------------------------')

        FmaxF=438; %Heaviest wheel load possible (Front wheel at GVW), kg
        n=np(sss);


        logCF=-n*log10(Del_static) + log10(FmaxF);
        CF=10^logCF;
        CF1=CF;
        CF2=CF;
        dell=0:0.1:50;
        F=CF*dell.^n;                    % kg
        dfddel=CF*n*dell.^(n-1);         % kg/mm
        dfddel_Npm=dfddel*9.81*1000;     % N/m
        logdel_F=(log10(mtf/2+mFaxle/2)-logCF)/n;
        delstatf=10^logdel_F/1000;          % Front static deflection, m
```

```
        logdel_R=(log10(mtr/2+mRaxle/2)-logCF)/n;
        delstatr=10^logdel_R/1000;          % Rear static deflection, m
        Zs_ini=9.5787e-2;
        Ztf_ini=1.1736e-2;
        Ztr_ini=4.2488e-3;
        theta_ini=-9.3611e-3;
        Ze_ini=1.121e-1;

        elseif sss==2
        check2=0;
        Del_static=Del_static1(eee);
        disp('-----------------------------------------------------
-------------------------------------')
        fprintf('\n****** delta max =%3.0f mm NONLINEAR TWEEL
STIFFNESS VALUE ********\n',Del_static)
        disp('-----------------------------------------------------
-------------------------------------')
        FmaxF=438; %Heaviest wheel load possible (Front wheel at GVW), kg
        n=np(sss);

        logCF=-n*log10(Del_static) + log10(FmaxF);
        CF=10^logCF;
        CF1=CF;
        CF2=CF;
        dell=0:0.1:50;
        F=CF*dell.^n;                    % kg
        dfddel=CF*n*dell.^(n-1);         % kg/mm
        dfddel_Npm=dfddel*9.81*1000;     % N/m
```

```
        logdel_F=(log10(mtf/2+mFaxle/2)-logCF)/n;
        delstatf=10^logdel_F/1000;          % Front static deflection, m
        logdel_R=(log10(mtr/2+mRaxle/2)-logCF)/n;
        delstatr=10^logdel_R/1000;          % Rear static deflection, m

        Zs_ini=9.7453e-2;
        Ztf_ini=1.2736e-2;
        Ztr_ini=6.4695e-3;
        theta_ini=-8.8666e-3;
        Ze_ini=1.1302e-1;

        elseif sss==3
        check2=0;
        Del_static=Del_static1(eee);
        disp('-----------------------------------------------------------
---------------------------------')
        fprintf('\n****** delta max =%3.0f mm NONLINEAR TWEEL
STIFFNESS VALUE ********\n',Del_static)
        disp('-------------------------------------------------------------
--------------------------------')
        FmaxF=438; %Heaviest wheel load possible (Front wheel at GVW),kg
        n=np(sss);

        logCF=-n*log10(Del_static) + log10(FmaxF);
        CF=10^logCF;
        CF1=CF;
        CF2=CF;
        dell=0:0.1:50;
```

```
        F=CF*dell.^n;                    % kg
        dfddel=CF*n*dell.^(n-1);         % kg/mm
        dfddel_Npm=dfddel*9.81*1000;     % N/m
        logdel_F=(log10(mtf/2+mFaxle/2)-logCF)/n;
        delstatf=10^logdel_F/1000;          % Front static deflection, m
        logdel_R=(log10(mtr/2+mRaxle/2)-logCF)/n;
        delstatr=10^logdel_R/1000;          % Rear static deflection, m
        Zs_ini=9.8519e-2;
        Ztf_ini=1.3268e-2;
        Ztr_ini=7.9832e-3;
        theta_ini=-8.4687e-3;
        Ze_ini=1.1349e-1;

        elseif sss==4
        check2=0;
        Del_static=Del_static1(eee);
        disp('-----------------------------------------------------
-----------------------------------')
        fprintf('\n****** delta max =%3.0f mm NONLINEAR TWEEL
STIFFNESS VALUE ********\n',Del_static)
        disp('-----------------------------------------------------
-----------------------------------')
        FmaxF=438; %Heaviest wheel load possible (Front wheel at GVW), kg
        n=np(sss);
        logCF=-n*log10(Del_static) + log10(FmaxF);
        CF=10^logCF;
        CF1=CF;
        CF2=CF;
```

```
        dell=0:0.1:50;
        F=CF*dell.^n;                    % kg
        dfddel=CF*n*dell.^(n-1);         % kg/mm
        dfddel_Npm=dfddel*9.81*1000;     % N/m
        logdel_F=(log10(mtf/2+mFaxle/2)-logCF)/n;
        delstatf=10^logdel_F/1000;          % Front static deflection, m
        logdel_R=(log10(mtr/2+mRaxle/2)-logCF)/n;
        delstatr=10^logdel_R/1000;          % Rear static deflection, m

        Zs_ini=9.9254e-2;
        Ztf_ini=1.3598e-2;
        Ztr_ini=9.0565e-3;
        theta_ini=-8.1674e-3;
        Ze_ini=1.1377e-1;

        elseif sss==5
        disp('****** OEM TIRE VALUES ********')
        check2=1;
         delstatf=((mtf/2+mFaxle/2)*g)/(KTF(sss)/2);
% This calculates the static defelction of the pneumatic tire
% which is then used to limit the extension of tire when it unloads.
         delstatr=((mtr/2+mRaxle/2)*g)/(KTR(sss)/2);
        Zs_ini=1.0186e-1;
        Ztf_ini=1.6788e-2;
        Ztr_ini=1.1181e-2;
        theta_ini=-8.5991e-3;
        Ze_ini=1.1703e-1;
        end
```

```
ktf=KTF(sss);
ktr=KTR(sss);
ctf=CTF(sss);
ctr=CTR(sss);
%% Run The Model
%
% check=1 runs linear shock model
% check=0 runs nonlinear shock model
check=0;
% road_choice=1 runs 4_post input
% road_choice=2 runs WA road input
% road_choice=3 runs Discrete Bump input
% road_choice=2;
% DOF5
% [T,X,Y]=sim('DOF8_Anup_ABS',20);  %,options
% [T,X,Y]=sim('DOF8_Anup_ABS_NL_Spring',20);  %,options
[T,X,Y]=sim('DOF8_Anup_ABS_No_Engine',20);  %,options
% [T,X,Y]=sim('DOF8_Anup_ABS_Static',20);  %,options
%% PLOTS
%
% Since the simulation does not run for a specified time the vectors are of
% different lenghts and hence for ease of plotting this section helps to
% put these different vectors in a matrix by padding const values towards
% the end.
    if sss==1,
          Fxf1(eee,:)=Fxf;
          Fxr1(eee,:)=Fxr;
```

```
        Fzf1(eee,:)=Fzf;
        Fzr1(eee,:)=Fzr;
        kappaf1(eee,:)=kappaf;
        kappar1(eee,:)=kappar;
        Tbf1(eee,:)=Tbf;
        Tbr1(eee,:)=Tbr;
        longi_postn1(eee,:)=longi_postn;
        longi_vel1(eee,:)=longi_vel;
        omegaf1(eee,:)=omegaf;
        omegar1(eee,:)=omegar;
        To1(eee,:)=To;
        Ztr1(eee,:)=Ztr;
        Ztf1(eee,:)=Ztf;
        Zroadf1(eee,:)=Zroadf;
        Zroadr1(eee,:)=Zroadr;
        Zs1(eee,:)=Zs;
        theta1(eee,:)=theta;
        longi_accel1(eee,:)=longi_accel;
        f_tire_comp1(eee,:)=f_tire_comp;
        r_tire_comp1(eee,:)=r_tire_comp;


elseif sss==2

        Fxf2(eee,:)=Fxf;
        Fxr2(eee,:)=Fxr;
        Fzf2(eee,:)=Fzf;
        Fzr2(eee,:)=Fzr;
```

```
        kappaf2(eee,:)=kappaf;
        kappar2(eee,:)=kappar;
        Tbf2(eee,:)=Tbf;
        Tbr2(eee,:)=Tbr;
        longi_postn2(eee,:)=longi_postn;
        longi_vel2(eee,:)=longi_vel;
        omegaf2(eee,:)=omegaf;
        omegar2(eee,:)=omegar;
        To2(eee,:)=To;
        Ztr2(eee,:)=Ztr;
        Ztf2(eee,:)=Ztf;
        Zroadf2(eee,:)=Zroadf;
        Zroadr2(eee,:)=Zroadr;
        Zs2(eee,:)=Zs;
        theta2(eee,:)=theta;
        longi_accel2(eee,:)=longi_accel;
%         f_tire_comp2(eee,:)=f_tire_comp;
%         r_tire_comp2(eee,:)=r_tire_comp;
%

    elseif sss==3
        Fxf3(eee,:)=Fxf;
        Fxr3(eee,:)=Fxr;
        Fzf3(eee,:)=Fzf;
        Fzr3(eee,:)=Fzr;
        kappaf3(eee,:)=kappaf;
        kappar3(eee,:)=kappar;
        Tbf3(eee,:)=Tbf;
```

```
        Tbr3(eee,:)=Tbr;
        longi_postn3(eee,:)=longi_postn;
        longi_vel3(eee,:)=longi_vel;
        omegaf3(eee,:)=omegaf;
        omegar3(eee,:)=omegar;
        To3(eee,:)=To;
        Ztr3(eee,:)=Ztr;
        Ztf3(eee,:)=Ztf;
        Zroadf3(eee,:)=Zroadf;
        Zroadr3(eee,:)=Zroadr;
        Zs3(eee,:)=Zs;
        theta3(eee,:)=theta;
        longi_accel3(eee,:)=longi_accel;
        f_tire_comp3(eee,:)=f_tire_comp;
        r_tire_comp3(eee,:)=r_tire_comp;

    elseif sss==4
        Fxf4(eee,:)=Fxf;
        Fxr4(eee,:)=Fxr;
        Fzf4(eee,:)=Fzf;
        Fzr4(eee,:)=Fzr;
        kappaf4(eee,:)=kappaf;
        kappar4(eee,:)=kappar;
        Tbf4(eee,:)=Tbf;
        Tbr4(eee,:)=Tbr;
        longi_postn4(eee,:)=longi_postn;
        longi_vel4(eee,:)=longi_vel;
        omegaf4(eee,:)=omegaf;
```

```
            omegar4(eee,:)=omegar;
            To4(eee,:)=To;
            Ztr4(eee,:)=Ztr;
            Ztf4(eee,:)=Ztf;
            Zroadf4(eee,:)=Zroadf;
            Zroadr4(eee,:)=Zroadr;
            Zs4(eee,:)=Zs;
            theta4(eee,:)=theta;
            longi_accel4(eee,:)=longi_accel;
%             f_tire_comp4(eee,:)=f_tire_comp;
%             r_tire_comp4(eee,:)=r_tire_comp;

    else

            Fxf5(eee,:)=Fxf;
            Fxr5(eee,:)=Fxr;
            Fzf5(eee,:)=Fzf;
            Fzr5(eee,:)=Fzr;
            kappaf5(eee,:)=kappaf;
            kappar5(eee,:)=kappar;
            Tbf5(eee,:)=Tbf;
            Tbr5(eee,:)=Tbr;
            longi_postn5(eee,:)=longi_postn;
            longi_vel5(eee,:)=longi_vel;
            omegaf5(eee,:)=omegaf;
            omegar5(eee,:)=omegar;
            To5(eee,:)=To;
            Ztr5(eee,:)=Ztr;
```

```
          Ztf5(eee,:)=Ztf;
          Zroadf5(eee,:)=Zroadf;
          Zroadr5(eee,:)=Zroadr;
          Zs5(eee,:)=Zs;
          theta5(eee,:)=theta;
%           Ze5(eee,:)=Ze;
          longi_accel5(eee,:)=longi_accel;
%           f_tire_comp5(eee,:)=f_tire_comp;
%           r_tire_comp5(eee,:)=r_tire_comp;
  end
end
save('Runny','T','Fzf','Fzr','Fxf','Fxr','omegaf','omegar',
'kappaf','kappar','Tbf','Tbr','theta','Zs','Ztf','Ztr',
'Zroadf','Zroadr','longi_accel','longi_vel','longi_postn',
'Ffh','Frh','omegafdot','omegardot')
figure
subplot(2,1,1)
plot(T,kappaf,'linewidth',1.5)
xlabel('Time, sec','fontweight','bold','fontsize',12);
ylabel('Tire Longitudinal Slip','fontweight','bold','fontsize',12)
title(strcat('Tire Longitudinal Slip'),'fontweight','bold','fontsize',12)
% legend(leg1,leg2,leg3,leg4,leg5,'location','SouthWest')
xlim([0 0.5])
% ylim([0 -0.2])
grid
% saveas(gcf, strcat('Front Tire Longitudinal Slip',param,
'del= ',num2str(Del_static1(eee)),' mm',' @ ',num2str(vmph),
' mph',' on ',roadtype), 'jpg');
```

```
subplot(2,1,2)
plot(T,Tbf,'linewidth',1.5)
xlabel('Time, sec','fontweight','bold','fontsize',12);
ylabel('Brake Torque (N-m)','fontweight','bold','fontsize',12)
title(strcat('Brake Torque'),'fontweight','bold','fontsize',12)
% legend(leg1,leg2,leg3,leg4,leg5,'location','SouthWest')
xlim([0 0.5])
ylim([0 3500])
grid
saveas(gcf,'ABS Operation', 'ai')

%%
% Legend Setup
leg1=(strcat ('TWEEL, N = ',num2str(np(1)),'
\delta_m_a_x = ',num2str(Del_static1(eee)),' mm '));
%Corrected to display proper N and delta value by ADK
leg2=(strcat ('TWEEL, N = ',num2str(np(2)),'
\delta_m_a_x = ',num2str(Del_static1(eee)),' mm '));
%Corrected to display proper N and delta value by ADK
leg3=(strcat ('TWEEL, N = ',num2str(np(3)),'
\delta_m_a_x = ',num2str(Del_static1(eee)),' mm '));
leg4=(strcat ('TWEEL, N = ',num2str(np(4)),'
\delta_m_a_x = ',num2str(Del_static1(eee)),' mm '));
leg5='OE TIRE';
figure
plot(T,-Fxf./Fzf,'linewidth',1.5);
xlabel('Time, sec','fontweight','bold','fontsize',12);
ylabel('Front Tire \mu','fontweight','bold','fontsize',12)
```

```
title(strcat('Front Tire \mu ------- ',param,' Brake from
',num2str(vmph),' mph',' on ',roadtype),'fontweight','bold','fontsize',12)
grid
figure
plot(-kappaf,-Fxf./Fzf,'linewidth',1.5);
xlabel('Front Tire Slip','fontweight','bold','fontsize',12);
ylabel('Front Tire \mu','fontweight','bold','fontsize',12)
title(strcat('Front Tire \mu ------- ',param,' Brake from ',
num2str(vmph),' mph',' on ',roadtype),'fontweight','bold','fontsize',12)
grid
plot(To1,kappaf1,'-',To2,kappaf2,'k',To3,kappaf3,'r',To4,kappaf4,
'm',To5,kappaf5,'g','linewidth',1.5)
xlabel('Time, sec','fontweight','bold','fontsize',12);
ylabel('Front Tire Longitudinal Slip','fontweight','bold','fontsize',12)
title(strcat('Front Tire Longitudinal Slip ------- ',param,'
Brake from ',num2str(vmph),' mph',' on ',roadtype),'fontweight',
'bold','fontsize',12)
legend(leg1,leg2,leg3,leg4,leg5,'location','SouthWest')
grid
% saveas(gcf, strcat('Front Tire Longitudinal Slip',param,
'del=',num2str(Del_static1(eee)),' mm',' @ ',num2str(vmph),' mph',
' on ',roadtype), 'jpg');
figure
plot(To1,kappar1,'-',To2,kappar2,'k',To3,kappar3,'r',To4,kappar4,
'm',To5,kappar5,'g','linewidth',1.5)
xlabel('Time, sec','fontweight','bold','fontsize',12);
ylabel('Rear Tire Longitudinal Slip','fontweight','bold','fontsize',12)
title(strcat('Rear Tire Longitudinal Slip ------- ',param,
```

```
' Brake from ',num2str(vmph),' mph',' on ',roadtype),
'fontweight','bold','fontsize',12)
legend(leg1,leg2,leg3,leg4,leg5,'location','SouthWest')
grid
% saveas(gcf, strcat('Rear Tire Longitudinal Slip',param,
'del=',num2str(Del_static1(eee)),' mm',' @ ',num2str(vmph),
' mph',' on ',roadtype), 'jpg');
%
figure
plot(To1,longi_postn1,'-',To2,longi_postn2,'k',To3,longi_postn3,
'r',To4,longi_postn4,'m',To5,longi_postn5,'g','linewidth',1.5)
xlabel('Time, sec','fontweight','bold','fontsize',12);
ylabel('Longitudinal Position (ft)','fontweight','bold','fontsize',12)
title(strcat('Longitudinal Position ------- ',param,
'Brake from ',num2str(vmph),' mph',' on ',roadtype),
'fontweight','bold','fontsize',12)
legend(leg1,leg2,leg3,leg4,leg5,'location','SouthWest')
grid
% saveas(gcf, strcat('Longitudinal Position',param,
'del= ',num2str(Del_static1(eee)),' mm',' @ ',num2str(vmph),
' mph',' on ',roadtype), 'jpg');
%
figure
plot(To1,longi_vel1,'-',To2,longi_vel2,'k',To3,longi_vel3,
'r',To4,longi_vel4,'m',To5,longi_vel5,'g','linewidth',1.5)
xlabel('Time, sec','fontweight','bold','fontsize',12);
ylabel('Longitudinal Velocity (mph)','fontweight','bold','fontsize',12)
title(strcat('Longitudinal Velocity ------- ',param,
```

```
' Brake from ',num2str(vmph),' mph',' on ',roadtype),
'fontweight','bold','fontsize',12)
legend(leg1,leg2,leg3,leg4,leg5,'location','SouthWest')
grid
% saveas(gcf, strcat('Longitudinal Velocity',param,
' del= ',num2str(Del_static1(eee)),' mm',' @ ',num2str(vmph),
' mph',' on ',roadtype), 'jpg');
figure
% plot(To1,Fzf1,'-',To2,Fzf2,'k',To3,Fzf3,'r',To4,Fzf4,
'm',To5,Fzf5,'g','linewidth',1.5)
plot(To2,Fzf2,'-r',To5,Fzf5,'--k','linewidth',1.5)
xlabel('Time, sec','fontweight','bold','fontsize',12);
ylabel('Vertical Force (N)','fontweight','bold','fontsize',12)
title(strcat('Front Vertical Force @',num2str(vmph),' mph',
'on ',roadtype),'fontweight','bold','fontsize',12)
% legend(leg1,leg2,leg3,leg4,leg5,'location','SouthWest')
legend(leg2,leg5,'location','SouthWest')
grid
saveas(gcf, strcat('Fz Front',param,' del= ',
num2str(Del_static1(eee)),' mm',' @ ',num2str(vmph),
' mph',' on ',roadtype), 'jpg');
figure
% plot(To1,Fzf1,'-',To2,Fzf2,'k',To3,Fzf3,'r',To4,Fzf4,
'm',To5,Fzf5,'g','linewidth',1.5)
plot(To2,f_tire_comp2.*1000,'-r',To5,f_tire_comp5.*1000,
'--k','linewidth',1.5)
xlabel('Time, sec','fontweight','bold','fontsize',12);
ylabel('Front Tire Compression (mm)','fontweight','bold','fontsize',12)
```

```
title(strcat('Front Tire Compression @',num2str(vmph),' mph',
'on',roadtype),'fontweight','bold','fontsize',12)
% legend(leg1,leg2,leg3,leg4,leg5,'location','SouthWest')
legend(leg2,leg5,'location','SouthWest')
grid
saveas(gcf, strcat('Front tire compression',param,
' del= ',num2str(Del_static1(eee)),' mm',' @ ',num2str(vmph),
' mph',' on ',roadtype), 'jpg');
figure
% plot(To1,Fzf1,'-',To2,Fzf2,'k',To3,Fzf3,'r',To4,Fzf4,'m',
To5,Fzf5,'g','linewidth',1.5)
plot(To2,r_tire_comp2.*1000,'k',To5,r_tire_comp5.*1000,'g',
'linewidth',1.5)
xlabel('Time, sec','fontweight','bold','fontsize',12);
ylabel('Rear Tire Compression (mm)','fontweight','bold','fontsize',12)
title(strcat('Rear Tire Compression ------- ',param,
' Brake from ',num2str(vmph),' mph',' on ',roadtype),
'fontweight','bold','fontsize',12)
% legend(leg1,leg2,leg3,leg4,leg5,'location','SouthWest')
legend(leg2,leg5,'location','SouthWest')
grid
% saveas(gcf, strcat('Fz Front',param,' del= ',
num2str(Del_static1(eee)),' mm',' @ ',num2str(vmph),
' mph',' on ',roadtype), 'jpg');
figure
% plot(To1,Fzr1,'-',To2,Fzr2,'k',To3,Fzr3,'r',To4,Fzr4,
'm',To5,Fzr5,'g','linewidth',1.5)
plot(To2,Fzr2,'-r',To5,Fzr5,'--k','linewidth',1.5)
```

```
xlabel('Time, sec','fontweight','bold','fontsize',12);
ylabel('Vertical Force (N)','fontweight','bold','fontsize',12)
title(strcat('Rear Vertical Force ------- ',param,
' Brake from ',num2str(vmph),' mph',' on ',roadtype),
'fontweight','bold','fontsize',12)
% legend(leg1,leg2,leg3,leg4,leg5,'location','SouthWest')
legend(leg2,leg5,'location','SouthWest')
grid
% saveas(gcf, strcat('Fz Rear',param,' del= ',num2str(Del_static1(eee)),
' mm',' @ ',num2str(vmph),' mph',' on ',roadtype), 'jpg');
long=[longi_postn1(end);longi_postn2(end);longi_postn3(end);
longi_postn4(end);longi_postn5(end)]
rmsf=[rms(Fzf1),rms(Fzf2),rms(Fzf3),rms(Fzf4),rms(Fzf5)]
rmskappaf=[rms(kappaf1),rms(kappaf2),rms(kappaf3),rms(kappaf4),
rms(kappaf5)]
rmsr=[rms(Fzr1),rms(Fzr2),rms(Fzr3),rms(Fzr4),rms(Fzr5)]
rmskappaf=[rms(kappar1),rms(kappar2),rms(kappar3),rms(kappar4),
rms(kappar5)]
% figure
% plot(To1,Fxf1,'linewidth',1.5)%,'-',To2,Fzf2,'k',To3,Fzf3,'r',
To4,Fzf4,'m',To5,Fzf5,'g','linewidth',1.5)
% xlabel('Time, sec','fontweight','bold','fontsize',12);
ylabel('Longitudinal Force (N)','fontweight','bold','fontsize',12)
% title(strcat('Front Longitudinal Force ------- ',param,'
Brake from ',num2str(vmph),' mph',' on ',roadtype),'fontweight',
'bold','fontsize',12)
% legend(leg1)%,leg2,leg3,leg4,leg5,'location','SouthWest')
% grid
```

```
% saveas(gcf, strcat('Fx Front',param,' del= ',num2str(Del_static1(eee)),
' mm',' @ ',num2str(vmph),' mph',' on ',roadtype), 'jpg');
%
% figure
% plot(To1,Fxr1,'linewidth',1.5)%,'-',To2,Fzr2,'k',To3,Fzr3,'r',
To4,Fzr4,'m',To5,Fzr5,'g','linewidth',1.5)
% xlabel('Time, sec','fontweight','bold','fontsize',12);
ylabel('Longitudinal Force (N)','fontweight','bold','fontsize',12)
% title(strcat('Rear Longitudinal Force ------- ',param,
' Brake from ',num2str(vmph),' mph',' on ',roadtype)
,'fontweight','bold','fontsize',12)
% legend(leg1)%,leg2,leg3,leg4,leg5,'location','SouthWest')
% grid
% saveas(gcf, strcat('Fx Rear',param,' del= ',
num2str(Del_static1(eee)),' mm',' @ ',num2str(vmph)
,' mph',' on ',roadtype), 'jpg');
%
% figure
% plot(To1,theta1.*(180/pi),'linewidth',1.5)%,'-',To2,Fzr2,
'k',To3,Fzr3,'r',To4,Fzr4,'m',To5,Fzr5,'g','linewidth',1.5)
% xlabel('Time, sec','fontweight','bold','fontsize',12);
ylabel('Pitch (deg)','fontweight','bold','fontsize',12)
% title(strcat('Sprung Mass Pitch ------- ',param,'
Brake from ',num2str(vmph),' mph',' on ',roadtype),
'fontweight','bold','fontsize',12)
% legend(leg1)%,leg2,leg3,leg4,leg5,'location','SouthWest')
% grid
%
```

```
% figure
% plot(To1,Zs1,'linewidth',1.5)%,'-',To2,Fzr2,'k',To3,Fzr3,
'r',To4,Fzr4,'m',To5,Fzr5,'g','linewidth',1.5)
% xlabel('Time, sec','fontweight','bold','fontsize',12);
ylabel('Heave (m)','fontweight','bold','fontsize',12)
% title(strcat('Sprung Mass Heave ------- ',param,
' Brake from ',num2str(vmph),' mph',' on ',roadtype),
'fontweight','bold','fontsize',12)
% legend(leg1)%,leg2,leg3,leg4,leg5,'location','SouthWest')
% grid
%
% figure
% plot(To1,(Ztr1-Zroadr1).*1000,'linewidth',1.5)%,'-',To2,Fzr2,'k',
To3,Fzr3,'r',To4,Fzr4,'m',To5,Fzr5,'g','linewidth',1.5)
% xlabel('Time, sec','fontweight','bold','fontsize',12);
ylabel('Relative Displacement at Rear (m)','fontweight','bold',
'fontsize',12)
% title(strcat('Relative Displacement at Rear ------- ',param,
' Brake from ',num2str(vmph),' mph',' on ',roadtype),'fontweight',
'bold','fontsize',12)
% legend(leg1)%,leg2,leg3,leg4,leg5,'location','SouthWest')
% grid
%
% figure
% plot(To1,(Ztf1-Zroadf1).*1000,'linewidth',1.5)%,'-',To2,Fzr2,
'k',To3,Fzr3,'r',To4,Fzr4,'m',To5,Fzr5,'g','linewidth',1.5)
% xlabel('Time, sec','fontweight','bold','fontsize',12);
ylabel('Relative Displacement at Front (m)','fontweight','bold',
```

```
'fontsize',12)
% title(strcat('Relative Displacement at Front ------- ',param,
'Brake from ',num2str(vmph),' mph',' on ',roadtype),'fontweight',
'bold','fontsize',12)
% legend(leg1)%,leg2,leg3,leg4,leg5,'location','SouthWest')
% grid
%
%
% figure
% plot(To1,Ztr1,'linewidth',1.5)%,'-',To2,Fzr2,'k',To3,Fzr3,'r',
To4,Fzr4,'m',To5,Fzr5,'g','linewidth',1.5)
% xlabel('Time, sec','fontweight','bold','fontsize',12);
ylabel('Rear Wheel Displacement (m)','fontweight','bold',
'fontsize',12)
% title(strcat('Rear Wheel Displacement ------- ',param,'
Brake from ',num2str(vmph),' mph',' on ',roadtype),
'fontweight','bold','fontsize',12)
% legend(leg1)%,leg2,leg3,leg4,leg5,'location','SouthWest')
% grid
%
% figure
% plot(To1,Ztf1,'linewidth',1.5)%,'-',To2,Fzr2,'k',To3,Fzr3,
'r',To4,Fzr4,'m',To5,Fzr5,'g','linewidth',1.5)
% xlabel('Time, sec','fontweight','bold','fontsize',12);
ylabel('Front Wheel Displacement (m)','fontweight','bold',
'fontsize',12)
% title(strcat('Front Wheel Displacement ------- ',param,
' Brake from ',num2str(vmph),' mph',' on ',roadtype),'fontweight',
```

```
'bold','fontsize',12)
% legend(leg1)%,leg2,leg3,leg4,leg5,'location','SouthWest')
% grid
%
figure
plot(To2,longi_accel2,'-',To5,longi_accel5,'g','linewidth',1.5)
%To3,longi_accel3,'r',To4,longi_accel4,'m',To5,longi_accel5,
xlabel('Time, sec','fontweight','bold','fontsize',12);
ylabel('Longitudinal Acceleration (gs)','fontweight','bold','fontsize',12)
title('Longitudinal Acceleration','fontweight','bold','fontsize',12) %param,
' Brake from ',num2str(60),' mph',' on ',roadtype),
% legend(leg1)%,leg2,leg3,leg4,leg5,'location','SouthWest')
grid
%
%%
%Pacjeka Magic Formula for longitudinal force
%This is intended purely as an estimation of the longitudinal force since
%no data actually exists.  Some of this will be based off the Pacejka data
%for lateral force the other parts will be guesses based on what the curve
%should approximately look like.   The goal is to have the peak Fx at 10%
%slip with mu at the same for lateral force.  then at steady state have it
%drop off to 70% off peak for large slip ratio
Z=1.0:0.5:6.5; % range of vertical loads in kN
ZN=Z*1000; %vertical load in N
g=0:0.5:100; %slip ratio
trang=g'/100;
X=zeros(length(g),length(Z)); %preallocate
for i=1:length(g)
```

```
    for k=1:length(Z)
      D=a1*Z(k)^2+a2*Z(k);
      C=1.615;
      B=(a3*Z(k)^2+a4*Z(k))/(C*D*exp(a5*Z(k)));
      E=a6*Z(k)^2+a7*Z(k)+a8;
      theta=(1-E)*g(i)+(E/B)*atan(B*g(i));
      X(i,k)=D*sin(C*atan(B*theta));
   end
end
figure(1)
plot(g,X(:,1),g,X(:,2),g,X(:,3),g,X(:,4)...
    ,g,X(:,5),g,X(:,6),g,X(:,7),g,X(:,8)...
    ,g,X(:,9),g,X(:,10),g,X(:,11),g,X(:,12),'linewidth',1.5)
ylabel('Longitudinal Force, kN','fontweight','bold','fontsize',14)
xlabel('Slip Ratio (%) ','fontweight','bold','fontsize',14)
title(strcat('Longitudinal Force vs. Slip Ratio','----',param,'
Brake from ',num2str(vmph),' mph',' on ','----',roadtype),'fontweight',
'bold','fontsize',14)
legend('1.0 kN','1.5 kN','2.0 kN','2.4 kN', '3.0 kN', '3.5 kN', '4.0 kN',...
    '4.5 kN','5.0 kN','5.5 kN','6.0 kN','6.5 kN','Location','best')
grid on
saveas(gcf,strcat('mu vs Slip Ratio IP',' on ',roadtype), 'jpg')
figure
plot(g,X(:,1)./ZN(1),g,X(:,12)./ZN(12),'linewidth',1.5)
legend('1.0 kN','6.5 kN','Location','best')
hold on
plot(-kappaf1*100,-Fxf1./Fzf1,':k','linewidth',2)
ylabel('\mu = Fx/Fz','fontweight','bold','fontsize',14)
```

```
xlabel('Slip Ratio (%)','fontweight','bold','fontsize',14)
title(strcat('\mu vs. Slip Ratio','-',' on ','-',roadtype,'-',
'TWEEL N=',num2str(np(1))),'fontweight','bold','fontsize',14)
grid on
saveas(gcf,strcat('mu vs Slip Ratio',' on ',roadtype,'TWEEL N=',
num2str(np(1)*10)), 'jpg')
figure
plot(g,X(:,1)./ZN(1),g,X(:,12)./ZN(12),'linewidth',1.5)
legend('1.0 kN','6.5 kN','Location','best')
hold on
plot(-kappaf2*100,-Fxf2./Fzf2,':k','linewidth',2)
ylabel('\mu = Fx/Fz','fontweight','bold','fontsize',14)
xlabel('Slip Ratio (%)','fontweight','bold','fontsize',14)
title(strcat('\mu vs. Slip Ratio','-',' on ','-',roadtype,'-',
'TWEEL N=',num2str(np(2))),'fontweight','bold','fontsize',14)
grid on
saveas(gcf,strcat('mu vs Slip Ratio',' on ',roadtype,'TWEEL N=',
num2str(np(2)*10)), 'jpg')
figure
plot(g,X(:,1)./ZN(1),g,X(:,12)./ZN(12),'linewidth',1.5)
legend('1.0 kN','6.5 kN','Location','best')
hold on
plot(-kappaf3*100,-Fxf3./Fzf3,':k','linewidth',2)
ylabel('\mu = Fx/Fz','fontweight','bold','fontsize',14)
xlabel('Slip Ratio (%)','fontweight','bold','fontsize',14)
title(strcat('\mu vs. Slip Ratio','-',' on ','-',roadtype,'-',
'TWEEL N=',num2str(np(3))),'fontweight','bold','fontsize',14)
grid on
```

```
saveas(gcf,strcat('mu vs Slip Ratio',' on ',roadtype,'TWEEL N=',
num2str(np(3)*10)), 'jpg')
figure
plot(g,X(:,1)./ZN(1),g,X(:,12)./ZN(12),'linewidth',1.5)
legend('1.0 kN','6.5 kN','Location','best')
hold on
plot(-kappaf4*100,-Fxf4./Fzf4,':k','linewidth',2)
ylabel('\mu = Fx/Fz','fontweight','bold','fontsize',14)
xlabel('Slip Ratio (%)','fontweight','bold','fontsize',14)
title(strcat('\mu vs. Slip Ratio','-',' on ','-',roadtype,'-',
'TWEEL N=',num2str(np(4))),'fontweight','bold','fontsize',14)
grid on
saveas(gcf,strcat('mu vs Slip Ratio',' on ',roadtype,'TWEEL N=',
num2str(np(4)*10)), 'jpg')
figure
plot(g,X(:,1)./ZN(1),g,X(:,12)./ZN(12),'linewidth',1.5)
legend('1.0 kN','6.5 kN','Location','best')
hold on
plot(-kappaf5*100,-Fxf5./Fzf5,':k','linewidth',2)
ylabel('\mu = Fx/Fz','fontweight','bold','fontsize',14)
xlabel('Slip Ratio (%)','fontweight','bold','fontsize',14)
title(strcat('\mu vs. Slip Ratio','-',' on ','-',roadtype,'-',
'OE Tire'),'fontweight','bold','fontsize',14)
grid on
saveas(gcf,strcat('mu vs Slip Ratio',' on ',roadtype,'OE Tire'), 'jpg')
%
%%
% figure
```

```
% loglog(whzc,specrmsfdynf1(eee,:),'-',whzc,specrmsfdynf2(eee,:),
'k',whzc,specrmsfdynf3(eee,:),'r',whzc,specrmsfdynf4(eee,:),'m',
whzc,specrmsfdynf5(eee,:),'g','linewidth',1.5)
% xlabel('Frequency, Hz','fontweight','bold','fontsize',12)
% ylabel('RMS Front tire-to-road Force, N','fontweight','bold',
'fontsize',12)
% title(strcat('RMS Front tire-to-road Force, ------- ',param,
' @ ',',',num2str(vmph),' mph',' on ',',',roadtype),'fontweight',
'bold','fontsize',12)
% legend(leg1,leg2,leg3,leg4,leg5,'location','SouthWest')
% grid
% % saveas(gcf, strcat('RMS Front tire-to-road Force--',param,
' del= ',num2str(Del_static1(eee)),' mm',' @ ',num2str(vmph),
' mph',' on ',roadtype), 'jpg');
%
%
% figure
% loglog(whzc,specrmsfdynr1(eee,:),'-',whzc,specrmsfdynr2(eee,:)
,'k',whzc,specrmsfdynr3(eee,:),'r',whzc,specrmsfdynr4(eee,:),
'm',whzc,specrmsfdynr5(eee,:),'g','linewidth',1.5)
% xlabel('Frequency, Hz','fontweight','bold','fontsize',12)
% ylabel('RMS Rear tire-to-road Force, N','fontweight','bold',
'fontsize',12)
% title(strcat('RMS Rear tire-to-road Force, ------- ',param,
' @ ',',',num2str(vmph),' mph',' on ',',',roadtype),
'fontweight','bold','fontsize',12)
% legend(leg1,leg2,leg3,leg4,leg5,'location','SouthWest')
% grid
```

```
% saveas(gcf, strcat('RMS Rear tire-to-road Force--',param,
'del= ',num2str(Del_static1(eee)),' mm',' @ ',num2str(vmph),' mph',
' on ',roadtype), 'jpg');
end
%%%%%%%%%%%%%%%
% END OF MAIN LOOP
%%%%%%%%%%%%%%%
n2=histc(Fzf2,[0:3600:7200])
n5=histc(Fzf5,[0:3600:7200])
% n2=histc(Fzf2,[0:1000:7000])
% n5=histc(Fzf5,[0:1000:7000])
n=[(n2*100/sum(n2));(n5*100/sum(n5))];
figure
bar([0:3600:7200],n')
n2r=histc(Fzr2,[0:2600:5200])
n5r=histc(Fzr5,[0:2600:5200])
% n2r=histc(Fzr2,[0:1000:7000])
% n5r=histc(Fzr5,[0:1000:7000])
nr=[(n2r*100/sum(n2r));(n5r*100/sum(n5r))];
figure
bar([0:2600:5200],nr')
%%
% Fzf2=1:50;
clear greater smaller oo pp i
oo=1
pp=1
qq=1
% Fzf2=Fzf2-Fzf2(1);
```

```
%
for i=1:length(Fzf2)
if Fzf2(i)>3895
greater(oo)=Fzf2(i);
oo=oo+1;
elseif Fzf2(i)<3895
smaller(pp)=Fzf2(i);
pp=pp+1;
else
equal(qq)=3895;
qq=qq+1;
end
end
greater2=greater;%-Fzf2(1);
smaller2=smaller;%-Fzf2(1);
%%%%%%%%%%%%%%%%%%%%%%%%%%%%%%%%%%%%%%%%%%%%%%%%%%%%%%%%
clear greater smaller oo pp i
oo=1
pp=1
qq=1
for i=1:length(Fzf5)
if Fzf5(i)>3895
greater(oo)=Fzf5(i);
oo=oo+1;
elseif Fzf5(i)<3895
smaller(pp)=Fzf5(i);
pp=pp+1;
else
```

```
equal(qq)=3895;
qq=qq+1;
end
end
greater5=greater;%-Fzf5(1);
smaller5=smaller;%-Fzf5(1);
%%%%%%%%%%%%%%%%%%%%%%%%%%%%%%%%%%%%%%%%%%%%%%%%%%%%
clear greater smaller oo pp i
oo=1
pp=1
qq=1
% Fzf2=Fzf2-Fzf2(1);
%
for i=1:length(f_tire_comp2)
if f_tire_comp2(i)>1.1736e-2
greater(oo)=f_tire_comp2(i);
oo=oo+1;
elseif f_tire_comp2(i)<1.1736e-2
smaller(pp)=f_tire_comp2(i);
pp=pp+1;
else
equal(qq)=1.1736e-2;
qq=qq+1;
end
end
greater_comp2=greater;%-Fzf2(1);
smaller_comp2=smaller;%-Fzf2(1);
%%%%%%%%%%%%%%%%%%%%%%%%%%%%%%%%%%%%%%%%%%%%%%%%%%%%
```

```
clear greater smaller oo pp i
oo=1
pp=1
qq=1
% Fzf2=Fzf2-Fzf2(1);
%
for i=1:length(f_tire_comp5)
if f_tire_comp5(i)>1.6788e-2
greater(oo)=f_tire_comp5(i);
oo=oo+1;
elseif f_tire_comp5(i)<1.6788e-2
smaller(pp)=f_tire_comp5(i);
pp=pp+1;
else
equal(qq)=1.6788e-2;
qq=qq+1;
end
end
greater_comp5=greater;%-Fzf2(1);
smaller_comp5=smaller;%-Fzf2(1);
```

## D.4 Braking_Road_PSD.m

```
%%%%%%%%%%%%%%%%%%%%%%%%%%%%%%%%%%%%%%%%%%%%%%%%%%%%%%%%%%%%%%%%%%%%%%%%%%%%%%%
%
%  modification of road_psd.m DEVELOPED BY D. MOLINE - Date Unknown
%
%   modified by: MAP 12/1/08
%   modified to create more type of roads by ADK on 05/25/09
%   roadx.m is a manually saved output of road profile in order to yield
%   repetetive results.
%   Modified by ADK in June 2009
%   Added more road types and corrected some labels
%
% Any modifications to this program should result in road.mat being updated
%   road=[tout*v road(:,3)]
%%%%%%%%%%%%%%%%%%%%%%%%%%%%%%%%%%%%%%%%%%%%%%%%%%%%%%%%%%%%%%%%%%%%%%%%%%%%%%%
% A little program to check the results of random road profile generation via
% summation of sine waves in Simulink.
%for nfreq=[50 100 200 300 400]
% First, basic data
clc
clear all
close all
format short g
%%%%%%%%%%%%%%%%%%%%%%%%%%%%%%%%%%%%%%%%%%%%%%%%%%%%%%%%%%%%%%%%%%%%%%%%%%%%%%%
% Description                       N             Csp (m^2/cycle/m)
% ------------------------------------------------------------------------
```

```
% Smooth Runway                    3.8              4.3e10-11
%
% Rough Runway                     2.1              8.1e10-6
%
% Smooth Highway                   2.1              4.8e10-7
%
% Highway with Gravel              2.1              4.4e10-6
%
% Pasture                          1.6              3.0e10-4
%
% Plowed Field                     1.6              6.5e10-4
%%%%%%%%%%%%%%%%%%%%%%%%%%%%%%%%%%%%%%%%%%%%%%%%%%%%%%%%%%%%%%%%%%%%%%%%%%%%%%%%
% Csp1=[8.1e-6 4.8e-7 4.4e-6 2.5e-8];        % make sure that the Csp1
and N1 are of same length...
% N1=[2.1 2.1 2.1 2.3];                   % This would mean working on
a combination of Csp and N for the said raod
% Csp1=[2.9e-5 7.5e-6 4.5e-7 2.5e-8];        % make sure that the Csp1
and N1 are of same length...
% N1=[2.3 2.3 2.3 2.3];                     % This would mean working
on a combination of Csp and N for the said road
Csp1=[1.08e-7 5.5e-7 1.5e-6 1.5e-7 4.8e-7 4.4e-6 2.5e-8];        % make
sure that the Csp1 and N1 are of same length...
N1=[2.6 2.1 2.3 2.3 2.1 2.1 2.3];                   % This would mean
working on a combination of Csp and N for the said road
for i=1:length(Csp1)
randn('state',0);
minfreq=.5; % Minimum, Hz
% maxfreq=60; % Maximum, Hz
```

```
maxfreq=50;
% nfreq=600; % No. of components
nfreq=400;
% Q=-.11; % our exponent on amplitude
Q=1.0000e-002;
phases0=randn(1,nfreq)*pi; % vector of phases
phases1=randn(1,nfreq)*pi; % a second vector of phases for
creating different tracks.
sc=0;
% fraction scaling for mixing the two tracks. 0 for identical.
freqs0=linspace(minfreq,maxfreq,nfreq); % vector of frequencies, Hz.
Linear gives flat vel PSD
vmph=60;    %vehicle speed, mph
v=vmph*.44704;  %vehicle speed, m/s
vmps=v;
A=.0022;
diff=1;
while abs(diff)>.1
    % amp0=.00056*freqs0.^(Q);
% Amplitude. Either constant or frequency dependent.
    amp0=A*freqs0.^(Q);
    % now some custom stuff for switching between 1 and 2 "wheels" at a time
    ith=3;
freq=[freqs0; freqs0];
phases=[phases0; phases0+sc*freqs0/max(freq).*phases1];
amp=[amp0; amp0]; % 2 wheels, displacement in 3rd and 4th col
    %ith=2; freq=freqs0; phases=phases0; amp=amp0;
% 1 wheels, displacement in 2nd col
```

```
    %tic, sim untitled, toc  % the simulation, for now
    %             tic,
    sim('road_test',20,simset('reltol',1e-3,...
       'abstol',1e-3,'refine',1,'solver','FixedStepDiscrete',
'fixedstep',1e-2)), %toc
    % Time results: 2 wheels take twice as long as 1 wheel,
both with matrices
    % Matrices or "nat'l" vectors makes no difference for one wheel.
    %Desired PSD
%     Csp=2.5e-8;
%     N=2.3;
    Csp=Csp1(i);
    N=N1(i);
    step=.1;
    whz=minfreq:step:maxfreq;      % Frequency range in Hz
    w_cyc_m=whz./vmps;             % Spatial Frequency in cycle/m
    w=2*pi*whz;                   % Frequency range in rad/s
    %
    % ROAD PSD
    %
    for kk=1:length(whz),
       rpsd(kk)=(2*pi*vmps)^(N-1)*Csp/(w(kk)^N);    % PSD in m^2/(rad/s)
       rpsd_spatial(kk)=Csp/(w_cyc_m(kk)^N);        % PSD in m^2/(cyc/m)
    end

    area1=trapz(whz,rpsd*2*pi); % desired PSD area,
comment added by ADK
    check(i)=area1;
```

```
    % now the analysis...
    % First, get the PSD
    % [p,f]=psd(road(:,2),2^11,1/(tout(2)-tout(1)));
    [p,f]=pwelch(road(:,ith),[],[],2^13,1/(tout(2)-tout(1)));
    % pick off the range of interest
    jj=find(f<=maxfreqandf>=minfreq);
    ii=jj; %(4:end);
    % Do the fit, assuming a power model over the range of interest
    c=[ones(size(ii(:))) log(f(ii))]\log(p(ii));
    %Area under fit
    %fit values
    Prr=exp(c(1))*f(ii).^c(2);
    area2=trapz(f(ii),Prr);        % road PSD area,
comment added by ADK
    diff=(area1-area2)/area1*100;
    if abs((abs(c(2))-N)/N*100)<1
        if area1>area2
            A=A+.05*A;
        else
            A=A-.01*A;
        end
    elseif abs(c(2))>N
        Q=Q+.01;
        diff=1;
    else
        Q=Q-.005;
        diff=1;
```

```
    end
end
fprintf('Q: %.2f RMS: %.7f,  AMP: %.9f,  Exp: %.5f,  n %i\n',...
    [Q, rms(road(:,3)), exp(c(1)), c(2), nfreq])
%end
figure
loglog(f(jj),p(jj),f(ii),exp(c(1))*f(ii).^c(2))
figure
loglog(f,p,f,exp(c(1))*f.^c(2),':',whz,2*pi*rpsd,'--','linewidth',1.5)
legend('PSD of Created Road','Desired PSD','Curve Fit to Road PSD')
% added by ADK
FGG
% for multiple track profiles
if size(freq,1)==2,
   figure
   % Neither of these seem particularly useful...
to sensitive to NFFT ([] right now)
   %csd(road(:,3),road(:,4),[],1/(tout(2)-tout(1)))
   %cohere(road(:,3),road(:,4),[],1/(tout(2)-tout(1)))
   %subplot(211),
   plot(tout,road(:,3:4)),fgg
   %subplot(224), plot(road(:,3),road(:,4)),fgg,axis square
end
% dist=tout*v;
rpsdi(i,:)=rpsd;
rpsdi_spatial(i,:)=rpsd_spatial;
if i==1
road1=[tout*v road(:,3)];
```

```
elseif i==2
road2=[tout*v road(:,3)];
elseif i==3
road3=[tout*v road(:,3)];
elseif i==4
road4=[tout*v road(:,3)];              % add another line to
take care of any additional Csp and N entries...
elseif i==5
road5=[tout*v road(:,3)];               % add another line to
take care of any additional Csp and N entries...
elseif i==6
road6=[tout*v road(:,3)];               % add another line to
take care of any additional Csp and N entries...
elseif i==7
road7=[tout*v road(:,3)];               % add another line to
take care of any additional Csp and N entries...
else
end
% save(strcat('road',num2str(i)),strcat('road',num2str(i)))
end
figure
loglog(whz,2*pi*rpsdi(1,:),'-',whz,2*pi*rpsdi(2,:),':',whz,
2*pi*rpsdi(5,:),'-.*',whz,2*pi*rpsdi(6,:),'--',whz,2*pi*rpsdi(7,:),
'-o','linewidth',1.5,'markersize',3.5)
legend(strcat('Rough Road Const RMS # 1',',',',' C_s_p','=',
num2str(Csp1(1)),',',' Nroad','=',num2str(N1(1))),
strcat('Rough Road Const RMS # 2',',',',' C_s_p','=',
num2str(Csp1(2)),',',' Nroad','=',num2str(N1(2)))...
```

```
    ,strcat('Smooth Highway',',',' C_s_p','=',num2str(Csp1(5)),
',',' Nroad','=',num2str(N1(5))),...
    strcat('Gravel Road',',',' C_s_p','=',num2str(Csp1(6)),
',',' Nroad','=',num2str(N1(6))),strcat('LPG Weathered Asphalt Road',
',',' C_s_p','=',num2str(Csp1(7)),',',' Nroad','=',num2str(N1(7))),
'location','SouthWest') % added by ADK
xlabel('Frequency ,\omega, Hz','fontsize',14,'fontweight','bold')
ylabel('Szr (\Omega),m^2/Hz','fontsize',14,'fontweight','bold')
title(strcat('Spectral Density Szr (\Omega)= C_s_p x \Omega^-^N^r^o^a^d',
' @ ',num2str(vmph),' mph'),'fontsize',14,'fontweight','bold')
grid
saveas(gcf, strcat('Spectral Densities',' @ ',num2str(vmph),' mph'),
'jpg');
figure
loglog(whz,2*pi*rpsdi(3,:),'-',whz,2*pi*rpsdi(4,:),':',whz,
2*pi*rpsdi(5,:),'-.*',whz,2*pi*rpsdi(6,:),'--',whz,2*pi*rpsdi(7,:),
'-o','linewidth',1.5,'markersize',3.5)
legend(strcat('Rough Road Const Nroad # 1',',',' C_s_p','=',
num2str(Csp1(3)),',',' Nroad','=',num2str(N1(3))),
strcat('Rough Road Const Nroad # 2',',',' C_s_p','=',
num2str(Csp1(4)),',',' Nroad','=',num2str(N1(4)))...
    ,strcat('Smooth Highway',',',' C_s_p','=',num2str(Csp1(5)),
',',' Nroad','=',num2str(N1(5))),...
strcat('Gravel Road',',',' C_s_p','=',num2str(Csp1(6)),
',',' Nroad','=',num2str(N1(6))),strcat('LPG Weathered Asphalt Road',
',',' C_s_p','=',num2str(Csp1(7)),',',' Nroad','=',num2str(N1(7))),
'location','SouthWest') % added by ADK
xlabel('Frequency ,\omega, Hz','fontsize',14,'fontweight','bold')
```

```
ylabel('Szr (\Omega),m^2/Hz','fontsize',14,'fontweight','bold')
title(strcat('Spectral Density Szr (\Omega)= C_s_p x \Omega^-^N^r^o^a^d',
' @ ',num2str(vmph),' mph'),'fontsize',14,'fontweight','bold')
grid
saveas(gcf, strcat('Spectral Densities (SPATIAL)',' @ ',
num2str(vmph),' mph'), 'jpg');
% xlabel('Spatial Frequency, cycle/m','fontsize',14,
'fontweight','bold')
% ylabel('Szr (\Omega),m^2/(cycle/m)','fontsize',14,
'fontweight','bold')
% title(strcat('Spectral Density (SPATIAL) Szr (\Omega)=
C_s_p x\Omega^-^Nroad'),'fontsize',14,'fontweight','bold')
figure
plot(road1(:,1),road1(:,2),road2(:,1),road2(:,2),road3(:,1),
road3(:,2),road4(:,1),road4(:,2),road5(:,1),road5(:,2),
road6(:,1),road6(:,2),road7(:,1),road7(:,2),'linewidth',1.5)
legend(strcat('Rough Road Const RMS # 1',',',',' C_s_p','=',
num2str(Csp1(1)),',',',' Nroad','=',num2str(N1(1))),strcat
('Rough Road Const RMS # 2',',',',' C_s_p','=',num2str(Csp1(2)),
',',',' Nroad','=',num2str(N1(2)))...
    ,strcat('Rough Road Const Nroad # 1',',',',' C_s_p','=',
num2str(Csp1(3)),',',',' Nroad','=',num2str(N1(3))),strcat
('Rough Road Const Nroad # 2',',',',' C_s_p','=',num2str(Csp1(4)),
',',',' Nroad','=',num2str(N1(4))),strcat('Smooth Highway',',',','
C_s_p','=',num2str(Csp1(5)),',',',' Nroad','=',num2str(N1(5))),...
    strcat('Gravel Road',',',',' C_s_p','=',num2str(Csp1(6)),
',',',' Nroad','=',num2str(N1(6))),strcat('LPG Weathered Asphalt Road',
',',',' C_s_p','=',num2str(Csp1(7)),',',',' Nroad','=',num2str(N1(7))))
```

```
% added by ADK
xlabel('Positon on Road (m)','fontsize',14,'fontweight','bold')
ylabel('Elevation of Road (m)','fontsize',14,'fontweight','bold')
title(strcat('Road Profiles',' @ ',num2str(vmph),' mph'),
'fontsize',14,'fontweight','bold')
grid
saveas(gcf, strcat('Road Profiles',' @ ',num2str(vmph),' mph'), 'jpg');
% disp('Do you want to save this road profile?')
% choice=input('Y/Nroad ?','s');
% if or(choice=='Y',choice=='y')
%     cd('C:\Documents and Settings\mparadi\My Documents\
Research Project\MATLAB_PROGRAMS')
%     save('road','road')
% end
```

## D.5 TWEEL™_Stiffness_selector.m

```
%
%  TWEEL23C.m
%
%  Developed by E.H. Law Nov.2007
%   TWEEL Force vs. Deflection Law is of form F=C*del^n
%   Static Deflection held constant at Del_static, mm
%
%   Program Calculates front and rear stiffnesses using
%   same C and n for the two axles (n=.5,.7,.9)
%
%   Choice of max deflection / N added 6/08 - MAP
%%%%%%%%%%%%%%%%%%%%%%%%%%%%%%%%%%%%%%%%%%%%%%%%%%%%%%%%%%%%%%%%%%%%%%%%
%%%%%%%%%%%%%%%%%%%%%%%%%%%%%%%%%%%%%%%%%%%%%%%%%%%%%%%%%%%%%%%%%%%%%%%%
%   Major changes made to facilitate the saving and printing o
f figures and tables by ADK in May 09
%
%   Whatever few modifications and lines that I added are about
the sweetest lines I have ever written in
%   MATLAB. This takes care of book-keeping for the user.
This code would
%   write the data generated by this program in form of tables
in EXCEL. The labels for the
%   tables and the name of the sheets are updated and written
automatically for any change in N or Del_static.
%   The user must only change the n and the Del_static arrays
to whatever is
```

```
%   needed. The code takes care of the rest.
%   TRIED AND TESTED BY ANUP D. KHEKARE ON THIS DARK NIGHT
OF MAY 11th 2009...
%%%%%%%%%%%%%%%%%%%%%%%%%%%%%%%%%%%%%%%%%%%%%%%%%%%%%%%%%%%%%%%%%%%%%%%
%%%%%%%%%%%%%%%%%%%%%%%%%%%%%%%%%%%%%%%%%%%%%%%%%%%%%%%%
clc
clear all
close all
format short g
format compact
%diary d:TWEEL_mini.out
disp('TWEEL Force vs. Deflection Law is of form F = C*del^n')
disp('Static Deflection held constant at Del_static, mm')
disp('  ')
disp('Program calculates front and rear stiffnesses using ')
disp('same C and n for the two axles')
disp('  ')
disp('  ')
disp('INPUT DESIRED MAX WHEEL LOAD')
disp('  ')
% Del_static=input('Max static deflection, mm = ');
% disp('  ')
% Fmax=input('Max wheel load, kg = ');
% disp('  ')
Fmax=438 ;           % Max static load in kg corresponds to GVW front
n=[0.4 0.6 0.8 1];
Del_static=15;
for i=1:length(Del_static)
```

```
    for j=1:length(n)
    logC(i,j)=-n(j).*log10(Del_static(i)) + log10(Fmax);
    C(i,j)=10.^logC(i,j);
    stiff_kg(i,j)=C(i,j).*n(j).*Del_static(i).^(n(j)-1);
    stiff_Npm(i,j)=9.81*1000.*stiff_kg(i,j);

% disp('  ')
% disp('Values of n, C, and Stiffness for Fmax and delmax')
% disp('  ')
% disp('C            n         Stiff (per wheel), N/m')
% disp([C' n' stiff_Npm'])
% disp('  ')
    del=0:0.1:40;
    F(i,j,:)=C(i,j).*del.^n(j);
    dfddel(i,j,:)=C(i,j).*n(j).*del.^(n(j)-1);
    dfddel_Npm(i,j,:)=dfddel(i,j,:)*9.81*1000;

%     F2(j)=C(i,j).*del.^n(j);
%     dfddel_2=C(2).*n(2).*del.^(n(2)-1);
%
%     F1(j)=C(i,j).*del.^n(j);
%     dfddel_3=C(3).*n(3).*del.^(n(3)-1);
%
%     F1(j)=C(i,j).*del.^n(j);
%     dfddel_4=C(4).*n(4).*del.^(n(4)-1);
    end

    temp1(1,:)=F(i,1,:);
```

```
    temp2(1,:)=F(i,2,:);
    temp3(1,:)=F(i,3,:);
    temp4(1,:)=F(i,4,:);

    figure(i)
    plot(del,temp1,del,temp2,'-.',del,temp3,':',del,temp4,'--',
'linewidth',2)
    xlabel('Del, mm','fontweight','bold','fontsize',11)
    ylabel('F, kg','fontweight','bold','fontsize',11)
    grid
    title(strcat('F vs Del, \deltamax = ',
int2str(Del_static(i)),' mm') ,'fontweight','bold','fontsize',11)
    legend(strcat('N= ',num2str(n(1))),strcat('N= ',num2str(n(2)))
,strcat('N= ',num2str(n(3))),strcat('N= ',num2str(n(4))),
'location','NorthWest')      % Changed to update automatically...May 09
    saveas(i, strcat('F vs Del, Static Deflection = ',
int2str(Del_static(i))), 'jpg');
%     print -djpeg -r300 strcat('F vs Del, Static Deflection =
', int2str(Del_static(i)))
  end


%% REFERENCE CODE FOR DYNAMIC FIGURE generation and saving
% for i=1:1:10
%     figure(i);
%     plot(rand(1,100)) % put something in the figure
%
%     saveas(i, strcat('filex_', int2str(i)), 'fig');
```

```
% end
% print -djpeg -r300 TWEEL_F_vs_Delta_Static
%%
%%%%%%%%%%%%%%%%%%%%%%%%%%%%%%%%%%
% Do Front First at GVW
%%%%%%%%%%%%%%%%%%%%%%%%%%%%%%%%%%
%Del_static=input('Input max desired static deflect of
TWEEL in mm,Del =  ')
% Del_static=30;
for ii=1:length(Del_static)
    temp_label=char('A');  % create index for the cell in excel

    for jj=1:length(n)
%FmaxF=input('Max wheel load (GVW) at front in kg, FmaxF =  ')
FmaxF=438;
% n=input('Please Enter Desired Value of N, .5-.9\n>');
logCF(ii,jj)=-n(jj)*log10(Del_static(ii)) + log10(FmaxF);
CF(ii,jj)=10^logCF(ii,jj);
logdel_F_GVW(ii,jj)=(log10(FmaxF)-logCF(ii,jj))/n(jj);
delF_GVW(ii,jj)=10^logdel_F_GVW(ii,jj);                  % mm
dfddelF_GVW(ii,jj)=CF(ii,jj)*n(jj)*delF_GVW(ii,jj)^(n(jj)-1); % kg/mm
dfddelF_GVW_Npm(ii,jj)=dfddelF_GVW(ii,jj)*9.81*1000;     % N/m
%%%%%%%%%%%%%%%%%%%%%%%%%%%%%%%%%%
% Now do Rear at GVW
%%%%%%%%%%%%%%%%%%%%%%%%%%%%%%%%%%
%FmaxR=input('Max wheel load at rear (GVW) in kg, FmaxR =  ')
FmaxR=344;
logdel_R_GVW(ii,jj)=(log10(FmaxR)-logCF(ii,jj))/n(jj);
```

```
delR_GVW(ii,jj)=10^logdel_R_GVW(ii,jj);   % mm
dfddelR_GVW(ii,jj)=CF(ii,jj)*n(jj)*delR_GVW(ii,jj)^(n(jj)-1); % kg/mm
dfddelR_GVW_Npm(ii,jj)=dfddelR_GVW(ii,jj)*9.81*1000;   % N/m
%
%%%%%%%%%%%%%%%%%%%%%%%%%%%%%%%%%%%%%%%%%%%%%%%%%%%%%%%%%%%%%%%%%%%%%%%
% Now do front and Rear at Conf 1 (Curb+Driver).Corrected by ADK in May 09
%%%%%%%%%%%%%%%%%%%%%%%%%%%%%%%%%%%%%%%%%%%%%%%%%%%%%%%%%%%%%%%%%%%%%%%
%%%%%%%%%%%%%%%%%%%%%%%%%%%%%%%%%%%%%%%%%%%%%%%%
% Do Front First at Conf 1
%%%%%%%%%%%%%%%%%%%%%%%%%%%%%%%%%%%%%%%%%%%%%%%%
%FC1F=input('Wheel load (Conf1) at front in kg, FC1F =  ')
FC1F=397;
logdel_F_C1(ii,jj)=(log10(FC1F)-logCF(ii,jj))/n(jj);
delF_C1(ii,jj)=10^logdel_F_C1(ii,jj);                  % mm
dfddelF_C1(ii,jj)=CF(ii,jj)*n(jj)*delF_C1(ii,jj)^(n(jj)-1);% kg/mm
dfddelF_C1_Npm(ii,jj)=dfddelF_C1(ii,jj)*9.81*1000;     % N/m
%%%%%%%%%%%%%%%%%%%%%%%%%%%%%%%%%%%%%%%%%%%%%%%%
% Now do Rear at at Conf 1
%%%%%%%%%%%%%%%%%%%%%%%%%%%%%%%%%%%%%%%%%%%%%%%%
%FC1R=input('Wheel load (Conf1)at rear in kg, FC1R =  ')
FC1R=265;
logdel_R_C1(ii,jj)=(log10(FC1R)-logCF(ii,jj))/n(jj);
delR_C1(ii,jj)=10^logdel_R_C1(ii,jj);                   % mm
dfddelR_C1(ii,jj)=CF(ii,jj)*n(jj)*delR_C1(ii,jj)^(n(jj)-1);% kg/mm
dfddelR_C1_Npm(ii,jj)=dfddelR_C1(ii,jj)*9.81*1000;     % N/m
%%%%%%%%%%%%%%%%%%%%%%%%%%%%%%%%%%%%%%%%%%%%%%%%

%The following statement creates a temp matrix with
```

```
strings,characters and numbers to be entered in a table in EXCEL
temp_string={" strcat('N = ', num2str(n(jj))),
strcat('Static Deflection (mm) = ', num2str(Del_static(ii)));
" 'Fmax (N)' 'Stiffness(N/m)';'Front_GVW' FmaxF*9.81
dfddelF_GVW_Npm(ii,jj);...
'Rear_GVW' FmaxR*9.81 dfddelR_GVW_Npm(ii,jj);'Front_C+D'
FC1F*9.81dfddelF_C1_Npm(ii,jj);
'Rear_C+D' FC1R*9.81 dfddelR_C1_Npm(ii,jj); };
% The following command writes the above matrix to a EXCEL sheet
% Every new Del_Static uses a new Sheet and every such sheet
contains table
% for all the N values used..As I said this is a pretty sweet
piece of code...
% please read about strings and char before attempting to change it.
s = xlswrite('TWEEL_Stiffness.xls', temp_string,
strcat('Del Static (mm) = ', int2str(Del_static(ii))),
strcat(temp_label, (int2str((1)))));
temp_label=char(temp_label+4);
    end


end
% fprintf('\nn = %6.2f, del max = %6.2f, GVW, C = %.3g \n',
n,Del_static,CF)
% disp('  ')
% disp('  ')
% data_stiff_GVW=[FmaxF  Del_static  dfddelF_GVW_Npm/1000;...
%                 FmaxR  delR_GVW    dfddelR_GVW_Npm/1000];
%
```

```
% disp('Wheel Load, kg     Del, mm     Stiffness, kN/m')
% disp('  ')
% disp([data_stiff_GVW])
% disp('   ')
%
% %
%
% fprintf('\nn = %6.2f, del max = %6.2f, Conf 1, , C = %.3g \n'
,n,Del_static,CF)
% disp('  ')
% data_stiff_C1=[FC1F  delF_C1  dfddelF_C1_Npm/1000;...
%                FC1R  delR_C1  dfddelR_C1_Npm/1000];
%
% disp('Wheel Load, kg     Del, mm     Stiffness, kN/m')
% disp('  ')
% disp([data_stiff_C1])
% disp('   ')
%% REFERENCE CODE FOR SETTING MULTIPLE LEGENDS
% % the plot with 9 traces...
%      ph=plot(rand(20,9));
%      set(gca,'ylim',[-2,5]);
% % the engine
% % - label trace 1 and 5
%     legend(ph(1),'trace one');
%     ah=axes('position',get(gca,'position'),...
%             'visible','off');
%     legend(ah,ph(5),'trace five','location','west')
%%%%%%%%%%%%%%%%%%%%%%%%%%%%%%%%%%%%%%%%%%%%%%%%%%%%%%%%%%%%%%%%%%%%%%%
```

```
%%%%%%%%%%%%%%%%%%%%%%%%%%
%%
% Now plot F vs Delta
    for kk=1:length(Del_static)
    figure(kk)
    temp1(1,:)=F(kk,1,:);
    temp2(1,:)=F(kk,2,:);
    temp3(1,:)=F(kk,3,:);
    temp4(1,:)=F(kk,4,:);

    FmaxF=FmaxF.*ones(size(dfddelF_GVW));
    FmaxR=FmaxR.*ones(size(dfddelF_GVW));
    FC1F=FC1F.*ones(size(dfddelF_GVW));
    FC1R=FC1R.*ones(size(dfddelF_GVW));


    ha=plot(del,temp1.*9.81,del,temp2.*9.81,'-.',del,temp3.*9.81,
':',del,temp4.*9.81,'--','linewidth',2);
    xlabel('Del, mm','fontweight','bold','fontsize',11)
    ylabel('F, kg','fontweight','bold','fontsize',11)

    line(delR_GVW(kk,:),FmaxR(kk,:).*9.81,'linewidth',2,'color','k')
    text(delR_GVW(kk,end),FmaxR(kk,end).*9.81,{'\leftarrow GVW Rear'},
'fontweight','bold','FontSize',10) %,'BackgroundColor',
[.7 .9 .7],'Margin',0.1)
    text(delF_GVW(kk,end),FmaxF(kk,end).*9.81,{'GVW Front \rightarrow'},
'fontweight','bold','FontSize',10,'HorizontalAlignment',
'right') %,'BackgroundColor',[.7 .9 .7],'Margin',0.1)
```

```
    line(delF_C1(kk,:),FC1F(kk,:).*9.81,'linewidth',2,'color','k')
    text(delF_C1(kk,end),FC1F(kk,end).*9.81,{'\leftarrow C+D Front'},
'fontweight','bold','FontSize',11) %,'BackgroundColor',
[.7 .9 .7],'Margin',0.1)
    line(delR_C1(kk,:),FC1R(kk,:).*9.81,'linewidth',2,'color','k')
    text(delR_C1(kk,end),FC1R(kk,end).*9.81,{'\leftarrow C+D Rear'},
'fontweight','bold','FontSize',11) %,'BackgroundColor',
[.7 .9 .7],'Margin',0.1)
    grid
    title(strcat('F vs Del, \deltamax = ', int2str(Del_static(kk)),' mm'),
'fontweight','bold','fontsize',11)
    legend(strcat('N= ',num2str(n(1))),strcat('N= ',num2str(n(2))),
strcat('N= ',num2str(n(3))),strcat('N= ',num2str(n(4))),'location',
'NorthWest')      % Changed to update automatically...May 09
    saveas(kk, strcat('F vs Del, Marked,Del = ',int2str(Del_static(kk))),
'jpg');
    end


    clear kk
%%
    for kk=1:length(Del_static)
    figure(kk)


    temp1(1,:)=dfddel_Npm(kk,1,:);
    temp2(1,:)=dfddel_Npm(kk,2,:);
    temp3(1,:)=dfddel_Npm(kk,3,:);
    temp4(1,:)=dfddel_Npm(kk,4,:);
    h=plot(del,temp1/1000,del,temp2/1000,'-.',del,temp3/1000,':',
```

```
del,temp4/1000,'--',...
         delF_GVW(kk,:),dfddelF_GVW_Npm(kk,:)/1000,'k*',...
         delR_GVW(kk,:),dfddelR_GVW_Npm(kk,:)/1000,'kx',...
         delF_C1(kk,:),dfddelF_C1_Npm(kk,:)/1000,'b+',...
         delR_C1(kk,:),dfddelR_C1_Npm(kk,:)/1000,'bo',del,
232.02.*ones(length(del)),
'-.k','linewidth',2,'MarkerSize',7.5);

    title(strcat('Stiffness vs Del,  \deltamax = ',
int2str(Del_static(kk)),' mm'),'fontweight','bold','fontsize',11)
    legend([h(1),h(2),h(3),h(4),h(9)],strcat('N= ',num2str(n(1))),
strcat('N= ',num2str(n(2))),strcat('N= ',num2str(n(3))),
strcat('N= ',num2str(n(4))),'OE Tire')
    xlabel('Del, mm','fontweight','bold','fontsize',11)
    ylabel('dF/d(del), kN/m','fontweight','bold','fontsize',11)
    grid
    ah=axes('position',get(gca,'position'),'visible','off');
    legend(ah,[h(5),h(6),h(7),h(8)],'GVW Front','GVW Rear',
'C+D Front','C+D Rear','location','NorthWest')
    saveas(kk, strcat('Stiffness vs Del, Marked,Del = ',
int2str(Del_static(kk))), 'jpg');
    end




%     plot(delF_GVW,dfddelF_GVW_Npm/1000,'*',...
%          delR_GVW,dfddelR_GVW_Npm/1000,'*',...
```

```
%          delF_C1,dfddelF_C1_Npm/1000,'o',...
%          delR_C1,dfddelR_C1_Npm/1000,'o','linewidth',2)


%     %Input offset lines to show change in force
%     rmsf=.39;       %rms front deflection C1, mm
%     rmsr=.47;       %rms rear deflection C1, mm
%     rmsfgvw=.4;    %rms front deflection GVW, mm
%     rmsrgvw=.47;    %rms rear delfection GVW, mm

%     plot((delF_GVW-rmsfgvw)*ones(1,51),(dfddelF_GVW_Npm/1000-25):
(dfddelF_GVW_Npm/1000+25),'b',...
%         (delF_GVW+rmsfgvw)*ones(1,51),(dfddelF_GVW_Npm/1000-25):
(dfddelF_GVW_Npm/1000+25),'b',...
%         (delR_GVW-rmsrgvw)*ones(1,51),(dfddelR_GVW_Npm/1000-25):
(dfddelR_GVW_Npm/1000+25),'g',...
%         (delR_GVW+rmsrgvw)*ones(1,51),(dfddelR_GVW_Npm/1000-25):
(dfddelR_GVW_Npm/1000+25),'g',...
%         (delF_C1-rmsf)*ones(1,51),(dfddelF_C1_Npm/1000-25):
(dfddelF_C1_Npm/1000+25),'r',...
%         (delF_C1+rmsf)*ones(1,51),(dfddelF_C1_Npm/1000-25):
(dfddelF_C1_Npm/1000+25),'r',...
%         (delR_C1-rmsr)*ones(1,51),(dfddelR_C1_Npm/1000-25):
(dfddelR_C1_Npm/1000+25),'c',...
%         (delR_C1+rmsr)*ones(1,51),(dfddelR_C1_Npm/1000-25):
(dfddelR_C1_Npm/1000+25),'c','linewidth',1.5)
```

## D.6 Ideal_brake_distribution.m

```
clc
clear all
close all
a=987.2; % Front axle to CG, mm
L=2468; % Wheelbase, mm
b=L-a; % Rear axle to CG, mm
h=517; % Height of CG
%%%%%%%%%%%%%%%%%%%%%%%%%%%%%%%%%%%%%%%%%%%%%%%%%%%%%%%%%%%%%%%%%%%%%%%%%%%%%%%
% Index of terms
% Ff= ratio of Fbf to Wf
% Fr= ratio of Fbr to Wr
% ao= the ratio of ax/g
% Kbf,Kbr= respective brake distribution at fron and rear
%%%%%%%%%%%%%%%%%%%%%%%%%%%%%%%%%%%%%%%%%%%%%%%%%%%%%%%%%%%%%%%%%%%%%%%%%%%%%%%
% Constant a/g Lines
Ff=0:0.1:1;
Fr=abs(Ff-1);
Ff1=0:0.1:0.8;
Fr1=abs(Ff1-0.8);
Ff2=0:0.1:0.6;
Fr2=abs(Ff2-0.6);
Ff3=0:0.1:0.4;
Fr3=abs(Ff3-0.4);
Ff4=0:0.1:0.2;
Fr4=abs(Ff4-0.2);
% Ideal Distribution
```

```
ao=0:0.1:1;
Fbf_ideal=((b/L)+((h/L).*ao)).*ao;
Fbr_ideal=((a/L)-((h/L).*ao)).*ao;
% Kbf Lines
Ff5=0:0.1:0.9;
Fr5=(0.1/0.9).*Ff5;
Ff6=0:0.1:0.8;
Fr6=(0.2/0.8).*Ff6;
Ff7=0:0.1:0.7;
Fr7=(0.3/0.7).*Ff7;
Ff8=0:0.1:0.6;
Fr8=(0.4/0.6).*Ff8;
plot(Ff,Fr,'k',Ff1,Fr1,'k',Ff2,Fr2,'k',Ff3,Fr3,'k',Ff4,Fr4,'k',Ff5,
Fr5,'k--',Ff6,Fr6,'k--',Ff7,Fr7,'k--',Ff8,Fr8,'k--','linewidth',1.2)
hold on
plot(Fbf_ideal,Fbr_ideal,'linewidth',2)
xlabel('Fbf/W, Front Brake Force / Normal Front Load','fontweight',
'bold','fontsize',12)
ylabel('Fbr/W, Rear Brake Force / Normal Rear Load','fontweight',
'bold','fontsize',12)
title('Ideal Braking Proportions','fontweight','bold','fontsize',12)
grid
saveas(gcf,'Ideal Brake Proportions', 'ai')
```

## D.7 Param_Curb_Driver_ADK.m

```
%
% Param_Curb_Driver_ADK.m
%
%   Paramater File of BMW Mini Cooper at Curb Weight + Driver
%   "Configuration 1"
%
%   Paramater Values as reported in:
%   Law, E.H., "Development of INput Parameters for a Simulation of the
%   Vertical Ride Response of a Model Year 2007, MBW Mini", Report
%   TR-07-113-ME-MMS, Dept. of Mechanical Engineering, Clemson University,
%   May 2007.
%
%   Parameter Values Updated as per TR-07-120-ME-MMS, 5/6/08
%   Parameter Values Updated as per simulation tuning, 12/08
%   Edited by ADK to add parameters for longitudinal dynamics. May 09
%   Pitch inertia updated to match Carsim..
%%%%%%%%%%%%%%%%%%%%%%%%%%%%%%%%%%%%%%%%%%%%%%%%%%%%%%%%%%%%%%%%%%%%%%%%%%%%
%% Vehicle Parameters
%
g=9.81;             %acceleration due to gravity, m/s^2
r=0.293;            % tire dyn rolling radius, m (175/65 R15)
L=2.468;              % wheelbase, m
% me=272;
me=0;             % engine and trans mass, kg
de=-.157;           %distance of engine cg behind the Front Axle, m
%% Load Dependent Parameters
```

```
% hs=.602;           % sprung mass CG above ground, m
hs=.570;           % sprung mass CG above ground, m
%A check to validate in carsim. Carsim considers engine
and chassis as sprung mass
htotal=0.517;
msc=1071;           % combined engine and chassis mass, kg
asc=0.963;          % distance of combined eng and chassis CG from F axle, m
ms=msc-me;         % chassis sprung mass, kg
% icar=680.4;      % pitch inertia of sprung mass with two front
seat passengers, kg m^2
icar=970.9;      % pitch inertia of sprung mass with two front
seat passengers, kg m^2
%% Calculated Parameters
bsc=L-asc;            % distance of combined eng and chassis CG from R axle, m
as=(msc*asc-me*de)/ms; % chassis sprung mass cg to front axle, m
bs=L-as;               % chassis sprung mass cg to rear axle, m
c=as-de;              % engine to CG of chassis sprung mass, m
%
% kev=870.5e3;         % eng mount stiff, N/m
% cev=263.9;          % eng mount damping, N/(m/s)
freqeng=10.5;             % assumed natural freq of one DOF engine, Hz
zetaeng=0.01;           % assumed zeta of one DOF engine
kev=((2*pi*freqeng)^2)*me;         % eng mount stiff, N/m
cev=2*zetaeng*(2*pi*freqeng)*me;    % eng mount damping, N/(m/s)
% kev=1e10;         % eng mount stiff, N/m
% cev=2000;    % eng mount damping, N/(m/s)
%% Unsprung Mass Parameters
mtf=141;           % unsprung mass, front axle, kg
```

```
mtr=111;           % unsprung mass, rear axle, kg
%
kf=66.3*1000;           % front susp stiff, per axle, N/m
kr=50.6*1000;           % rear susp stiff, per axle, N/m
%
%
% cf=6030;          % front susp damp, per axle, N/(m/sec)
% cr=9961;          % rear susp damp, per axle, N/(m/sec)
cf=7839;
cr=5180;
%
ktf=464.04e3;            % front tire stiff, per axle, N/m
ktr=464.04e3;         % rear tire stiff, per axle, N/m
ctf=93.6;        % front tire damp, per axle, N/(m/sec)
ctr=93.6;        % rear tire damp, per axle, N/(m/sec)
%
mFaxle=msc*(L-asc)/L;   %mass on front axle
mRaxle=msc*asc/L;       %mass on rear axle
%% Addition to accomodate longitudinal dynamics added in
april 09 by ADK
mtotal=msc+mtf+mtr;
rf=0.29; % Wheel radius front in meters
rr=0.296; % Wheel radius rear in meters
% rf=0.31483; % Wheel radius front in meters
% rr=0.30991; % Wheel radius rear in meters
% hwc=hs-rf; %height of sprung mass CG above wheel centers
% hwc=0.1;
he=0.1397;         % height of engine CG above ground, m
```

```
added in april 09 by ADK
% Itf=2*1.637;  % front wheel assembly inertia in kgm^2
% Itr=2*1.376;  % rear wheel assembly inertia in kgm^2
Itf=2*1.637;  % front wheel assembly inertia in kgm^2 per axle
Itr=2*1.376;  % rear wheel assembly inertia in kgm^2 per axle
```

# References


[1] Rangelov, K. 2004. "Simulink Model of a Quarter-Vehicle with an Anti-lock Braking System". Masters Thesis, Eindhoven University of Technology, Stan Ackerman Institute, Eindhoven.

[2] Ashrafi, B. 1991. "Modeling, Simulation and Sensitivity Analysis of a road vehicle during emergency braking". Doctoral Thesis, Drexel University, Philadelphia.

[3] Nantais, N. 2006. "Active brake proportioning and its its effects on safety and performance". Masters Thesis, University of Windsor, Windsor.

[4] Nigam, S. 1993. "Modeling, Simulation and Response analysis of antilock braking systems". Doctoral Thesis, West Virginia University, Morgantown.

[5] Delaigue, P. and A. Eskandarian. 2004. "A comprehensive vehicle braking model for predictions of stopping distances". Proceedings of the Institution of Mechanical Engineers, Part D: Journal of Automobile Engineering. Volume 218, Number 12. Page(s): 1409-1417.

[6] Alptekin, M. 1991. "An investigation of the interactions of the braking and suspension systems of automobiles". Masters Thesis, Clemson University, Clemson.

[7] Infantini, M., Perondi, E. and N. Ferreira. 2005. "Development of an anti-lock braking system model". SAE technical paper 2005-01-4032, SAE Brazil Congress and Exhibit, Sao Paulo, Brazil.

[8] Day, T. and S. Roberts. 2002. "A simulation model for vehicle braking systems fitted with ABS". SAE technical paper 2002-01-0559, SAE World Congress, Detroit, Michigan, USA.

[9] Cabrera, J., Ortiz, A., Castillo, J. and A. Simon. 2005. "A Fuzzy Logic Control for Antilock Braking System Integrated in the IMMa Tire Test Bench". IEEE Transactions on Vehicular Technology, Vol.54 (no.6), Page(s): 1937- 1949

[10] Jun, S. 2003. "Development of Fuzzy Logic Anti-Lock Braking System for Light Bus". SAE technical paper 2003-01-0458, SAE World Congress, Detroit, Michigan, USA.

[11] Wambold, J., Brickman, A., Park, W. and J. Ingram. 1973. "Effect of road roughness on vehicle braking". Highway Research Board, 52nd annual meeting, Highway Research Record No. 4, Washington D.C., Page(s): 76-82

[12] Reed, W. and A. Keskin. 1989 "Vehicular deceleration and its relationship to friction". SAE technical paper 890736, SAE International Congress and Exposition, Detroit, Michigan, USA.

[13] Hazare, M. and E. H. Law. 2009. "Trade-Off Study for Ride Comfort and Tire Grip for a 2007 BMW Mini Equipped with TWEELs™ Traversing a Randomly Irregular Road",Clemson Dept. of Mechanical Engineering Report TR-09-102- ME-MMS, May 21.

[14] Calvo, J., Díaz, V., Román, J. and D. García-pozuelo. 2008. "Influence of Shock Absorber Wearing on Vehicle Brake Performance". International Journal of Automotive Technology, Vol. 9, No. 4, Page(s): 467−472

[15] Paradiso, M. 2009. "Development of a Nonlinear Ride Quality Model to Aid in TWEEL™ Parameter Selection". Masters thesis, Clemson University, Clemson.

[16] Pacejka, H. 2006. "Tire and Vehicle Dynamics, Second Edition". SAE International and Elsevier.

[17] Law, E. H. " Dynamics of Road Vehicles", ME 453/653 Class Notes, Spring 2006, Clemson University.

[18] McKibben, D. 2007. "2007 BMW MINI: Examination of Suspension and Steering Kinematics and Compliance", Michelin Tire CTA/PE3/V, MARC Report No. FW576.

[19] Law, E. H. 2007. "Development of Input Parameters For a Simulation of the Vertical Ride Response of a Model Year 2007, BMW Mini, REVISED", Clemson University, Dept. of Mechanical Engineering Report TR-07-120-ME-MMS, December 28.

[20] Anon. 1976. "Surface Vehicle Recommended Practice – Vehicle Dynamics Terminology", SAE International, SAE J670e.

[21] Fisher, D. 1970. "Brake System Component Dynamic Performance Measurement and Analysis", SAE technical paper 700373, International Automobile Safety Conference, Detroit, Michigan, USA.

[22] Schafer, T., Howard, D. and R. Carp. 1968. "Design and Performance Considerations for a Passenger Car Adaptive Braking System", SAE Technical Paper 680458, Mid-Year Meeting, Detroit, Michigan, USA.

[23] Aurora, R. 1972. "Simulation of Vehicle Dynamic Braking Characteristics", Journal of Automotive Engineering, 3(e).

[24] Bosch Automotive Handbook, 2000, Page 662.

[25] Yamada, T., Sawada, M. 2001. "Development and Implementation of Simulation Tool for Vehicle Brake System", SAE technical paper 2001-01-0034, SAE World Congress, Detroit, Michigan, USA.

[26] A. Fortina, M. Velardocchia, A. Sorniotti. 2003. "Braking System Components Modeling" , SAE technical paper 2003-01-3335, 21st Annual Brake Colloquium and Exhibition, Hollywood, Florida, USA.

[27] Pang, P. and Agnew, D. 2004. "Brake System Component Characterization for System Response Performance: A System Level Test Method and Associated Theoretical Correlation", SAE technical paper 2004-01-0726

[28] Miyashitaa, N., Kawazuraa, T. and K. Kab. 2003 "Analytical model of mu–S curve using generalized skewed-parabola", JSAE Review, Volume 24, Issue 1, January, Page(s): 87-92

[29] Salaani, M. 2007. "Analytical Tire Forces and Moments Model With Validated Data", SAE Paper No. 2007-01-0816, Meeting Name:SAE World Congress, Detroit, Michigan, USA.

[30] Lacombe, J. 2000. "Tire Model for Simulations of Vehicle Motion on High and Low Friction Road Surfaces". Proceedings of the 2000 Winter Simulation Conference.

[31] Rhyne, T. " Mechanics of Pneumatic Tires ", AuE 829 Course Notes, Spring 2008.

[32] Wong, J. 2001. "Theory of Ground Vehicles", third edition, John Wiley and Sons, New York.

[33] Paradiso, M. and E. H. Law. 2008. "Investigation of Ride Response for a Nonlinear Model of the 2007 BMW Mini with TWEELs™ with a Range of Static Deflections from 10 to 20 mm", Clemson University, Dept. of Mechanical Engineering Report TR-08-118-ME-MMS, November 4.

[34] Khekare, A., Powell, R., Ayalew, B. and E. H. Law. 2009. "Transient Handling Analysis of a 2007 BMW Mini Equipped with TWEELs™: Comparison of Tests and Simulation and Parameter Studies", Clemson University, Dept. of Mechanical Engineering Report TR-08-119-ME-MMS, March 31.

[35] Quarterly Meetings and Updates from BMW and Michelin (2007-09).

[36] E. H. Law. 2008. "Sensitivity of Ride and Tire-to-Road Grip to Changes in the Suspension Stiffness and Damping for a TWEEL™-Equipped BMW Mini", Clemson University, Dept. of Mechanical Engineering Report TR-08-107-ME-MMS, May 15.

[37] E-mail, 2009. From Tim Rhyne to Harry Law, March 19.